TOPICAL AND LOCAL CONTROLLED RELEASE OF STRATIFIN FOR THE IMPROVEMENT OF HYPERTROPHIC SCARRING IN OPEN AND SURGICALLY CLOSED WOUNDS

by

ELHAM RAHMANI NEISHABOOR

Pharm. D., Tehran University, 2002

A THESIS SUBMITTED IN PARTIAL FULFILLMENT OF
THE REQUIREMENTS FOR THE DEGREE OF

DOCTOR OF PHILOSOPHY

in

THE FACULTY OF GRADUATE STUDIES

(Experimental Medicine)

THE UNIVERSITY OF BRITISH COLUMBIA

(Vancouver)

February 2011

Abstract

Hypertrophic scar (HS), which results from the uncontrolled synthesis and excessive deposition of extracellular matrix (ECM) at sites of dermal injury, represents an undesirable endpoint of wound healing. Stratifin (SFN) was recently identified as a potent matrix methaloproteinase-1 (MMP-1) stimulatory factor in dermal fibroblasts. In this research project, it is hypothesized that stratifin can modulate the deposition of ECM components and prevent HS formation when it is applied topically to open wounds or locally delivered to surgically closed wounds.

Four specific objectives were accomplished in this project. Under objective 1, a hydrogel /microsphere dermal implant was fabricated, specifically to be placed in surgical wounds before closure and locally deliver stratifin in a controlled manner to reduce HS formation. Microencapsulating stratifin complexed chitosan particles into PLGA microspheres allowed bioactive stratifin to be controllably released over 30 days with a reduced burst release. Under objective 2, use of a rat surgical wound model showed that the local controlled delivery of stratifin markedly reduced fibrosis and inflammation induced by drug-free implants, confirmed by a reduced collagen deposition, total tissue cellularity, and infiltrated $CD3^+$ immune cells.

Under objective 3, the anti-fibrogenic effect of topically applied stratifin was investigated on open wounds created in a rabbit ear fibrotic model. Qualitative wound assessment showed a reduced HS in wounds treated with stratifin-impregnated CMC gel (0.002%, w/w) applied twice a day, confirmed with reduced scar volume including deposited collagen and total tissue cellularity. Under objective 4, CMC gel was modified into a thermoreversible emulgel, which demonstrated a significant effect on scar reduction through its occlusive effect. Using this emulgel and combining stratifin with acetylsalicylic acid significantly reduced HS, even with once a day application.

In conclusion, the findings presented in this thesis provide further support for the importance and feasibility of using stratifin as an MMP-1 stimulatory factor for the improvement/prevention of dermal fibrosis in open and surgically closed wounds. These findings also provide additional information regarding controlled delivery of proteins to any kind of wounds, such as those resulting from surgical or burns.

Preface

The work presented in this thesis has already been published or prepared for publication in peer-reviewed journals as co-authored manuscripts. I am the first author of all of the publications shown below:

Chapter 2: Rahmani-Neishaboor, E., J. Jackson, H. Burt, and A. Ghahary. 2009. Composite hydrogel formulations of stratifin to control MMP-1 expression in dermal fibroblasts. *Pharm Res*. 26:2002–2014.

Chapter 3: Rahmani-Neishaboor, E., R. Hartwell, E. Brown, J. Jackson, and A. Ghahary. Controlled release of stratifin from composite wound implants reduces post-surgical scarring. [Submitted]

Chapter 4: Rahmani-Neishaboor, E., F.M. Yau, R. Jalili, R.T. Kilani, and A. Ghahary. 2010. Improvement of hypertrophic scarring by using topical anti-fibrogenic/anti-inflammatory factors in a rabbit ear model. *Wound Repair Regen*. 18:401–408.

Chapter 5: Rahmani-Neishaboor, E., R. Jalili, R. Hartwell, N. Carr, and A. Ghahary. Controlled release of stratifin and acetylsalicylic acid from a topically applied thermoreversible submicron emulgel reduces hypertrophic scarring. [Submitted]

Dr. Aziz Ghahary was the supervising investigator of the research project, and the original identification of stratifin as a keratinocyte-releasable factor is credited to him. In addition, he supervised all experimental designs and analysis and critically reviewed all the published manuscripts included in this thesis. The financial support for this thesis was provided by CIHR grants held by Dr. Ghahary. I was responsible for the identification and design of the experiments, performing the research, data analysis, and manuscript preparation for all the work described here. All of the animal works were reviewed and approved by the University of British Columbia Animal Care Committee (Animal Care protocol number: A10-0147). All research work involving biological hazards was conducted in accordance with the University of British Columbia Policies and Procedures, Biosafety Practices and Public Health Agency of Canada guidelines (Biohazard Protocol Number: B09-0298).

Table of Contents

List of Tables

List of Figures

List of Acronyms

ASA	acetylsalicylic acid
bFGf	basic fibroblast growth factor
BSA	bovine serum albumin
cDNA	complementary DNA
CMC	carboxymethylcellulose
DAPI	4',6-diamidino-2-phenylindole
DDW	double distilled water
DMEM	Dulbecco's modified Eagle's medium
ECM	extracellular matrix
EDAC	ethyl-3-(dimethylamino) carbodiimide
EDTA	ethylenediaminetetraacetic acid
EGF	epidermal growth factor
ETI	epidermal thickness index
FBS	fetal bovine serum
FGF	fibroblast growth factor
FITC	fluorescein isothiocyanate
GAPDH	glyceraldehyde-3-phosphate dehydrogenase
GF	growth factor
GM-CSF	granulocyte-macro-phage colony-stimulating factor
GST	glutathione S transferase
H&E	hematoxylin and eosin
HA	hyaluronic acid
hpf	high power field
HS	hypertrophic scar
IFN	interferon
IGF-1	insulin-like growth factor
IPTG	isopropyl-beta-D-thiogalactopyranoside
KDAF	keratinocyte derived anti-fibrogenic factor
KSFM	keratinocyte serum free medium
LB	lysogeny broth
MAPK	mitogen-activated protein kinase
MePEG-b-PDLLA	methoxy poly(ethylene glycol)block-poly(D,L-lactide)
MMP	matrix metalloproteinase
MTT	methyl thiazolyl tetrazolium
OA	oleylamine
OD	outside diameter
ODN	oligonucleotide
PBS	phosphate buffered saline
PCR	polymerase chain reaction
PDGF	platelet derived growth factor
PEG	polyethylene glycol
PLDF	polyvinylidene difluoride
PLGA	poly(lactic-*co*-glycolic acid)

PVA	polyvinyl alcohol
RT-PCR	reserved transcription-polymerase chain reaction
SCC	squamous cell carcinoma
SD	Sprague-Dawley
SDS-PAGE	sodium dodecyl sulfate polyacrylamide gel electrophoresis
SEI	scar elevation index
SEM	scanning electron microscope
SFN	stratifin
Si-RNA	small interfering RNA
SME	submicron emulsion
SOD	superoxide dismutase
TGF	transforming growth factor
TNF	tumor necrosis factor
UBC	University of British Columbia
VEGF	vascular endothelial growth factor

Acknowledgements

I am grateful to Dr. Aziz Ghahary for being an exceptional supervisor. I am indebted to him for his continuous support, guidance, and inspiration.

I am thankful to the members of my advisory committee: Dr. Erin Brown, Dr. Nicholas Carr, and Dr. Frank Ko, for their valuable guidance, insight and magnificent support.

My warm regards to Dr. Effat Farboud from whom I learned most of my pharmaceutical knowledge.

My sincere thanks to John Jackson in Pharmaceutics laboratory at UBC for his great comments on controlled release drug delivery formulation.

I also thank the amazing group of people in BC professional fire fighters' burn and wound healing research laboratory at UBC. Their friendship, support, and wisdom have improved the quality of my work and life. I am grateful to Amir Akbari, Matthew Carr, Claudia Chavez, Farshad Forouzandeh, Abdi Ghaffari, Darya Habibi, Ryan Hartwell, Reza Jallili, Ruhangiz Kilani, Amy Lai, Yanyuan Li, Abelardo Medina, AliReza Moeen, and Azadeh Tabatabai.

I acknowledge the funding agencies Work Safe BC, the CIHR/Skin Research Training Program, and MSFHR/Transplantation Research Training Program for their financial support.

Finally and most importantly, I thank my family, siblings and my cousin for their continued love, support, and strength, and especially my husband, Mehran for his unconditional love and inspiration. Special thanks to his family for their wonderful support throughout the course of my Ph.D.

To my parents, who taught me to value knowledge and education

Chapter 1. Introduction

1.1 Biology of Wound Healing

Tissue injury initiates a cascade of wound repair processes that restore tissue integrity. The repair cascade consists of overlapping phases of inflammation, proliferation, and remodeling (Clark, 1996). Inflammation is the first stage of wound healing and includes hemostasis. At the injury site lacerated vessels immediately constrict. Thrombotic tissue products from the subendothelium are exposed. Platelets aggregate and form the initial hemostatic plug. The intrinsic and extrinsic coagulation pathways are initiated and lead to the formation of fibrin, which is subsequently polymerized into a stable clot. The aggregated platelets degranulate, releasing potent chemoattractants for inflammatory cells, activation factors for local fibroblasts and endothelial cells, and vasoconstrictors. The initial influx of white blood cells into the wound is composed of neutrophils. The early neutrophil infiltrate scavenges cellular debris, foreign bodies, and bacteria. Within 2 to 3 days, the inflammatory cell population begins to shift to monocytes. Circulating monocytes are attracted to the injured tissue, differentiate into macrophages, and organize the repair process (Clark, 1996). Macrophages phagocytose bacterial debris and secrete multiple growth factors to recruit endothelial cells, keratinocytes, and fibroblasts to begin their repair function. During the proliferation phase, fibroblasts synthesize and deposit extracellular matrix (ECM) at the wound site. Fibronectin and glycosaminoglycan (GAG) hyaluronic acid compose the initial wound matrix (Singer and Clark, 1999). Hyaluronic acid provides a matrix that enhances cell migration because of its large water content. Adhesion glycoproteins, including fibronectin, laminin, and tenascin, are present throughout the early matrix and facilitate cell attachment and migration. As fibroblasts enter and populate the wound, they utilize hyaluronidase to digest the provisional hyaluronic-acid-rich matrix, and larger, sulfated GAGs are subsequently deposited. Concomitantly, collagens are deposited onto the fibronectin and GAG scaffold in a disorganized array.

Collagen types I and III are the major fibrillar collagens compromising the ECM and are the major structural proteins in both wounded and unwounded skin. The ratio of

collagen types I:III is 4:1 in skin and wound scar. Type III collagen is initially present in relatively large amounts in wounds but always less than type I collagen in mature scar (Miller and Gay, 1992). The final phase is remodeling, which is commonly described as scar maturation. The ECM is the scaffold that supports the cells both in unwounded and wounded states. It is dynamic and constantly undergoes remodeling during repair. The balance among synthesis, deposition, and degradation of ECM regulates remodeling. Collagenases, gelatinases, and stromelysins are matrix metalloproteinases (MMPs) that degrade ECM components. Lysyl oxidase is the major intermolecular collagen crosslinking enzyme. Collagen crosslinking improves wound tensile strength (Kobayashi et al., 1994).

Ultimately, the outcome of wound healing is scar formation. Scar has no epidermal appendages (hair follicles and sebaceous glands). Scar has a collagen pattern that is distinctly different from unwounded skin. The collagen pattern in scar tissue is densely packed and does not possess the regular pattern found in unwounded dermis. During remodeling, wounds gradually become stronger with time. Wound tensile strength increases rapidly from 1 to 8 weeks after wounding, which correlates with collagen crosslinking by lysyl oxidase (Levenson et al., 1965). However, the tensile strength of wounded skin reaches at best only 80% of the tensile strength of unwounded skin (Levenson et al., 1965). Mature scar is brittle and less elastic than normal skin.

1.2 Wound Pathology

1.2.1 Non-healing wounds

Chronic or non-healing wounds are open wounds that fail to epithelialize and close in a reasonable amount of time, usually within 30 days (Norton J.A. et al., 2000; **Norton**, 2008). Many factors can contribute to wound healing failure, with no predominant reason for non-healing of wounds. Medical conditions such as diabetes, arterial insufficiency, venous disease, steroid use, connective tissue disease, chemotherapy, and radiation injury inhibit wound healing. Non-healing wounds can also be due to pressure necrosis, infection, skin cancer, malnutrition, and chronic dermatological and other metabolic conditions (Norton, 2008; Singer and Clark, 1999). Treatment of these wounds frequently involves the debridement of necrotic tissue.

Despite optimal management of various clinical conditions these wounds may not heal, and surgical intervention may be required (Norton J.A. et al., 2000; **Norton**, 2008).

1.2.2 Excessive healing

Normal wounds receive "stop" signals that halt the repair process when the wound is closed and epithelialization is complete. When these signals are absent or infinitesimal, the repair process may continue and result in excessive scarring. The underlying regulatory mechanisms for excessive scarring are not yet known. Delayed epithelialization (Ghahary et al., 2004; Medina et al., 2007), prolonged inflammatory phase (Tredgetet al., 1997), profibrotic cytokine overexpression (Tredget et al., 1997), and a lack of programmed cell death for activated fibroblasts have been implicated in scar formation (Wassermann et al., 1998; Yang et al., 2003). There are no good animal models of excessive scar formation. There have been some models that are making some headway into the pathophysiology of scarring (Morris et al., 1997; Zhu et al., 2007).

1.2.3 Hypertrophic scar

Hypertrophic scar (HS) and keloids (Fig. 1.1), which result from the uncontrolled synthesis and excessive deposition of extracellular matrix (ECM) at sites of dermal injury (Tredget et al., 1997), represent an undesirable endpoint of wound healing. HS is defined as thick, raised scars that remain confined to the borders of the original wound and usually retain their shape. Keloids are benign dermal fibrotic tumors that grow beyond the boundaries of the initial wound. (Atiyeh et al., 2005). Hypertrophic scar and keloids show a tendency to form in areas with increased tension, such as the shoulders, sternum, mandible, and arms. This is more common in Asians and dark-skinned races (Mutalik, 2005b). In the majority of cases, HS enlarges for a period of months and eventually regresses spontaneously over a few years (Scott et al., 2000). If left untreated, however, the scar tissue may undergo a remodeling, leading to the development of contractures that further contribute to the functional impairment, discomfort, and cosmetic problems suffered by the patient (Kwan et al., 2009; Ladak and Tredget, 2009).

Fig. 1.1. Hypertrophic scarring and keloid scarring:(**a**) post-burn hypertrophic scarring (Courtesy of Dr. E. Tredget at University of Alberta and (**b**) keloid scarring (Aarabi et al., 2007).

1.3 Extracellular Matrix Components

The main components of extracellular matrix are collagens, elastic fibers, proteoglycan/glycosaminoglycan macromolecules, and several non-collagenous glycoproteins. The ability of resident cells, such as fibroblasts and smooth muscle cells, to synthesize and assemble the extracellular matrices is critical for wound healing.

Collagen, in its various forms, is the main fibrillar component of connective tissue and the major extracellular protein of the human body (Franzke et al., 2005; Myllyharju and Kivirikko, 2001; Pulkkinen et al., 2002). The physiologic role of collagen fibers in the skin is to provide tensile properties that allow the skin to serve as a protective organ against external trauma. In human skin, collagen fibers form the bulk of the extracellular matrix and comprise approximately 80% of the dry weight of the dermis. The prototype of the collagens is type I collagen, the most abundant collagen in the dermis.

1.4 Extracellular Matrix Degradation and Turnover

Extracellular matrix remodeling is a multi-step process involving localized degradation of the existing matrix components, followed by cytoskeletal rearrangement, cell translocation, and the deposition of new extracellular matrix components. Although each of these steps is controlled by a variety of molecular mechanisms, the initial step depends on the presence of proteinases capable of initiating the degradation of the matrix macromolecules. These enzymes comprise the matrix metalloproteinase (MMP) family

(Bauer et al., 1975; Bode et al., 1999; Eisen et al., 1968), which includes the collagenases, gelatinases, stromelysins, matrilysins, metalloelastase, enamelysin, and the membrane-type MMPs (Table 1.1). MMP-1 was the first enzyme of the MMP family to be discovered and was defined by its ability to break down triple-helical collagen, which is resistant to most proteases. MMP-1, like the other MMPs, requires zinc and calcium for its enzymatic activity (Pirard, 2007). MMP-1 degrades collagen types I, II, III, VII, and X, but it does not degrade collagen types IV and V. At physiologic pH and temperature the enzyme catalyzes a single cleavage three quarters of the distance from the amino terminus in each of the three polypeptide chains comprising the triple-helical, native collagen monomer.

At physiologic temperature, the collagen cleavage products (i.e., the three-quarter/one-quarter fragments), which are initially triple helical, become soluble, thermally unstable, and denature spontaneously to form gelatin (denatured collagen). These denatured gelatin polypeptides are then susceptible to digestion by other proteinases. Thus, the interstitial collagenases stand at a key point in connective tissue metabolism: They initiate the proteolytic events that result in the degradation of collagen and overall turnover of the extracellular matrices (Table 1.1).

Table 1.1. Matrix metaloproteinases (Klaus Wolff et al., 2007)

Enzyme	MMP number	Alternate name	Matrix substrate
Interstitial collagenase	MMP-1	Type 1 collagenase	Collagens I, II, III, VII, VIII, X, entactin, tenascin, aggrecan, denatured collagens
Neutrophil collagenase	MMP-8	—	Collagens I, II, III, VII, VIII, X, gelatin, aggrecan, fibronectin
Collagenase-3	MMP-13	—	Collagens I, II, IV, IX, X, XIV, aggrecan
Gelatinase A	MMP-2	72-KD type IV collagenase	Denatured collagens, collagens I, IV, V, VII, X, XI, XIV, elastin, fibronectin, laminin, aggrecan, entactin
Gelatinase B	MMP-9	92-KD type IV collagenase	Denatured collagens, collagens I, IV, V, VII, X, XI, XIV, elastin, fibronectin, laminin, aggrecan, entactin
Stromelysin-1	MMP-3	Proteoglycanase	Collagens I, IV, V, IX, X, XI, proteoglycans, laminin, fibronectin, gelatin, elastin, tenascin, aggrecan, entactin, decorin
Stromelysin-2	MMP-10	Transin-2	Collagens III, IV, V, proteoglycans, laminin, fibronectin, elastin, aggrecan
Stromelysin-3	MMP-11	—	α-1 proteinase inhibitor
Matrilysin	MMP-7	Matrilysin-1	Collagen IV, denatured collagens, laminin, fibronectin, elastin, aggrecan, tenascin
Matrilysin-2	MMP-26	Endometase	Gelatin, 1-proteinase inhibitor
Membrane type MMP-1	MMP-14	MTI-MMP	Progelatinase A, denatured collagen, fibronectin, laminin, entactin, proteoglycans
Membrane type MMP-2	MMP-15	MT2-MMP	Progelatinase A
Membrane type MMP-3	MMP-16	MT3-MMP	Progelatinase A
Membrane type MMP-4	MMP-17	MT4-MMP	Unknown
Membrane type MMP-5	MMP-24	MT5-MMP	Progelatinase A
Membrane type MMP-6	MMP-25	MT6-MMP	Unknown
Metalloelastase	MMP-12	—	Elastin, collagen IV, vitronectin, laminin, entactin, fibronectin
Enamelysin	MMP-20	—	Amelogenin, aggrecan
MMP-19	MMP-19	—	Gelatin, aggrecan, fibronectin
MMP-21	MMP-21	—	Unknown
MMP-22	MMP-22	—	Unknown
MMP-23	MMP-23	—	Unknown
Epilysin	MMP-28	—	Unknown

1.5 Stratifin

It is well established that when keratinocytes infiltrate and re-epithelialize a wound within 2–3 weeks, only one third of the anatomically matched wounds become hypertrophic. However, the incidence of hypertrophic wounds increases to 78% when wounds are epithelialized later than 21 days (Ghahary et al., 2005). These findings suggest that upon epithelialization some of the keratinocyte releasable factors may function as wound healing termination factors at a late stage of the wound healing process. In this regard, recent studies indicate that keratinocytes synthesize and release a strong collagenase stimulating factor for dermal fibroblasts; this factor was identified to be 14-3-3σ protein (Ghahary et al., 2004). 14-3-3σ is a member of a family of highly conserved and abundant 28–33 kDa acidic polypeptides called 14-3-3 proteins (β, γ, ε, η, σ, θ, and ς). Moore and Perez (1967) first described it in their research of acidic proteins of the nervous system by 2D chromatography. The unusual name was given during a systematic attempt to classify bovine brain proteins. The 14-3-3 proteins eluted in the 14th fraction of bovine brain extract and were found on positions 3.3 of subsequent starch-gel electrophoresis.

14-3-3σ is also known as stratifin (SFN), owing to its high expression in stratifying keratinocytes. Leffers et al. (1993) first identified "epithelial marker" stratifin in the Golgi apparatus, cytoplasm, and the conditioned medium of cultured human keratinocytes, suggesting partial secretion by these cells. Although no function was assigned to extracellular SFN, it has been unexpectedly but frequently found in various cells, including human MDA-MB-231 breast carcinoma (Butler et al., 2008), human uveal melanoma cells (Pardo et al., 2006), tumor-associated monocytes/macrophages (Kobayashi et al., 2009), and adult human epidermis keratinocytes (Katz and Taichman, 1999). Analysis of human epidermal keratinocyte secretome has made it possible to document that extracellular SFN functions as a potent MMP-1 stimulatory factor in fibroblasts (Ghahary et al., 2004). Recombinant stratifin demonstrated potent MMP-1 stimulatory activity in dermal fibroblasts (Ghahary et al., 2004; Ghahary et al., 2005).

Further investigation revealed that SFN markedly increases c-Fos/c-Jun, which are components of the AP-1 transcription complex (Fig. 1.2). A specific p38 mitogen-activated protein kinase (MAPK) inhibitor (SB203580) blocked the activation of

fibroblast MMP-1 mRNA expression by SFN, suggesting that extracellular SFN may function through the p38 signalling pathway (Lam et al., 2005).

One of the main strategies to reduce scar formation is to induce or accelerate scar degradation. Stratifin has been shown to function as a potent stimulator of fibroblast MMP-1, -3, -8, and -24 levels through the activation of c-Fos and mitogen-activated protein kinase pathway (Lam et al., 2005). As such, stratifin would be a good candidate to function as an anti-fibrogenic factor. Stratifin increases the expression of MMP-1 in wound tissue. It is expected that stratifin slows down the healing process by reducing the matrix accumulation. On the other hand, reducing the volume of the matured scar is very difficult if techniques to do so are applied at the very end of the maturation phase of healing. Consequently, an essential component of normal wound healing is its timely cession. Termination of wound healing, therefore, requires a fine balance between ECM deposition and its hydrolysis (Ghahary et al., 2004).

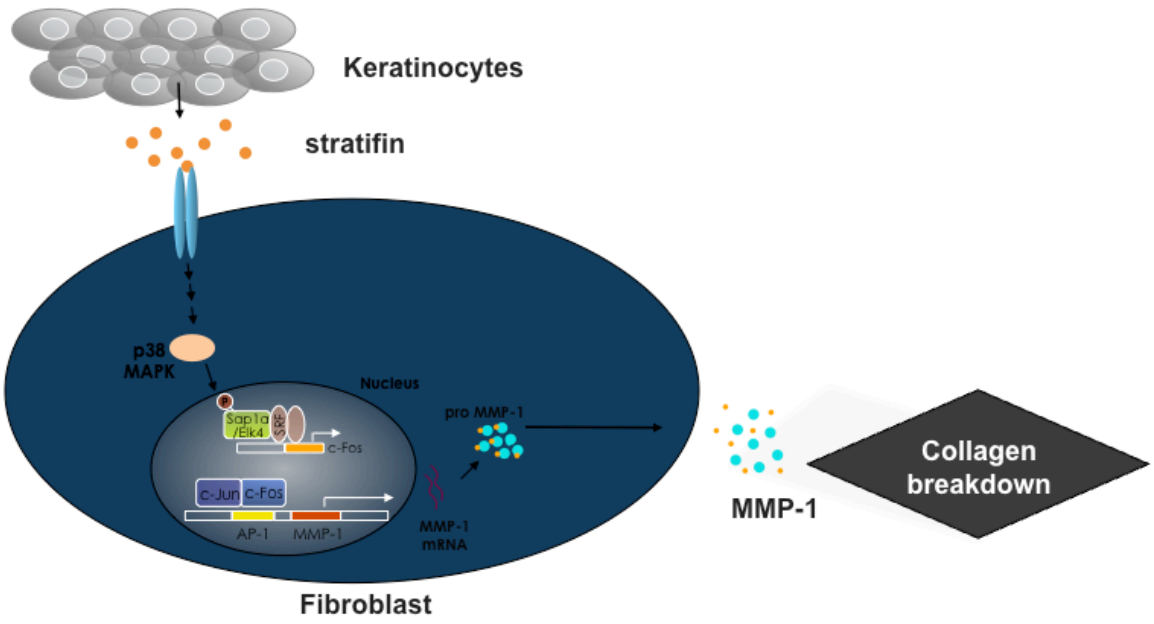

Fig. 1.2. Stratifin mechanism of action. Revised from (Medina et al., 2007).

1.6 Current Treatments of Hypertrophic Scar

There are two general techniques of wound treatment; primary intention, in which the wound is closed with suture material after completion of the operation; secondary intention, in which the wound is left open and closes naturally (Kirsner and Eaglstein, 1993). As such, the modalities for the prevention and treatment of hypertrophic scarring in closed and open wounds are different. These are described here (Norton J.A. et al., 2000; Norton, 2008).

1.6.1 Surgically closed wounds

Most surgical wounds heal by primary intention, in which the wound is closed by suturing. The amount of tissue injury and degree of contamination influence the length and quality of healing. Small, closed wounds heal quickly with less scar formation, whereas large, open, severe wounds heal slowly with significant scar. After a wound is closed by a surgical procedure, scar prevention options are limited. Topical scar prevention has been used infrequently, likely because surgically closed wounds are expected to present a drug permeation barrier similar to intact skin. Traditionally, for post-wound-closure scar prevention, corticosteroids are injected intralesionally. Triamcinolone acetonide, 10 mg/mL, is commonly used initially; if no response occurs, the dose should be increased to 40 mg/mL. Silicone gel sheeting should be used concurrently. Mature keloid lesions with the duration of months to years gradually become unresponsive to corticosteroids and silicone gel sheeting. Newer treatment modalities, such as intralesional injection of interferons (α, β, and γ), 5-fluorouracil, and bleomycin, may be useful. These act by decreasing inflammation and collagen synthesis (Slemp and Kirschner, 2006). However, intralesional injection is painful, invasive, and requires professional administration. With surgically closed wounds, which are very sensitive, injections should be avoided if possible (Gregg and Jones, 1999).

Thus far, a non-invasive treatment for scar prevention resulting from surgically closed wounds such as laparoscopy is demanded and has not been available. Drug-eluting scaffolds that can be implanted in a wound before closure and sustainably release an anti-fibrogenic factor such as stratifin may offer a promising new treatment modality for scar prevention after surgical procedures.

Drug-eluting coronary stents, such as sirolimus- and paclitaxel-eluting stents, have been used extensively to limit the growth of neointimal scar tissue (Garg and Serruys, 2010). However, the field of active scaffolds for wound healing is relatively new, and there is no report available on the use of drug-eluting scaffolds for post-surgical HS prevention.

1.6.2 Open wounds

Open wounds heal with the same basic processes of inflammation, proliferation, and remodeling as do closed wounds. The major difference is that each sequence is much longer, especially the proliferative phase. There is more granulation tissue formation and contraction. Open wound edges are separated, which requires epithelial cell migration across a longer distance. Delayed epithelialization (Ghahary et al., 2004; Medina et al., 2007), infection, and acute and chronic inflammation (Mutalik, 2005b; Norton J.A. et al., 2000; **Norton**, 2008) can impair repair and transform the healing wound into a clinically non-healing wound. When an open wound heals, which is generally defined as complete epithelialization, the dermal defect has been filled with collagen scar covered by epithelium.

Treatment of hypertrophic scar in open wounds remains extremely challenging, particularly in their variable response to treatment. No single therapy has been universally adopted as the standard of care for clinical practice (Franz et al., 2007; Meier and Nanney, 2006; Mustoe et al., 2002). The first step toward treatment of HS is early detection and initiation of therapy after surgery or trauma. Wound management to reduce both infection and suturing is necessary. A new concept for scar management is the prophylactic reduction of scarring by pharmaceutical agents that are given at the time of surgery. Currently, there are no pharmaceuticals marketed for the prophylactic improvement of scar appearance (Occleston et al., 2008).

Patients who are at increased risk of excessive scarring benefit from preventive techniques, which include silicone gel sheeting and ointments and intralesional corticosteroid injection (Mutalik, 2005b). Silicone gel sheeting is a soft, self-adhesive sheeting designed to be used on intact skin for preventing and treating both hypertrophic and keloid scars (Poston, 2000). The mechanism of action of silicone therapy has not been completely determined but is likely to involve occlusion and hydration of the

stratum corneum with subsequent cytokine-mediated signalling from keratinocytes to dermal fibroblasts (Mustoe, 2008). Silicone-based creams are an alternative for the treatment of scars on the face, scalp, or neck (Wong et al., 1996).

In patients who are at extremely high risk of forming problematic scars, such as those developed after excision of keloid and HS, intralesional injection of steroids can be given prophyla3ctically, but multiple injections and higher concentrations of triamcinolone (10 to 40 mg/ml) are often required. Often, cryotherapy will be used first to aid in the ease of the injection. This combination has proved beneficial in scar reduction over time (Boutli-Kasapidou et al., 2005). Intralesional steroids, when injected too deeply or aggressively, can cause atrophy. Other injectable treatments that have been proved to have varying success include bleomycin, 5-fluorouracil, tacrolimus, and interferon (Kim et al., 2001; Mutalik, 2005a; Saray and Gulec, 2005). Surgical excision of larger scars will often result in recurrent and sometimes even larger scars. Skin grafting, pressure garments for both the surgical site and the grafted site, and steroid or interferon injections to the excision site have been shown to reduce type I collagen gene expression, hence 3reducing keloid formation (Kauh et al., 1997). Other therapies, such as topical retinoids, laser therapy, self-adherent soft silicone dressings, and radiation, have had varying success rates (Daly and Weston, 1986; Majan, 2006; Sallstrom et al., 1989; Sherman and Rosenfeld, 1988). Intralesional collagenase has been proved ineffective (Kang et al., 2006).

1.7 Wound Management Products

1.7.1 Traditional healing products

Traditional dressings include cotton wool, natural or synthetic bandages, and gauzes. These dressings are dry and thus do not provide a moist wound environment. Traditional wound dressings for chronic wounds and burns have been largely replaced by more recent and advanced dressings that provide the desired moist environment for wound healing (Boateng et al., 2008).

1.7.2 Modern wound healing products

Many of the wound management products that have been introduced over the last 25 years affect tissue repair. Most are vapour permeable, enabling gaseous exchange but

not allowing passage of water or bacteria (Boateng et al., 2008). This prevents dehydration of the wound surface and provides a moist environment for the formation of granulation tissue and/or enhanced epidermal regeneration.

1.7.2.1 Hydrogels

Hydrogels are three-dimensional networks of hydrophilic polymers, such as gelatin, polysaccharides, and crosslinked synthetic polymers, that contain a large proportion of water. They are able to donate water to necrotic and dry wounds. They also interact with aqueous solutions by absorbing and retaining water within their structure without dissolving. Some hydrogels such as NU-GEL™ and Purilon™ are combined with alginate (Boateng et al., 2008). There are two types of hydrogels used in wound management:

- thin flexible sheets such as Geliperm™, Hydrosorb™, Novogel™, which swell as they absorb water
- amorphous gels such as Intrasite Gel™, Aquaform™, and Sterigel™, which decrease in viscosity as they absorb fluid until the gel is dispersed.

The high moisture content of hydrogels provides a moist wound surface. Amorphous gels are useful specifically in rehydrating necrotic tissue, debridement, and assisting its separation from underlying healthy tissue. Hydrogels are also indicated for lightly exuding granulating wounds. They cool the wound surface and so reduce pain and inflammation. They are transparent. Most need secondary dressing.

1.7.2.2 Hydrocolloids

Most hydrocolloid dressings such as Granuflex™, Aquacel™, and Tegasorb™ are complex formulations consisting of colloids, elastomers, and adhesives. The colloid is the gelling element and absorbent. Typical gel forming agents include carboxymethylcellulose (CMC), gelatin, and pectin. They are available in the form of thin films, sheets, and gels. In the sheet form these polymers are present as hydrophilic particles dispersed in a hydrophobic adhesive. The adhesive is bonded to a vapour-permeable polyurethane film. When a hydrocolloid is placed on an exuding wound, the hydrophilic particles absorb fluid and swell, forming a moist gel at the wound surface. By covering potentially exposed nerve endings, the gel reduces pain.

Hydrocolloids are used extensively in the treatment of leg ulcers and pressure sores. They rehydrate hard necrotic tissue, which softens and eventually separates. They can aid in the removal of the dead tissue from wounds.

1.7.2.3 Adhesive film dressings

The original nylon-derived film dressings have limited ability to absorb sufficient quantities of wound exudates, which results in the accumulation of excess exudates beneath the dressing. This leads to skin maceration, bacterial proliferation, and the risk of infection and therefore requires regular dressing changes as well as irrigation of the wound with saline. Opsite™ is a thin semi-permeable film made from polyurethane covered with acrylic derivatives and is more porous and permeable to water vapour and gases but not liquid from exudates. The films can be transparent, conform to contours such as elbows, knees, and sacral areas (owing to their elastic and flexible nature), and do not require additional taping. However, they are too thin to be packed into deep or cavity wounds and thus are suitable only for relatively shallow wounds. Other available products include Cutifilm™, Biooclusive™, and Tegaderm™ (Boateng et al., 2008).

1.7.3 Protein-eluting scaffolds and dressings for wound repair

One of the advanced technologies in wound repair is a scaffold that elutes bioactive agents. The field of active scaffolds for wound repair is relatively new, and only a small number of such scaffolds have been developed to date. Upon implantation of such scaffolds, cells from the body are recruited to the site and a tissue can be formed (Howard et al., 2008). Growth factors are essential for promoting cell proliferation and differentiation; however, their direct administration is problematic because of their poor *in vivo* stability (Babensee et al., 2000). It is therefore necessary to develop scaffolds with controlled delivery of bioactive agents that can achieve prolonged availability as well as protection of these bioactive agents, which might otherwise undergo rapid proteolysis (Zhu et al., 2008). The main obstacle to successful incorporation and delivery of small molecules, as well as proteins, from scaffolds is their inactivation during the process of scaffold manufacture owing to exposure to high temperatures or harsh chemical environments; this is why it is necessary to develop a method that minimizes protein inactivation.

There are three approaches for protein (growth factor) incorporation into biodegradable scaffolds: adsorption onto the surface of the scaffold, incorporation into scaffolds directly during the fabrication process, and encapsulation into microspheres and then integration into scaffolds (composite scaffold/microsphere structures) (Zilberman et al., 2010). It is important to note that incorporation of protein in all three approaches should be carried out with a method that preserves the protein activity, i.e., without exposure to elevated temperatures or organic solvents.

It has been reported that a variety of growth factors participate in the process of wound healing. These factors include epidermal growth factor (EGF), platelet-derived growth factor (PDGF), fibroblast growth factor (FGF), transforming growth factor (TGF-β1), insulin-like growth factor (IGF-1), human growth hormone, vascular endothelial growth factor (VEGF), and granulocyte-macro-phage colony-stimulating factor (GM-CSF) (Steenfos, 1994). Different dressings have been used to topically administer some of the above growth factors to wound sites. These include hydrogel dressings for delivering TGF-β1 (Puolakkainen et al., 1995), collagen film for delivering PDGF (Koempel et al., 1998), alginate dressings in the form of beads used to deliver VEGF (Gu et al., 2004), and polyurethane and collagen film dressings for delivery of EGF (Grzybowski et al., 1999). One product that has reached market is Regranex™, which is a gel containing 0.01% becaplermin, recombinant human-platelet-derived growth factor (GF). It enhances the formation of granulation tissue and is indicated for full thickness, neuropathic, chronic, and diabetic ulcers.

The polymeric dressings employed for controlled drug delivery to wounds are made of polymers, including poly (lactide-co-glycolide) (Katti et al., 2004), polyvinyl pyrrolidone (Hoffman, 2002), polyvinyl alcohol (Kietzmann and Braun, 2006), and polyurethane foam (Cho et al., 2002; Gottrup et al., 2007; Jorgensen et al., 2005). Other polymeric dressings reported for drug delivery to wounds comprise novel formulations prepared from polymeric biomaterials such as hyaluronic acid (Luo et al., 2000), collagen (Maeda et al., 2001), and chitosan (Aoyagi et al., 2007; Mi et al., 2002b).

1.8 Hypotheses and Specific Objectives

One of the main strategies to prevent dermal fibrosis is to induce or accelerate extracellular matrix degradation. It has been shown in previous studies that stratifin functions as a potent stimulator of MMP-1, -3, -8, and -24 expression in dermal fibroblasts and that effect is mediated through the activation of c-Fos and mitogen-activated protein kinase pathways (Lam et al., 2005). As such, stratifin would be a potential therapeutic option for the prevention of keloid and hypertrophic scarring.

It is expected that stratifin slows down the healing process by reducing matrix accumulation. Therefore, application of stratifin during the early phases of wound healing would theoretically compromise or delay healing. Conversely, application of stratifin near the cessation of the healing process would likely result in no significant change in the volume of the matured scar. An essential component of normal wound healing is its timely cession, suggesting that the timing of administration of stratifin is an important consideration for this proposed intervention. Ideal termination of wound healing, therefore, requires a fine balance between ECM deposition and its hydrolysis (Ghahary et al., 2004).

To investigate the therapeutic effect of stratifin in prevention of hypertrophic scarring in open and surgically closed wounds, the two hypotheses stated below were tested.

1.8.1 Hypothesis 1

Local controlled delivery of stratifin will reduce post-surgical hypertrophic scarring.

The following objective describes our approach in addressing this hypothesis.

1.8.1.1 Objective 1.1

To create a controlled release delivery system for stratifin. In chapter 2, a microencapsulation approach is described; this included preliminary complexing of stratifin with chitosan. This strategy led to the microencapsulation of stratifin without compromising its biological activity. Microspheres were further embedded into a hydrogel film. As a result, active stratifin was controlled released with a reduced burst

release. The findings in this study provide additional information regarding the potential delivery of other bioactive proteins.

1.8.1.2 Objective 1.2

To evaluate the therapeutic effect of a localized controlled release of stratifin to surgical wounds. Stratifin-releasing microsphere/hydrogel implants were tested in a rat surgical wound model. The results, described in chapter 3, confirmed that a localized controlled release of stratifin reduces fibrosis induced by microsphere/hydrogel implants. Moreover, when the ubiquitous nature of scarring within the body was taken into consideration, these results provided important potential treatment options for problematic scarring associated with implanted prostheses, such as vascular stents and breast implants.

1.8.2 Hypothesis 2

Topical application of stratifin will reduce hypertrophic scar formation in open wounds if it is applied before completion of epithelialization.

The following objectives describe the approach used here to address this hypothesis.

1.8.2.1 Objective 2.1

To evaluate the anti-fibrogenic effect of topically applied stratifin in open wounds. As described in chapter 4, a rabbit ear fibrotic model was used. Findings revealed that twice a day application of a stratifin-contained carboxymethyl cellulose gel (0.002%, w/w) reduces hypertrophic scarring in full thickness wounds created on the rabbit ears. All hypertrophic scar criteria including scar elevation index, epidermal thickness index, total tissue cellularity, and infiltrated $CD3^+$ immune cells were significantly reduced following topical application of stratifin.

1.8.2.2 Objective 2.2

To enhance the therapeutic efficacy of topically applied stratifin. In chapter 5, a thermoreversible submicron emulgel that forms an occlusive film following topical application is formulated. This emulgel formulation had the advantage of controlling the release of stratifin for 24 h. Using this emulgel and combining stratifin with acetylsalicylic acid significantly reduced HS when tested on the rabbit ear model, even

with once a day application. A significant reduction in hypertrophic scarring was observed in the wounds treated with the vehicle (empty emulgel). This effect could be described by the occlusive effect of emulgel and its function as a wound dressing. More importantly, incorporating stratifin and acetylsalicylic acid into the emulgel resulted in an additive effect on reduction of hypertrophic scarring.

Chapter 2. Composite Hydrogel Formulations of Stratifin to Control MMP-1 Expression in Dermal Fibroblasts[1]

2.1 Introduction

Collagen deposition is an essential component of normal wound healing but, if unregulated or excessively prolonged, contributes to the development of fibroproliferative disorders such as hypertrophic scarring and keloid induction (Tredget et al., 1997). There are no effective treatment modalities for these conditions (Leventhal et al., 2006).

It is well known that when keratinocytes infiltrate and epithelialize open wounds within 2–3 weeks only one third of the anatomically matched wounds become hypertrophic. However, the incidence of hypertrophic wounds increases to 78% when a wound is epithelialized later than 21 days (Ghahary et al., 2005). These findings suggest that the keratinocytes influence the adjacent fibroblasts to reduce additional scar formation. In fact, studies indicate that keratinocytes synthesize and release a strong collagenase stimulating factor for dermal fibroblasts; this factor was identified to be stratifin or 14-3-3σ protein (Ghahary et al., 2004).

These findings suggest that stratifin, whose anti-fibrogenic effect has previously been established, is an ideal natural factor for reducing and/or preventing excessive scarring. However, topical application of a protein of this size is not feasible because the epidermal barrier prevents penetration (Takeuchi et al., 1999). The objective of this study was to develop a controlled release delivery system for stratifin that can be applied at the time of wound closure.

This formulation should optimally release stratifin for extended periods following a lag time of 3 to 5 days post operation. Intra-wound application of stratifin may be complicated because the biological half-life of most proteins is short. To overcome this

[1] A version of this chapter has been published. Rahmani-Neishaboor, E., J. Jackson, H. Burt, and A. Ghahary. 2009. Composite hydrogel formulations of stratifin to control MMP-1 expression in dermal fibroblasts. *Pharm Res*. 26:2002–2014.

problem, stratifin should be encapsulated in a controlled release formulation that may be retained at the wound site.

A suitable biomaterial for the controlled delivery of proteins is the biocompatible biodegradable polymer poly(lactic-co-glycolic acid) (PLGA). The main potential problems with using PLGA for this purpose are protein aggregation during the loading process and a high burst phase of proteins (Diwan and Park, 2001; Sanchez et al., 2003). Some studies have shown that polymer microspheres containing both hydrophobic and hydrophilic regions successfully encapsulated proteins like bovine serum albumin (BSA), basic fibroblast growth factor (bFGF), and superoxide dismutase (SOD) showed controlled release properties with maintaining the bioactivity of the proteins (Li et al., 2006; Zheng et al., 2004). Geng et al. (2008) showed that erythropoietin could be successfully encapsulated in polysaccharide particles, achieving sustained release of the protein while preserving bioactivity. Other studies have shown that a reduction in the burst phase of protein release may be achieved by embedding microspheres in hydrogel scaffolds, which further restricts water movement and protein dissolution or diffusion (DeFail et al., 2006; Huang et al., 2006; Kempen et al., 2008; Lee et al., 2004).

In the present study, stratifin was encapsulated in PLGA microspheres that were embedded in a crosslinked hydrogel scaffold. Since stratifin is a negatively charged protein, it was electrostatically complexed to the positively charged polysaccharide, chitosan, before encapsulation in PLGA microspheres.

Chitosan (Fig. 2.1) is a hydrophilic polymer that is both biocompatible and biodegradable (Mi et al., 2002a). Furthermore, it has been used to enhance the delivery of plasmid DNA by condensing the DNA to protect it from nuclease degradation (Chen et al., 2004; MacLaughlin et al., 1998; Springate et al., 2005). Chitosan was also found to protect the activity of lysozyme during encapsulation in PLGA polymer (Li et al., 2008).

In this study, microparticulate chitosan (approximately 40 μm in diameter) was soaked in a stratifin solution and dried; the particles were then encapsulated in large (diameter ~ 300 μm) PLGA microspheres. These microspheres were homogenously distributed in crosslinked hyaluronic acid films. Hyaluronic acid is a glycoaminoglycan component of extracellular matrix with unique wound healing and anti-adhesion

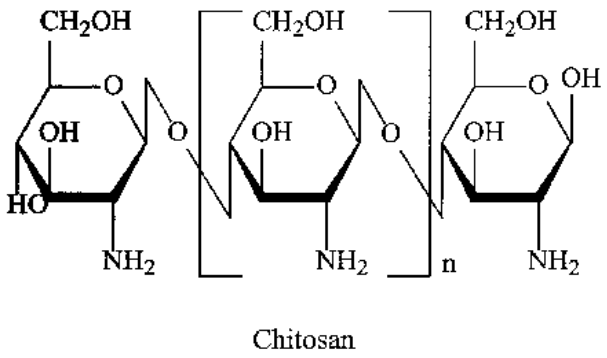

Chitosan

Fig. 2.1. Chitosan chemical structure.

properties, and it has been widely used as the base material for artificial skin as an injectable tissue expansion solution and biodegradable wound dressing (Jackson et al., 2002; Park et al., 2007; Yeo et al., 2007).

The ideal performance characteristics of this delivery system were, firstly, to create a lag phase and, secondly, to control the release of stratifin from the matrix while maintaining the biological activity of the protein. This multi-component formulation of stratifin in chitosan, encapsulated in PLGA microspheres and dispersed in a hyaluronic acid film, successfully achieved these objectives. The biological activity of sustained released stratifin was evaluated by measuring the level of MMP-1 expression in cultured dermal fibroblasts.

2.2 Materials and Methods

2.2.1 Materials

PGEX-6P-1 expression vector, PreScission protease, and glutathione sepharose-4B beads were obtained from GE Healthcare Bio-Sciences AB (Uppsala, Sweden). Protein expressing bacteria BL-21(DE3) was purchased from Novagene (Madison, WI). Anti-human MMP-1 IgG1 (R&D Systems Inc., Minneapolis, MN), mouse anti-ß-actin IgG1 (Sigma, MO), secondary horseradish peroxidase conjugated anti-mouse IgG (Bio-Rad Laboratories, Hercules, CA), Western Blotting detection reagent (Santa Cruz Biotechnology, Santa Cruz, CA), 3-(4,5-dimethyldiazol-2-yl)-2,5-diphenyl tetrazolium bromide (MTT; Sigma, MO), EZ-Label™ fluorescein isothiocyanate (FITC) protein

labeling kit (Pierce Biotechnology Inc., Rockford, IL), and D-Salt™ dextran desalting columns (Pierce Biotechnology Inc., Rockford, IL) were all used as received. Chitosan (ULTRASAN™) (MW.226000, degree of deacetylation = 74.2%) (Biosyntech Inc., Québec, QC), PLGA (85/15, IV = 0.61 dL/g) (Birmingham Polymers, Birmingham, AL), polyvinyl alcohol (PVA) (98% hydrolyzed, MW .25000) (Polysciences, Warrington, PA), and medical grade sodium hyaluronate (HA) (MW .1000000) (Lifecore Scientific, Chaska, NJ,) were used as supplied. Ethyl-3-(dimethylamino) carbodiimide (EDAC) was obtained from Sigma (St. Louis, MO). The diblock copolymer, methoxy poly(ethylene glycol)block-poly(D,L-lactide) (MePEG-b-PDLLA) (60:40 W/W),was synthesized as previously described (zhang et al., 1996). The MePEG molecular weight was 2000 Da, and the molecular weight of the diblock (measured by Gel Permeation Chromatography) was 5240 Da (zhang et al., 1996).

2.2.2 Expression of recombinant stratifin

Human recombinant stratifin protein was prepared as previously described with slight modification (Ghahary et al., 2004). Briefly, the cDNA of stratifin from human keratinocytes was cloned into a pGEX-6P-1 expression vector and transformed into protein expressing bacteria BL-21 (DE3). A single positive clone was grown in 100 mL of lysogeny broth (LB) medium containing 50 μg/mL of ampicillin for 4–6 h at 37°C until an Optical Density (OD) of 0.4–0.6 was reached at 600 nm. Bacteria were then diluted to 1:10 with LB medium plus 0.1 mM isopropyl β-D-1-thiogalactopyranoside (IPTG) for 12 h. To purify the protein, bacteria were centrifuged and lysed by sonication using short cut bursts (30 s intervals). Glutathion-S-transferase (GST)-fused stratifin was purified by adding to glutathione sepharose-4B beads and subsequently digested using PreScission protease according to the manufacturer's procedure. It was previously shown that the recombinant stratifin protein produced in bacteria is more than 95% pure (Ghahary et al., 2004).

2.2.3 Conjugation of stratifin with FITC

For detection and quantification purposes, stratifin was conjugated with fluorescein isothiocyanate (FITC). Fluorescent probe conjugation of stratifin was done using an EZ-Label™ FITC protein labeling kit. The excess fluorescent dye was removed

using a dextran desalting column (D-Salt™). Analytical quantification of FITC-conjugated stratifin was done in a Fluoroscan spectrofluorometer, and the fluorescence was measured at the maximum of the emission band, 520 nm (excitation at 485 nm). Sodium dodecyl sulfate polyacrylamide gel electrophoresis (SDS-PAGE) was used to determine the molecular weight of FITC-conjugated stratifin.

2.2.4 Preparation of stratifin-loaded PLGA microspheres incorporated in hyaluronic acid films

The schematic procedure of preparation of stratifin-loaded PLGA microspheres incorporated in hyaluronic acid films is presented in Fig. 2.2. Stratifin was electrostatically complexed within chitosan particles as follows. 5 mg chitosan particles, smaller than 45 μm, were swelled in 30 μL solution of SFN-FITC in phosphate buffer pH 5.5 (SFN-FITC:chitosan, 1 μg:1 mg) with the molar ratio of 7.5:1.0. The suspension was vortexed and incubated at room temperature for 1 h in order to form ionic complexes. To remove the free/uncomplexed stratifin from the complex, 500 μL phosphate buffered saline (PBS) 5.5 was added to the microtubes. The suspension was gently vortexed and centrifuged at 1000 rpm for 3 min. After the supernatant was removed the complexes were dried under nitrogen gas, and the particles were broken up into a fine powder using a pestle and mortar. These particles were passed through a sieve with a 40 μm pore size, and only particles smaller than 40 μm diameter were encapsulated in PLGA using a suspension-solvent evaporation technique described below. Stratifin bound chitosan particles were dispersed in a 12.5% solution of PLGA in dichloromethane (chitosan:PLGA, 1:12.5 (w/w)). The mixture was vortexed for 30 s. It was slowly pipetted into 100 mL aqueous solution of PVA 1% (w/v) and stirred at 400 rpm. After 2 h the microspheres were separated by gravity, washed 3 times with distilled water, and dried under nitrogen gas for 1 h. The same procedure was used to make PLGA microspheres loaded with 15% MePEG-b-PDLLA diblock. Crosslinked hyaluronic acid (HA) films were made according to the method previously described, with some modification (Jackson et al., 2002). Briefly, 3.2 g of the 1% HA solution (+20% glycerol) containing 8 mM EDAC was pipetted into 2.5 cm diameter plastic Petri dishes and dried for 24 h at 60°C. Microspheres were weighed and uniformly distributed between two layers of dry hydrogel films. The films were sealed by placing the compositions in a

humid chamber for 5 min. To evaluate the *in vitro* release rate of stratifin from different preparations, FITC-conjugated stratifin was used. The loading procedures and release studies were performed under dark conditions to preserve FITC fluorescence.

2.2.5 Microscopic images and particle size of microspheres

The morphology of empty and protein-loaded PLGA microspheres was examined using a scanning electron microscope (SEM) (HITACHI S-4700) after the samples were coated with a thin layer of gold under vacuum. Fluorescence microscope images were taken over a period of 30 days for particles loaded with SFN-FITC. Unencapsulated chitosan particles and particles encapsulated either in PLGA or PLGA/diblock microspheres were photographed at days 1 and 30 using a fluorescence microscope (Motic AE-31) and compared simultaneously.

The particle size analysis was performed using an optical microscope and Motic Images software. In all, measurements of at least 50 particles in four different fields were examined. This procedure was performed on four different preparations of microspheres.

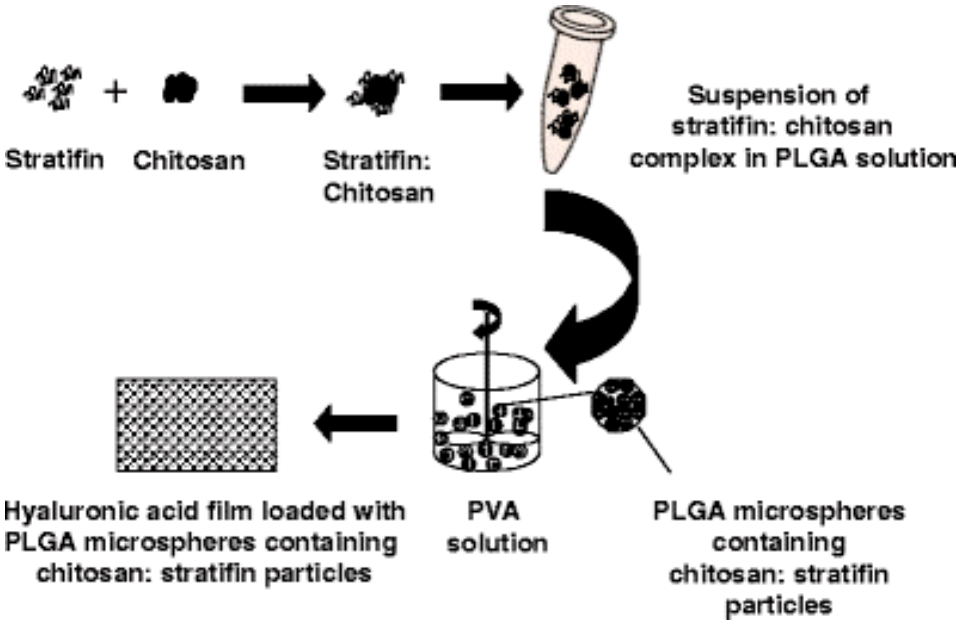

Fig. 2.2. Schematic drawing of the preparation of stratifin-loaded PLGA microspheres incorporated in hyaluronic acid films.

2.2.6. Evaluation of stratifin binding efficiency of chitosan particles and encapsulation efficiency of PLGA microspheres

The amount of stratifin complexed to chitosan particles was calculated by two methods.

The first method was the calculation of the difference between the total amount of SFN-FITC used and the amount of free unbound protein remaining dissolved in the aqueous suspending medium. To measure unbound protein, 5 mg of dried chitosan particles loaded with 5 μg SFN-FITC were suspended in a 1 mL phosphate buffer, pH 7.4, and the suspension was gently vortexed. The suspension was then centrifuged, and the supernatant was assayed for protein concentration by spectrofluorometer. The stratifin binding efficiency of chitosan particles was calculated as indicated below:

$$\text{Entrapment efficiency} = \frac{\text{Total amount of SFN-FITC loading} - \text{free SFN-FITC in supernatant}}{\text{Total amount of SFN-FITC loading}} \times 100$$

The second method for evaluation of stratifin bound to chitosan particles was an estimation of the protein directly bound to particles. For this method, 5 mg dry chitosan particles loaded with SFN-FITC (SFN-FITC:chitosan, 1 μg:1 mg) were suspended in 1 mL phosphate buffer, pH 11, and incubated for 30 min. Since both stratifin with isoelectric pH (pI 4.7) and chitosan with pKa 6.7 are negatively charged at pH 11, they will be separated under this pH. The suspension was sonicated for 15 s and then centrifuged. The concentration of SFN-FITC in supernatant was assayed and considered as the total bound amount.

The encapsulation efficiency of stratifin in PLGA microspheres was then calculated by measuring the difference between the total amount of SFN-FITC bound to chitosan particles (used in the microencapsulation procedure) and the amount of free SFN-FITC remaining in the PVA 1% (w/v) suspending medium at the end of the encapsulation procedure. The encapsulation efficiency of PLGA microspheres was calculated as indicated below:

Encapsulation efficiency =

$$\frac{\text{Total SFN-FITC bound to chitosan} - \text{free SFN-FITC in PVA 1\%}}{\text{Total amount of SFN-FITC bound to chitosan}} \times 100$$

2.2.7 *In vitro* release study

The *in vitro* release of stratifin was obtained from chitosan particles alone, chitosan particles encapsulated into PLGA or PLGA/diblock microspheres, and hyaluronic acid films containing stratifin, stratifin bound chitosan particles, and PLGA microspheres. Under these experimental conditions, stratifin was released within the sink condition determined. SFN-FITC was used to prepare formulations and was analyzed by spectrofluorometry.

Five milligrams of unencapsulated chitosan particles or 45 mg of microspheres were weighed into a microcentrifuge tube containing 1 mL of PBS, pH 7.4, and kept in an incubator at 37°C. Samples were taken at 1 h, 1, 3, 5, 10, 15, 20, and 30 days, and at each sampling time; the release medium was collected after centrifugation and replaced by the same amount of fresh buffer. The samples were analyzed using spectrofluorometry with excitation and emission wavelengths of 480 and 520 nm, respectively.

Hyaluronic acid films containing one of 7.5 μg SFN-FITC or 10 mg SFN-FITC bound chitosan particles or 100 mg PLGA microspheres were assessed for *in vitro* release studies. These films were put on top of the Millicell cell culture inserts (PTFE, 0.4 μm) (Millipore, Billerica, MA) and then placed into 6-well cell culture plates containing 1.5 mL PBS, pH 7.4, containing 0.1% BSA. The release media contained 0.1% BSA as a carrier to reduce protein adsorption to the surface of the plates. In fact, 0.1% BSA did not interfere with fluorescence measurement of FITC under these conditions. The plates were kept in an incubator at 37°C, and samples were taken at 1 h and 1, 3, 5, 10, 15, 20, and 30 days. At each sampling time, the release medium was removed from the bottom chamber and replaced by the same amount of fresh buffer. The samples were analyzed using spectrofluorometry, and percent cumulative release was determined for each time point. The experiments were repeated three times using $n = 4$ samples.

2.2.8 Fibroblast cell culture

Neonatal foreskin pieces were used as the source of fibroblasts and the procedure was done based on the approval of the Ethics Committee of the University of British Columbia (UBC). Cultures of human foreskin fibroblasts were established as described previously (Sarkhosh et al., 2003). In brief, punch biopsy samples were prepared from human foreskins. The tissue was collected in Dulbecco's modified Eagle's medium (DMEM); (GIBCO, Grand Island, NY) with 10% fetal bovine serum (FBS); (GIBCO, Grand Island, NY), minced into small pieces of <0.5 mm in any dimension, washed with sterile medium six times, and distributed into 60 ×15 mm Petri culture dishes (Corning Inc., Corning, NY), with four pieces per dish. A sterile glass coverslip was attached to each dish with a drop of sterile silicone grease to immobilize the tissue fragment. DMEM containing antibiotics (penicillin G sodium 100 U/mL, streptomycin sulfate 100 mg/mL, and amphotericin B 0.25 mg/mL; 3 mL, GIBCO) with 10% FBS was added to each dish and incubated at 37°C in a water-jacked humidified incubator in an atmosphere of 5% CO_2. The medium was replaced twice weekly. After 4 weeks of incubation, cells were released from dishes using 0.1% trypsin (Life technologies Inc., Gaithersburg, MD) and 0.02% ethylenediaminetetraacetic acid (EDTA) (Sigma, St. Louis, MO) in PBS, pH 7.4, and transferred to 75 cm^2 culture flasks (Corning Inc., Corning, NY). Cells were then subcultured 1:6, and fibroblasts from passages 4–7 were used for this study.

2.2.9 *In vitro* bioactivity assay

The bioactivity of stratifin released from the microspheres and hyaluronic acid films containing PLGA microspheres was evaluated by measuring its ability to stimulate expression of MMP-1 in cultured dermal fibroblasts using a procedure described previously (Ghahary et al., 2004). The fibroblasts were seeded onto 6-well plates at a density of 2.5 × 105 cells per well in DMEM with 10% FBS. After cell attachment, fibroblasts were treated for 24 h as described below.

Before preparing the formulations containing stratifin, the biological activity of recombinant stratifin and FITC-conjugated stratifin was determined. In this experiment, fibroblasts were treated with either 2.5 μg/mL recombinant stratifin or an equivalent amount of SFN-FITC. Untreated fibroblasts were considered as negative control. Stability and biological activity of recombinant stratifin in aqueous media at 37°C were

determined, and fibroblasts were treated with either fresh stratifin (day 0) or stratifin incubated in DMEM at 37°C for periods of 7, 14, 21, and 28 days. Untreated fibroblasts were considered as negative control.

To evaluate the biological activity of stratifin following encapsulation in PLGA, 150 mg of microspheres (recombinant stratifin was complexed to chitosan particles and then encapsulated into PLGA microspheres under aseptic conditions) were placed in a microcentrifuge tube containing 1 mL DMEM and incubated in 37°C for 24 h. The supernatant was collected after centrifugation and added to the cultured fibroblasts in 6-well plates. The fibroblasts treated with 2.5 μg/mL stratifin were considered as positive control for MMP-1 expression and the untreated fibroblasts considered as negative control. The cells treated with the media released from empty microspheres served as a control for MMP-1 stimulatory effect of vehicle.

The long-term bioactivity of stratifin released from PLGA microspheres was assessed at 3 and 30 days. 100 mg PLGA microspheres were placed in a microcentrifuge tube containing 1 mL DMEM and kept at 37°C. The tubes were centrifuged and the supernatant was removed after 3 days and kept at −20°C. The microspheres were resuspended in 1 mL fresh DMEM and incubated at 37°C up to 30 days. The fibroblasts were treated with the release medium of 3 and 30 days at the same time.

The stimulatory effect of stratifin released from hyaluronic acid films containing PLGA microspheres after 3 and 30 days was also determined. Hyaluronic acid films containing 100 mg PLGA microspheres were placed on top of Millicell cell culture inserts, and then they were placed into 6-well cell culture plates containing 1 mL DMEM containing 0.1% BSA. The plates were incubated at 37°C and samples were taken at 3 and 30 days. The release medium was removed from the bottom chamber and replaced by the same amount of fresh DMEM. Samples were kept at −20°C and used for treating fibroblasts at the same time. Hyaluronic acid films containing empty PLGA microspheres were considered as a control for MMP-1 expression due to the vehicle. The experiments were performed with three different preparations for each set ($n = 3$).

After harvesting the cells, the level of MMP-1 expression was evaluated by western blot analysis. Western blots were performed by loading 20 μg denatured protein into each lane and run on 10% (w/v) sodium dodecyl sulfate polyacrylamide gel

electrophoresis (SDS-PAGE). The fractionated proteins were transferred onto a polyvinylidene difluoride (PVDF) membrane (Millipore, Billerica, MA). Immunoblotting was performed using monoclonal mouse anti-human MMP-1 antibody (1:250 dilution). The membranes were then incubated with the appropriate secondary horseradish peroxidase conjugated anti-mouse IgG antibody (1:2500 dilution). Immunoreactive proteins were then visualized using the western blotting detection reagent. The protein bands were detected by exposure to X-ray film. The membrane was then stripped and reprobed with ß-actin antibody and used as a control for protein loading. Quantitative analysis of autoradiograms was accomplished by measuring density of bands using Scion Image digital image processing software.

2.2.10 *In vitro* cytotoxicity assay

The cytotoxicity of stratifin released from hyaluronic acid films containing PLGA microspheres was quantitatively assessed by 3-(4,5-dimethyl-2-thiazolyl)-2,5-diphenyl-2H-tetrazolium bromide (MTT) assay, which measures the metabolic reduction of 3-(4,5-dimethylthiazol-2-yl)-2,5, diphenyl tetrazolium bromide to a colored formazan by viable cells. MTT was prepared by dissolving in sterile PBS, pH 7.4, at a concentration of 5 mg/mL, and then filtering through a 0.22 μm filter. Fibroblasts were cultured in 12-well cell culture plates at a concentration of 1×10^5 cells per well in DMEM supplemented with 10% FBS and were incubated at 37°C, 5% CO_2 atmosphere for 24 h. After 24 h, the culture medium was removed from the wells and 1 mL of the experimental materials was added to each well. Toxicity was assessed on stratifin released from hyaluronic acid films containing PLGA microspheres in DMEM at 3 and 30 days. Hyaluronic acid films containing 100 mg PLGA microspheres were placed on top of Millicell cell culture inserts, and then they were placed into 6-well cell culture plates containing 1 mL DMEM containing 0.1% BSA. The plates were kept in an incubator at 37°C, and samples were taken at 3 and 30 days. The release medium was removed from the bottom chamber and replaced by the same amount of fresh DMEM. Samples were kept at −20°C until used to assess for cytotoxicity. In control (untreated) wells, 1 mL of DMEM was added. Cells incubated with the release media of hyaluronic acid films containing 100 mg empty microspheres served as a control for the vehicle, and cells incubated with 2.5 μg/mL stratifin served as a control for toxicity of soluble stratifin. Plates were kept for 24 h at

37°C in 5% CO_2 atmosphere. After 24 h, the treatment media was replaced with 500 μL of MTT solution. Plates were wrapped with aluminum foil and incubated at 37°C for 5 h. After removing the reagent solution and rinsing with PBS, 1 mL of dimethyl sulfoxide (DMSO) (Sigma, MO) was added to each well, and plates were shaken for 20 min to dissolve crystals of formazan. The absorbance of the resulting solution in each well was recorded immediately at 570 nm using an ultra microplate reader (ELX 808, Bio-Tek Instruments, Winooski, VT). MTT assays were performed in triplicate.

2.2.11 Statistical analysis

All data are given as mean ± standard deviation for $n = 4$ (release studies) and $n = 3$ (biological activity and cytotoxicity studies) and compared with a Student's t test or Kruskal-Wallis test (nonparametric ANOVA).

2.3 Results

2.3.1 FITC-conjugated stratifin

Stratifin was conjugated with FITC, a fluorescent label for quantification purposes. The excess fluorescent dye was removed using dextran desalting columns. The SDS-PAGE results showed that FITC-conjugated stratifin (SFN-FITC) had an apparent molecular weight of 30 kDa, similar to that of unconjugated stratifin (data not shown).

2.3.2 Morphology and particle size of microspheres

Scanning electron microscopy of microspheres shows that empty PLGA microspheres (Fig. 2.3 a, b) are smooth and spherical, whereas PLGA microspheres encapsulating either chitosan alone or stratifin-complexed chitosan particles are dimpled (Fig. 2.3 c–f).

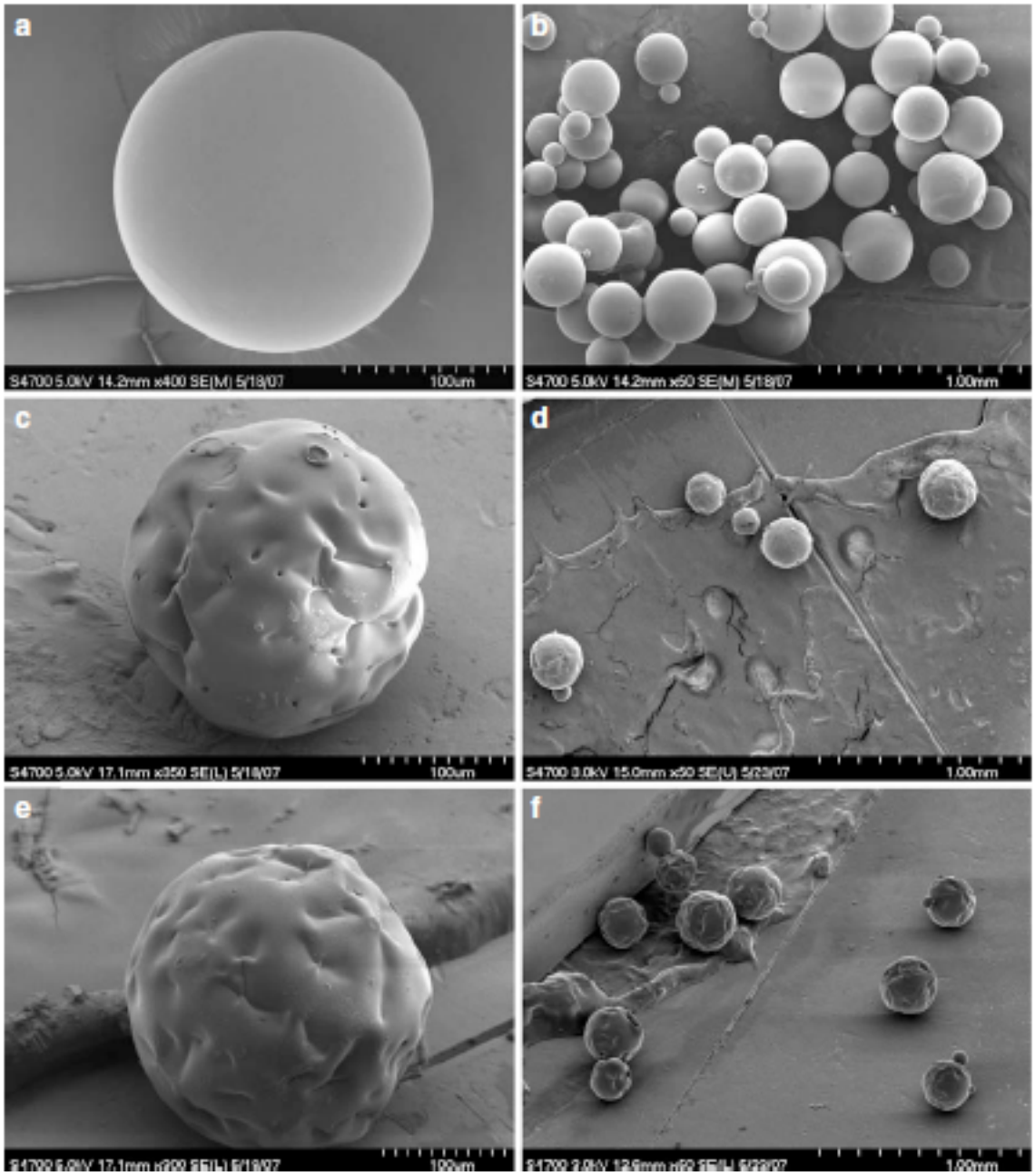

Fig. 2.3. Scanning electron microscopic images of PLGA microspheres. Empty PLGA microspheres are spherical (**a** and **b**) whereas PLGA microspheres encapsulating chitosan particles (**c** and **d**) or stratifin: chitosan complexed particles (**e** and **f**) are dimpled.

The average size of PLGA microspheres encapsulating chitosan particles was 317 ± 20 μm in diameter measured by optical microscopy.

Fluorescence microscopic images of SFN-FITC complexed chitosan particles and PLGA and PLGA/diblock microspheres showed that chitosan particles were encapsulated in both PLGA and PLGA/diblock microspheres (Fig. 2.4 a–c, upper line). After a 30 day incubation in PBS, pH 7.4, the presence of SFN-FITC is still visible in PLGA microspheres (Fig. 2.4 c, bottom), whereas it is barely visible in PLGA/diblock microspheres (Fig. 2.4 b, bottom) and absent in unencapsulated chitosan particles (Fig. 2.4 a, bottom).

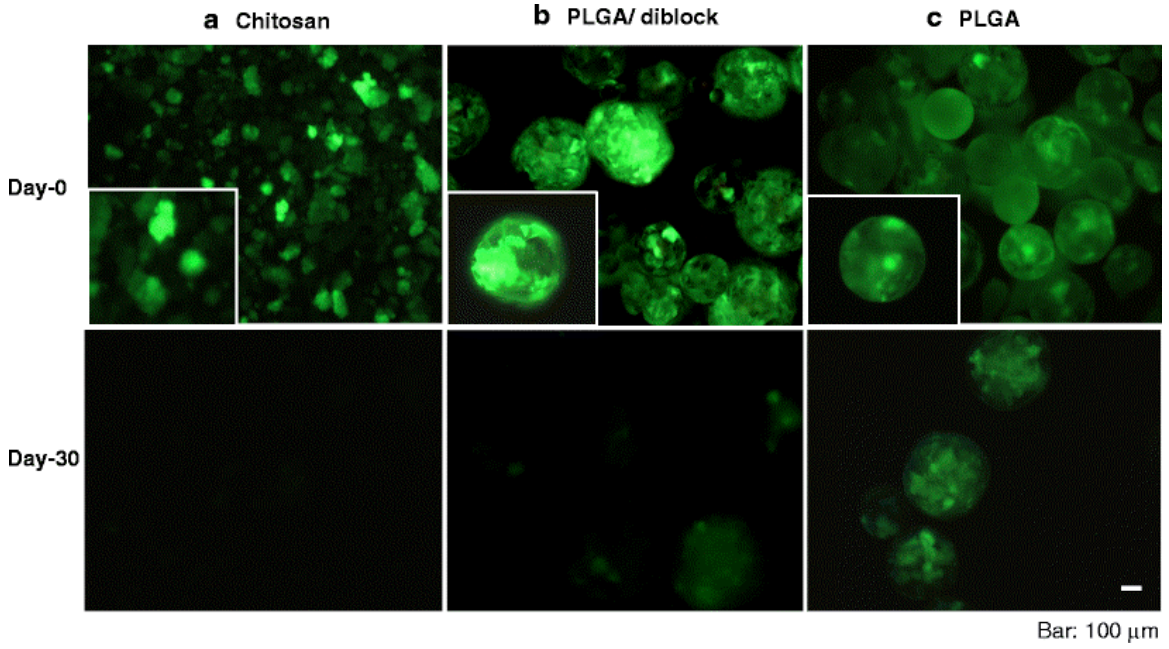

Fig. 2.4. Fluorescence microscopic images of SFN-FITC complexed chitosan particles alone (**a**) or loaded in PLGA/diblock (**b**) and PLGA microspheres (**c**). At day 0, images are shown as the upper line. After 30 days incubation in PBS, SFN-FITC is noticeably visible in PLGA microspheres (right bottom), whereas it is barely visible for PLGA/diblock microspheres (middle bottom) and absent for unencapsulated chitosan particles (left bottom). Scale bar: 100 μm.

2.3.3 Stratifin binding efficiency of chitosan particles and encapsulation efficiency of PLGA microspheres

Chitosan particles (1 mg) loaded with different amounts of SFN-FITC (0.5–3 μg) were tested for binding efficiency and release kinetics (data not shown). The average binding efficiency of stratifin with chitosan particles was calculated by measuring the free unbound SFN-FITC remaining dissolved at aqueous medium, pH 5.5. Under this condition, the maximum binding efficiency was seen for the complex with the ratio of stratifin:chitosan of 1 μg:1 mg, which was 74 ± 3%. This value was in good agreement with the result obtained by releasing the total bound SFN-FITC at pH 11, which was 72 ± 3%. When the release of SFN-FITC from chitosan was evaluated, the complex with the ratio of stratifin:chitosan of 1 μg:1 mg showed a suitable release profile (low burst release first and steady protein release after). At this ratio and at pH 5.5 stratifin and chitosan particles interacted with a charge ratio of approximately 1:10.

When chitosan particles were encapsulated in PLGA microspheres, the encapsulation efficiency was 78 ± 2.5%, determined by measuring the free SFN-FITC left in the suspending medium following encapsulation.

2.3.4 *In vitro* release of stratifin

The *in vitro* release of stratifin from different formulations was obtained over a period of 30 days using SFN-FITC. When SFN-FITC was directly encapsulated in PLGA microspheres, the encapsulation efficiency was lower than 50% (in agreement with previous publications demonstrating low encapsulation efficiency for proteins in polymeric microspheres) (Li et al., 2006; Zheng et al., 2004).

In Fig. 2.5 the SFN-FITC release from chitosan particles is compared with the release from PLGA and PLGA/diblock microspheres. There was a high initial burst release of stratifin from chitosan particles in the first day followed by a steady phase up to 30 days (Fig. 2.5 a). About 57 ± 4% of total SFN-FITC loaded was released in 1 h; that increased to 73 ± 6% by 24 h.

Encapsulation of chitosan particles into PLGA microspheres reduced this initial burst release to 9 ± 1% in 1 h and 18 ± 3% in 24 h. PLGA microspheres prolonged the release of SFN-FITC, and as a result only 54±6% of total loaded protein was released by

30 days. Adding diblock copolymer to PLGA resulted in almost complete release of SFN-FITC (86 ± 6%) in 30 days.

To further reduce the initial burst release of stratifin from PLGA microspheres, they were embedded in hyaluronic acid films. During the first week, water absorption and swelling were seen in all preparations. The burst release was almost eliminated, and a lag time in the release of stratifin was observed for 24 h (Fig.2.5 b). Following that, the release gradually increased to 5.38 ± 2% in 3 days. After 3 days, a constant release phase was observed with about 60% of total protein released in 30 days.

Figure 2.5 c shows the release profiles of SFN-FITC from hyaluronic acid films loaded with soluble SFN-FITC, SFN-FITC complexed chitosan particles, and PLGA microspheres encapsulating SFN-FITC complexed chitosan particles. Films containing soluble SFN-FITC exhibited a rapid release profile with a high burst release of 41 ± 6% by 24 h. It was followed by almost linear release for 10 days, which resulted in the release of 89 ± 11% of SFN-FITC within 10 days. The release rate of soluble SFN-FITC from hyaluronic acid films was reduced when the protein was complexed to chitosan particles and reduced even further when chitosan particles were encapsulated in PLGA microspheres (Fig. 2.5 c). Figure 2.5 d shows that hyaluronic acid films significantly reduced the initial burst release of SFN-FITC from chitosan particles, and as a result a lag time of 1 h in the release of protein was observed followed by only 8 ± 2% release by 24 h.

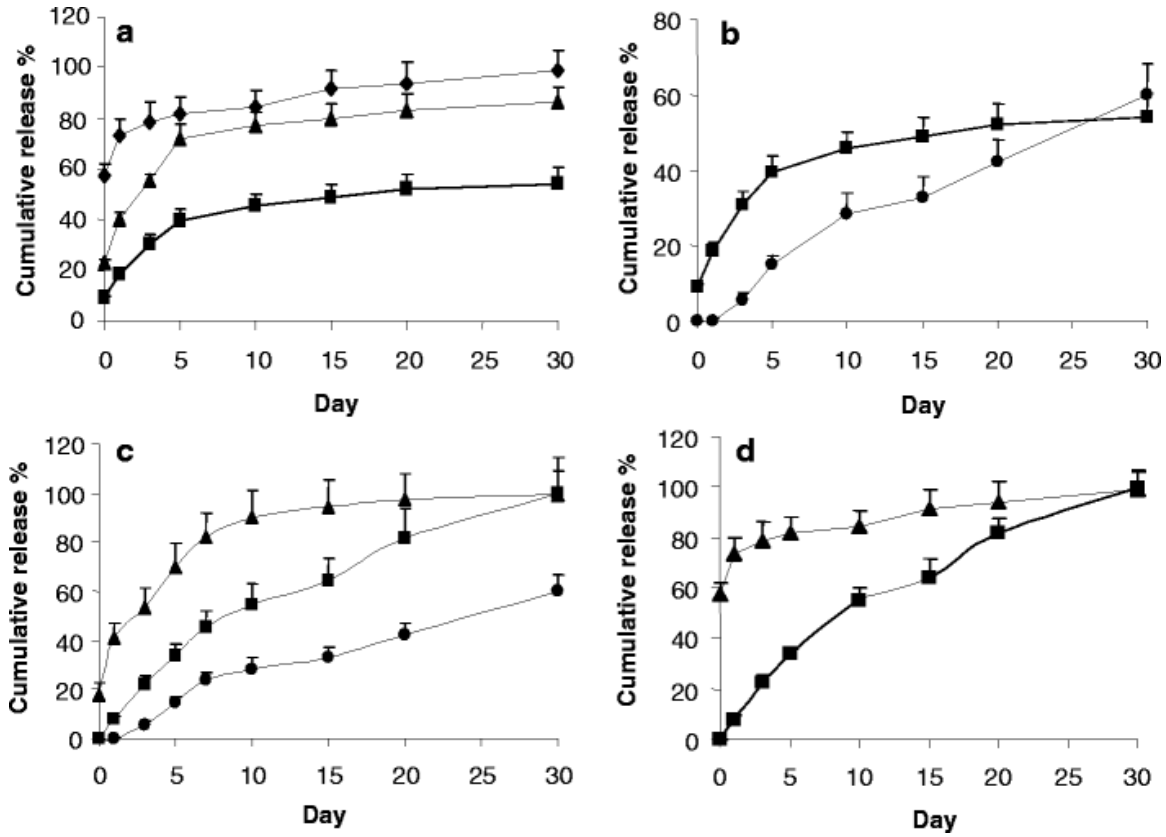

Fig. 2.5. *In vitro* release profiles of SFN-FITC from either SFN-FITC:chitosan particles, PLGA or PLGA/diblock microspheres containing SFN-FITC:chitosan particles or different formulations of hyaluronic acid films loaded with particles and microspheres. (**a**) SFN-FITC release from either chitosan particles (—◆—), PLGA microspheres containing chitosan particles (—■—) or PLGA/diblock microspheres containing chitosan particles (—▲—). (**b**) SFN-FITC release from either PLGA microspheres containing chitosan particles loaded in hyaluronic acid films (—●—) or PLGA microspheres (no film) containing chitosan particles (—■—). (**c**) SFN-FITC release kinetic from either hyaluronic acid films loaded with soluble SFN-FITC (—▲—), SFN-FITC:chitosan particles (—■—) or PLGA microspheres containing chitosan particles (—◆—). (**d**) SFN-FITC release from either SFN-FITC: chitosan particles (—▲—) or SFN-FITC: chitosan particles blended into hyaluronic acid films. (—■—). Error bars represent the mean ± SD for n=4.

2.3.5 *In vitro* bioactivity of stratifin

To demonstrate the in vitro bioactivity of stratifin, the level of MMP-1 expression was evaluated in dermal fibroblasts using western blot analysis. As expected, the level of MMP-1 expression in fibroblasts treated with recombinant stratifin was elevated. However, this effect was less pronounced for FITC conjugated stratifin (Fig. 2.6 a, MMP-1). To determine the total protein loadings, the same blot was probed with ß-actin antibody and similar loadings were found (Fig. 2.6 a, ß-actin). When the corresponding autoradiograms were quantified by densitometry, the level of MMP-1 expression in cells treated with recombinant stratifin was found to be significantly higher than control (837 ± 27%, $p < 0.05$, $n = 3$) (Fig. 2.6 b). In subsequent experiments addressing the biological activity of stratifin, unconjugated stratifin was used.

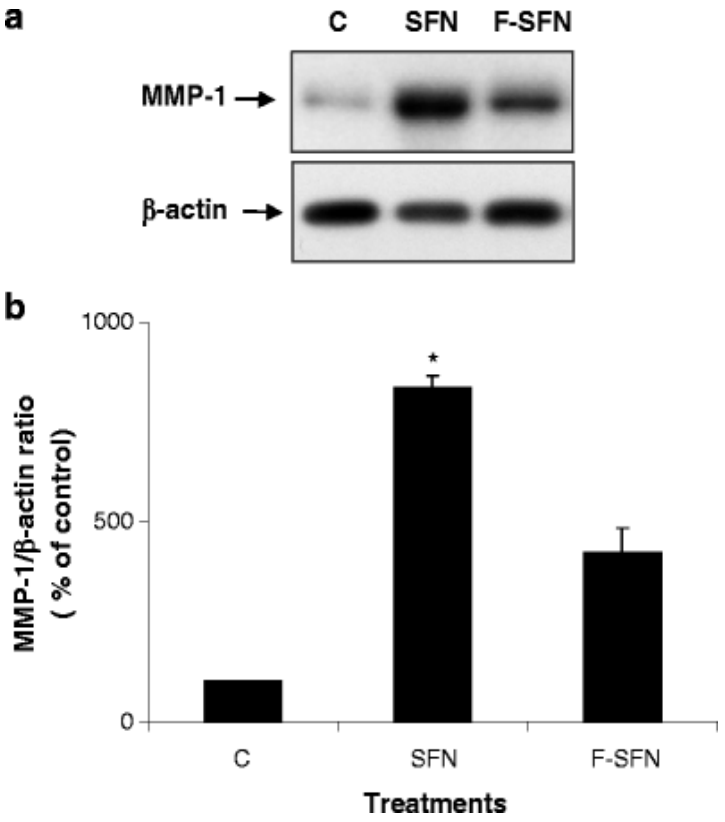

Fig. 2.6. Bioactivity of recombinant and FITC conjugated stratifin. (**a**) Western blot analysis of MMP-1 expression in fibroblasts treated with either recombinant stratifin (SFN) or FITC conjugated stratifin (F-SFN). Untreated fibroblasts were used as negative control (C), and protein loadings were compared using ß-actin bands. (**b)** Semi-quantitative level of MMP-1 expression for each treatment group was analyzed by densitometry of the corresponding bands and represented as the ratio of MMP-1 expression to ß-actin. Error bars represent the mean ± SD for *n*=3.

To address the stability and biological activity of stratifin in aqueous media, the protein was incubated in DMEM at 37°C up to 28 days. Figure 2.7 shows that the stimulatory effect of stratifin on the expression of MMP-1 was not compromised up to 28 days of incubation in aqueous media at 37°C (Fig. 2.7 a, MMP-1). ß-actin bands show the similar protein loadings (Fig. 2.7 a, ß-actin). The results of densitometry show that the relative levels of MMP-1 expression to ß-actin for the treatments of 7, 14, 21, and 28 days were equivalent to the fresh stratifin ($p > 0.05$, $n = 3$) (Fig. 2.7 b). These data confirm that stratifin was stable and biologically active in aqueous media at 37°C for at least 28 days.

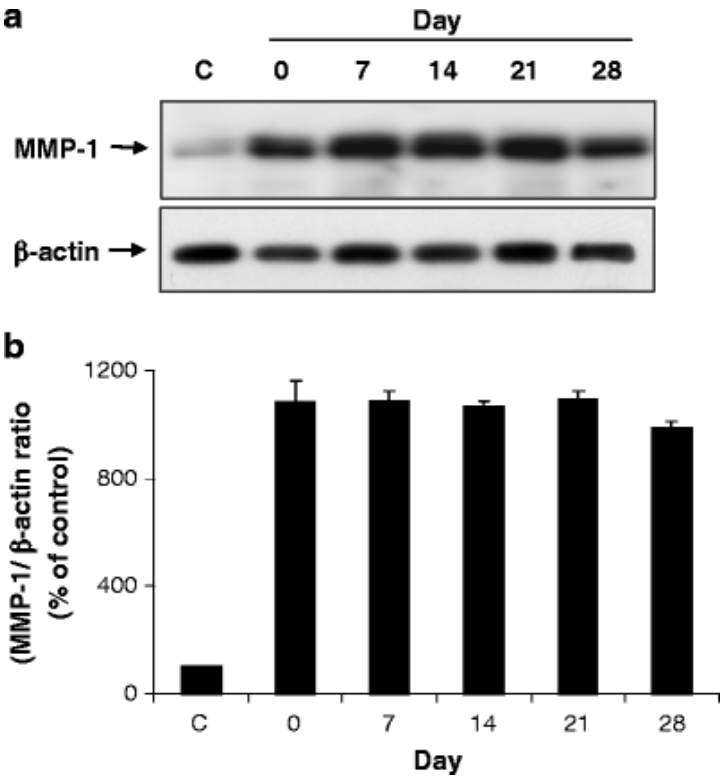

Fig. 2.7. Stability and biological activity of stratifin in aqueous media at 37°C. **(a)** Western blot analysis of MMP-1 expression in fibroblasts treated with either fresh stratifin (day 0) or stratifin incubated at 37°C for 7, 14, 21, and 28 days. Protein loadings were compared using ß-actin bands. **(b):** Semi-quantitative level of MMP-1 expression for each treatment group was analyzed by densitometry of the corresponding bands and represented as the ratio of MMP-1 expression to ß-actin. Error bars represent the mean ± SD for n=3.

The bioactivity of stratifin following encapsulation was evaluated by measuring the MMP-1 expression stimulatory effect of stratifin released from PLGA microspheres in 24 h; it was then compared with the bioactivity of the equivalent amount of naked stratifin. The naked stratifin encapsulated in PLGA microspheres did not show any MMP-1 stimulatory effect (data not shown). Therefore, to increase the stability of stratifin during the microencapsulation procedure in this study, it was complexed to chitosan particles and then encapsulated in PLGA microspheres. It was observed that the stratifin released from PLGA microspheres (first stratifin was complexed to chitosan particles and then encapsulated into PLGA microspheres) significantly increased the level of MMP-1 expression in fibroblasts (Fig. 2.8 a, MMP-1). This stimulatory effect was comparable to the effect of an equivalent amount of naked stratifin. The empty PLGA microspheres (containing unloaded chitosan particles) were tested to evaluate the stimulatory effect of polymeric vehicles on expression of MMP-1. The media released from empty microspheres did not show any stimulatory effect. Related ß-actin bands ensure the similar protein loadings (Fig. 2.8 a, ß-actin). The densitometry results indicated the equivalent ratio of MMP-1/ß-actin for fibroblasts treated with stratifin released from PLGA microspheres and fibroblasts treated with the naked stratifin (1398 ± 88% vs. 1240 ± 46%, $p > 0.05$, $n = 3$) (Fig. 2.8 b). These data indicate that neither complexing stratifin with chitosan particles nor the process of microencapsulating in PLGA reduce the biological activity and stimulatory effect of stratifin on expression of MMP-1 in cultured fibroblasts.

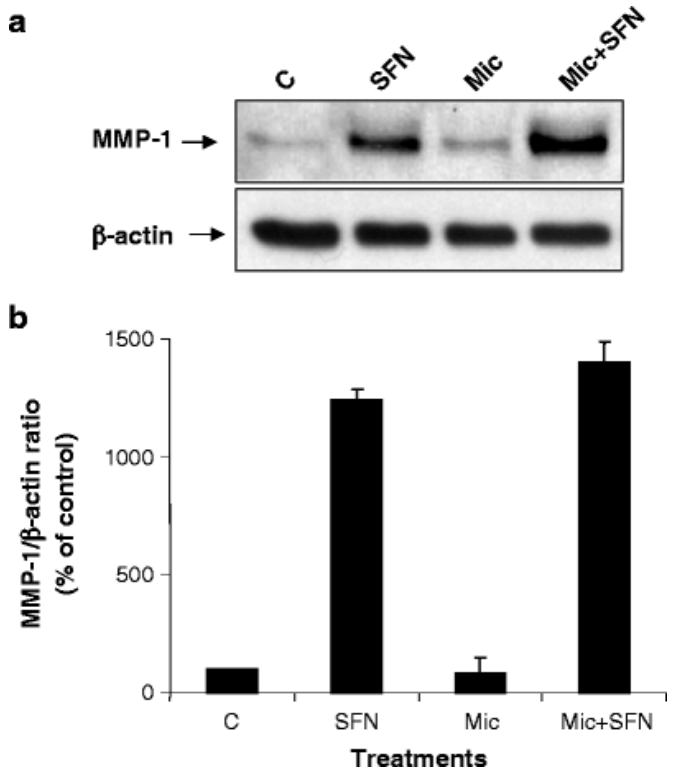

Fig. 2.8. Bioactivity of stratifin following encapsulation in PLGA microspheres containing chitosan particles**. (a)** MMP-1 expression in fibroblasts treated with stratifin released from PLGA microspheres containing stratifin complexed chitosan particles by 24 h (SFN+Mic), equivalent amount of naked stratifin (SFN) and PLGA microspheres containing unbound chitosan particles (Mic). Protein loadings were compared using ß-actin bands. **(b)** Semi-quantitative level of MMP-1 expression for each treatment group was analyzed by densitometry of the corresponding bands and represented as the ratio of MMP-1 expression to ß-actin. Error bars represent the mean ± SD for *n*=3.

The biological activity of stratifin released from PLGA microspheres and hyaluronic acid films containing PLGA microspheres was evaluated at 3 and 30 days (Fig. 2.9). As expected, the level of MMP-1 expression in fibroblasts treated with 3 day stratifin released from hyaluronic acid films containing PLGA microspheres was very low, whereas it was highly pronounced in fibroblasts treated with 3 day stratifin released from PLGA microspheres alone (Fig. 2.9 a, MMP-1). ß-actin bands ensure the similar protein loadings (Fig. 2.9 a, ß-actin). Measuring the density of the related bands and calculating the relative level of MMP-1 expression to ß-actin established that this difference was significant (74 ± 11% vs. 1265 ± 44%, $p < 0.05$, $n = 3$) (Fig. 2.9 b). These data agree with the result of the *in vitro* release of SFN-FITC, which revealed a reduced burst release of stratifin upon incorporating the PLGA microspheres in hyaluronic acid films.

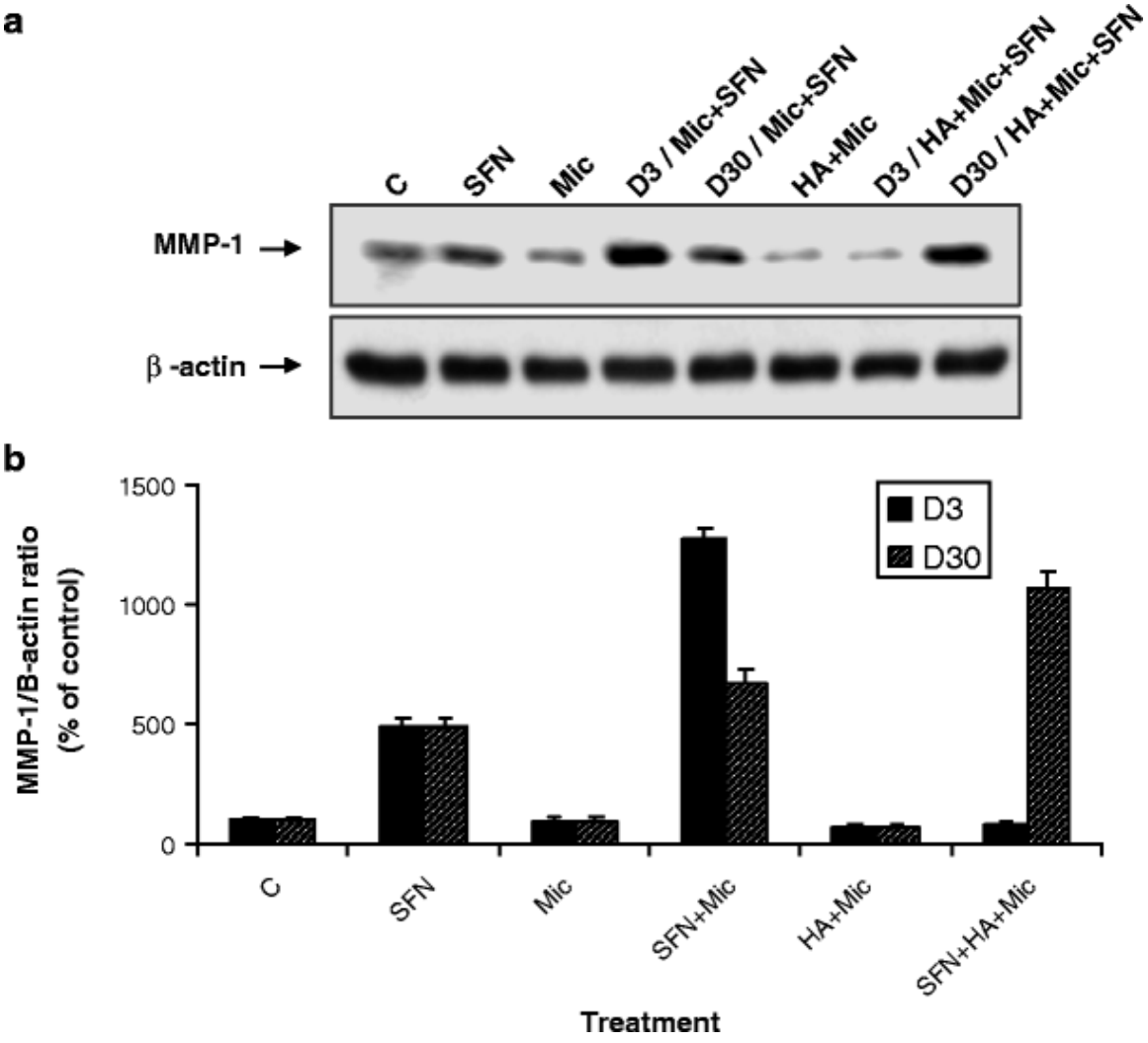

Fig. 2.9. Long-term bioactivity and burst phase of stratifin released from chitosan particles encapsulated in PLGA microspheres alone or loaded in hyaluronic acid films. *Panel a*: MMP-1expression in fibroblasts treated with stratifin released at 3 and 30 days from PLGA microspheres containing stratifin complexed chitosan particles (D3/Mic+SFN and D30/Mic+SFN) and hyaluronic acid films loaded with PLGA microspheres containing stratifin complexed chitosan particles (D3/HA+Mic+SFN, D30/HA+Mic+SFN). MMP-1 expression in fibroblasts treated with the media released from PLGA microspheres alone or in films, containing control (no protein) chitosan particles at 30 days served as control for polymeric vehicles. Protein loadings were compared using ß-actin bands. *Panel b*: Semi-quantitative level of MMP-1 expression analyzed by densitometry of the corresponding bands. The relative level of MMP-1 expression to ß-actin quantified by densitometry of the corresponding bands. *Error bars* represent the mean ± SD for $n = 3$.

The stratifin released from 3 to 30 days from both preparations showed a high stimulatory effect on expression of MMP-1 (Fig. 2.9, panel a, MMP-1). The relative level of MMP-1 expression to ß-actin for these treatments was greater for stratifin released from hyaluronic acid films containing PLGA microspheres than stratifin released from PLGA microspheres (1063 ± 74% vs. 667 ± 60%, $p < 0.05$, $n = 3$) (Fig. 2.9 b). The

incubation media obtained from both mentioned vehicles from 3 to 30 days did not show any stimulatory effect on expression of MMP-1 in fibroblasts. In contrast, controlled release of stratifin from PLGA microspheres was biologically active and had the ability to elevate expression ofMMP-1 in cultured fibroblasts for at least 30 days. Incorporation of these microspheres into hyaluronic acid films reduced the burst release of stratifin and caused a lag phase to occur.

2.3.6 *In vitro* cytotoxicity

The cytotoxicity of release media from hyaluronic acid films containing stratifin-loaded or empty PLGA microspheres was tested on human dermal fibroblasts using MTT assay. The number of viable cells was assessed after 24 h incubation with the release media. Statistical analysis showed no significant reduction in viable cells following incubation for samples from either day 3 or day 30 (Fig. 2.10) ($p > 0.05$, $n = 3$).

2.4 Discussion

Collagen deposition is an essential component of normal wound healing, but if unregulated or excessively prolonged it may contribute to the development of fibroproliferative disorders (Tredget et al., 1997). Such problems might be preventable by prolonged expression and release of matrix metalloproteinases to degrade the excessive mass of collagen at the late stage of healing process. It was previously found that keratinocyte releasable stratifin markedly stimulates the expression of matrix metalloproteinase-1 (MMP-1) in dermal fibroblasts, suggesting that this protein might be useful in the treatment of collagen-associated healing disorders (Ghahary et al., 2004). However, efficacy might depend on the presence of therapeutic concentrations of stratifin at later stages of wound healing and the absence of this protein during the early healing process. The objective of this study was to formulate a controlled release formulation for stratifin, with minimum burst release (and ideally an initial lag phase) followed by a sustained release to improve and/or prevent formation of keloid and hypertrophic scarring frequently seen in post-surgical procedures. This study successfully complexed stratifin to chitosan particles; these were encapsulated in PLGA microspheres and finally blended in hyaluronic acid films. The release of bioactive stratifin was negligible for up to 3 days; this was followed by controlled release.

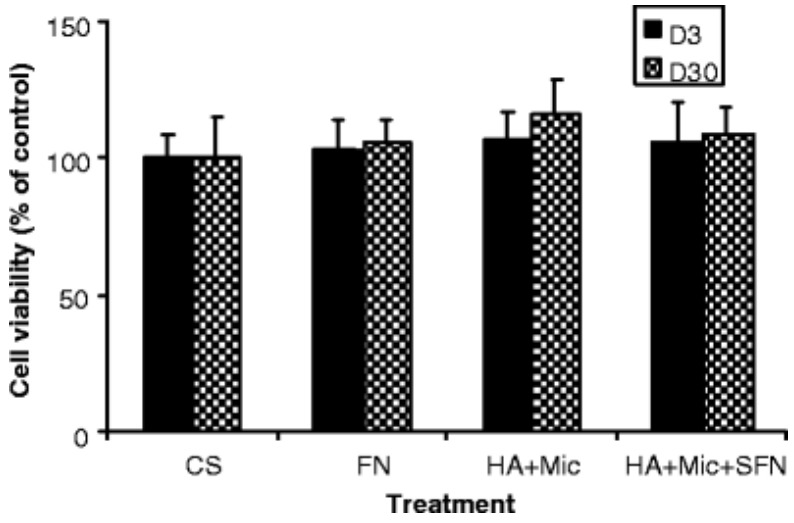

Fig. 2.10. Effect of stratifin and polymeric vehicles on cell viability. The fibroblasts were either untreated or treated with 2.5 μg stratifin (SFN), release media from hyaluronic acid films containing empty PLGA microspheres (HA+Mic) at 3 and 30 days, or hyaluronic acid films containing stratifin-complexed chitosan particles (SFN+HA+Mic) at 3 and 30 days. The result is represented as a percentage of the untreated group. Error bars represent the mean ± SD for *n*=3.

The use of polymeric microspheres for sustaining the release of bioactive proteins has been previously described (Li et al., 2006; Zheng et al., 2004); typically it produced a burst release of protein. For example, gelatin nanoparticles containing bFGF loaded in PLGA microspheres produced 30% release of bFGF in the first 24 h (Li et al., 2006). Using a composite of alginate-chitosan in PLGA microspheres, Zheng et al. (2004) reported a reduction in the burst phase of BSA release from 53% to 39%. To further reduce early protein release, some groups have blended protein-loaded microspheres in hydrogel films (DeFail et al., 2006; Huang et al., 2006; Kempen et al., 2008; Lee et al., 2004). Defail et al. (2006) reported the controlled release of TGF-ß1 from PLGA microspheres incorporated into PEG-genipin hydrogels. Within 1 day, the microspheres demonstrated a high burst release of protein (69 ± 29%), while the PEG-genipin scaffold delayed the burst release up to 17 days (72 ± 11%).

In this study, to avoid protein denaturation during the process of encapsulation and to reduce the burst release effect, stratifin was complexed with chitosan particles. These complexes were then encapsulated into PLGA, and the microspheres were blended into crosslinked hyaluronic acid films. SEM images showed that PLGA microspheres were dimpled as a result of encapsulating chitosan particles (Fig. 2.3), and fluorescent

microscopy showed significant amounts of chitosan and protein embedded in the microspheres (Fig. 2.4).

The encapsulation of chitosan particles in PLGA microspheres significantly reduced the burst release of stratifin from 73% to 18% in 24 h. It was shown that PLGA microspheres sustained the release of stratifin from chitosan particles so that 54% of the total loaded protein was released in 30 days. In some experiments an amphipathic diblock copolymer, methoxy poly(ethylene glycol)-block-poly(D,L-lactide) (MePEG-b-PDLLA) was incorporated into the PLGA microspheres at a ratio of 15% diblock to 85% PLGA. Previous studies have shown that this strategy allowed for increased drug release from PLGA microspheres because the diblock copolymer slowly partitions out of the PLGA matrix, allowing for increased microsphere porosity (Jackson et al., 2007). In this study microspheres made of 15% diblock polymer and 85% PLGA released stratifin almost completely in 30 days (Fig. 2.5). Although no significant burst phase of protein release was observed using this method, there was a steady release over the first 10 days without the preferred initial delay of release observed with PLGA-only microspheres.

Fluorescence microscopy of SFN-FITC demonstrated the presence of the protein in chitosan, PLGA and PLGA/diblock microspheres (Fig. 2.4, day 0). After 30 days there was little SFN-FITC in the chitosan or PLGA/diblock microspheres but evidence of residual protein in the PLGA-only microspheres (Fig. 2.4, day 30), in agreement with protein release profiles (Fig. 2.5). These findings demonstrated the success of the chitosan/PLGA encapsulation process in allowing the sustained release of the protein.

Blending PLGA microspheres into hyaluronic acid films significantly reduced the initial burst release of stratifin, so that only 5% of the protein was released in 3 days. As a result, most of the stratifin was released at later time points, thereby achieving the preferred release profile of an initial lag phase followed by controlled release. It was likely that the movement of water through the swollen, cross-linked hyaluronic acid film was restricted, so that the efflux of protein from the microsphere surface and subsequent diffusion processes were reduced.

Both stratifin and the FITC-conjugated stratifin were shown to be effective in stimulating MMP-1 expression in fibroblasts (Fig. 2.6), demonstrating the bioactivity of both forms of protein. Furthermore, following incubation in aqueous media, there was

little change in the bioactivity of the stratifin after 28 days, demonstrating the resistance of this protein to hydrolytic degradation processes (Fig. 2.7). To study the bioactivity of stratifin released from polymeric formulations, the aqueous release media from *in vitro* protein release studies was used as incubation media with fibroblasts; cells treated with the release media of the PLGA microspheres containing stratifin bound chitosan showed equivalent increases in MMP-1 expression to that induced by protein alone (Fig. 2.8). This study showed that the encapsulation and release processes did not degrade the protein and full bioactivity was maintained. More detailed bioactivity studies showed that the protein released from both types of formulations (i.e., chitosan in PLGA microspheres either free or blended in hyaluronic acid films) at day 3 or day 30 of the release study was non-degraded and effective at inducing MMP-1 expression in fibroblasts (Fig. 2.9). Interestingly, for the hyaluronic acid formulation, the *in vitro* protein release study showed a marked delay in protein release at 3 days. This was reflected in the detailed bioactivity study whereby the aqueous media from this study showed a reduced ability to increase MMP-1 expression. This scenario of a reduced expression of MMP-1 at day 3 followed by sustained increases in expression after that time satisfies a preferred therapeutic release profile for use in wound healing settings.

None of the release media from stratifin-bearing formulations had any cytotoxic effect on fibroblasts *in vitro* (Fig. 2.10). The release media from formulations incubated in media for 3 or 30 days was incubated with fibroblasts with no observed change in cell proliferation rates. This study suggests that any observed increases in MMP-1 expression caused by stratifin were not the result of cell stress induced by polymeric or protein materials.

Overall, these studies support the use of a hyaluronic-based microparticulate wound dressing for the prevention of abnormal wound healing processes. The compatibility of hydrocolloid dressings is well established, and materials such as carboxymethylcellulose (CMC), gelatin, and hyaluronic acid are commonly used as wound dressings. Commercially available hydrocolloid dressings include Granuflex™ and Aquacel™ (Conva Tec, Hounslow, UK), Comfeel™ (Coloplast, Peterborough, UK), and Tegasorb™ (3 M Healthcare, Loughborough, UK). They are manufactured in the form of thin films and sheets, and they have been used to topically administer some of the

growth factors to wound sites. These include hydrogel dressings for delivering transforming growth factor-β1 (TGF-β1) (Puolakkainen et al., 1995) collagen film for delivering PDGF (Koempel et al., 1998) and human growth hormone, alginate dressings (Maeda et al., 2001) in the form of beads used to deliver endothelial growth factor (Gu et al., 2004), and polyurethane and collagen film dressings for delivery of EGF (Grzybowski et al., 1999). Although all these previous studies support the application of thin sheets of hydrocolloid dressings to wound sites, none of these formulations have been developed for the delivery of an antifibrogenic agent that might require delayed drug release properties. Drug release from hydrogel wound dressings is mostly controlled by physical processes. For example, hydration resulting from wound exudate permits diffusion of the drug through the swollen gel and eventual erosion of polymer (Siepmann and Peppas, 2000). Therefore, factors such as rapid erosion of the polymer matrix following water diffusion and swelling are known to be the main reasons for immediate release of factors from these wound dressings. However, the microspheres in hyaluronic acid film formulation described in this study is the first report of a delayed and controlled release system prepared from biocompatible materials suitable for application to a wound site.

These *in vitro* studies established that a lag phase followed by a controlled release phase of bioactive stratifin had been successfully produced.

2.5 Conclusions

Hyaluronic acid embedded PLGA microspheres were developed to delay and then control the release of an antifibrogenic factor, stratifin. In these studies, stratifin bioactivity was preserved during the encapsulation process, and the release of the protein was successfully delayed for 3 days after which it was slowly released over 30 days. The stratifin released during these *in vitro* studies increased the level of MMP-1 expression in cultured fibroblasts at later time points without causing any cytotoxicity.

Chapter 3. Controlled Release of Stratifin from Composite Wound Implants Reduces Post-surgical Scarring[2]

3.1 Introduction

Surgical scarring is a major clinical problem that can be devastating and costly to both patients and health care providers (Chen and Davidson, 2005; Niessen et al., 1999; Singer and Clark, 1999). Aside from improved surgical techniques (Atkinson et al., 2005), the only primary treatment for scarring is the application of self-adhesive silicone gel sheets. The mechanism of the apparent effect of silicone sheets on scarring is unknown but may be due to the modulation of the physical wound environment rather than the molecular pathways involved in scarring. Moreover, the silicone needs to be used at least 20 h per day for 6 to 12 months (Clugston et al., 1995; Rhee et al., 2010). The advent of a delivery system containing anti-fibrogenic factors that can be secured in the incision before wound closure and locally release the anti-fibrogenic drug to control the healing process and prevent excessive scar formation would be an ideal strategy for prevention of surgical scars. The advantages of this implanted system would be the need for only a low therapeutic dose, bypassing of the skin barrier and the avoidance of daily medication application.

Stratifin or 14-3-3σ protein is a potent anti-fibrogenic factor that is normally synthesized and released from skin keratinocytes, thereby increasing the expression of collagenases in dermal fibroblasts (Ghahary et al., 2004). Collagen is the primary component of extracellular matrix and is essential for wound repair and tissue regeneration. However, when expressed in excess, it can lead to fibroproliferative disorders such as hypertrophic scarring and keloids. It has been recently demonstrated that the topical application of stratifin could prevent hypertrophic scarring in a rabbit ear fibrotic model (Rahmani-Neishaboor et al., 2010).

---

[2] A version of this chapter is submitted for publication. Rahmani-Neishaboor, E. Hartwell, R. Brown, E. Jackson, J. and A. Ghahary. Controlled Release of Stratifin from Composite Wound Implants Reduces Post-surgical Scarring.

Thus, stratifin is an ideal biologic factor for preventing excessive scarring by regulating the deposition of collagen during the healing process (Aarabi et al., 2007; Ghaffari et al., 2006; Lam et al., 2005; Medina et al., 2007).

Moreover, a composite implant composed of stratifin-associated PLGA microspheres embedded in hyaluronic acid hydrogels was previously developed (Rahmani-Neishaboor et al., 2009). This system exhibited a biphasic release profile that was tailored to the wound healing process, with an initial slow release phase followed by a more rapid release phase over 30 days. Unfortunately, the cost and the high swelling ratio were two major obstacles for the use of hyaluronic acid as the implant substrate. The degree of swelling associated with hyaluronic acid based implants resulted in inappropriate stress on the tissue and difficulty in surgical closure of the wound. In the current study, the composite implants have been modified using polyvinyl alcohol (PVA), a synthetic equivalent of hyaluronic acid with both a low propensity for swelling and a reduced cost. Using a rat surgical-wound model (Wu et al., 2007), it was hypothesized that the PVA:PLGA implant containing stratifin would serve as an effective anti-fibrogenic implant with improved tissue integration.

3.2 Materials and Methods

Ethics approval for this study was obtained from the University of British Columbia Clinical Research Ethics Board. All of the animal work was reviewed and approved by the University of British Columbia Animal Care Committee.

3.2.1 Materials

Chitosan (ULTRASAN®) (MW.226000, degree of deacetylation = 74.2%) (Biosyntech Inc., Canada), PLGA (85/15, IV = 0.61 dL/g) (LACTEL, USA) polyvinyl alcohol (PVA) (98% hydrolyzed, low MW 11000–31000), and PVA (86% hydrolyzed, medium MW 57000–66000) (Alfa Aesar, USA) were used as supplied. Sodium borate was purchased from Sigma (St. Louis, USA).

PGEX-6P-1 expression vector, PreScission protease, and glutathione sepharose-4B beads were obtained from GE Healthcare Bio-Sciences AB (Uppsala, Sweden). Protein expressing bacteria, BL-21(DE3), was purchased from Novagene (Madison, USA). EZ-Label™ FITC protein labeling kit (Pierce Biotechnology Inc., USA) and D-

Salt TM dextran desalting columns (Pierce Biotechnology Inc., USA) were used as received.

3.2.2 Preparation of human recombinant stratifin (14-3-3σ)

Human recombinant stratifin (SFN) protein was prepared as previously described (Ghahary et al., 2004) with slight modification. Briefly, the cDNA of stratifin from human keratinocytes was cloned into a pGEX-6P-1 expression vector (Amersham/ Pharmacia Biotech, USA) and transformed into protein expressing bacteria, BL-21(DE3) (Novagene, USA). After lysing the bacteria, GST-fused stratifin was purified by adding to glutathione sepharose-4B beads and subsequently digested using PreScission protease. Recombinant stratifin protein produced as described has previously been shown to be more than 95% pure (Ghahary et al., 2004).

3.2.3 Conjugation of stratifin with FITC

For detection and quantification purposes, stratifin was conjugated with fluorescein isothiocyanate. Fluorescence probe conjugation of stratifin was done by EZ-Label™ FITC protein labeling kit as described previously (Rahmani-Neishaboor et al., 2009). Analytical quantification of FITC-conjugated stratifin (SFN-FITC) was done using an Infinite™ F500 microplate reader (TECAN Trading AG, USA) set at excitation and emission wavelengths of 485 and 535 nm, respectively.

3.2.4 Preparation of PLGA microspheres containing chitosan particles

PLGA microspheres were prepared using a suspension-evaporation technique as previously reported (Rahmani-Neishaboor et al., 2009). Briefly, for stratifin-loaded microspheres, 5 mg chitosan particles, smaller than 45 μm, were swelled in 30 μL solution of SFN-FITC in phosphate buffer pH 5.5 (SFN-FITC: chitosan, 1 μg:1 mg) with molar ratio of 7.5:1.0. The suspension was vortexed and incubated at room temperature for 1 h to form ionic complexes. In order to remove the free/uncomplexed stratifin from the complex, 500 μL PBS 5.5 was added to the microtubes. The suspension was gently vortexed and centrifuged at 1000 rpm for 3 min. After removal of the supernatant the complexes were dried under nitrogen gas, and the particles were broken up into a fine powder using a mortar and pestle. These particles were passed through a sieve with a 45 μm pore size, and only particles smaller than 45 μm diameter were encapsulated in

PLGA using the suspension-solvent evaporation technique described below. Chitosan was chosen as a solid carrier to stabilize stratifin during the microencapsulation procedure in PLGA. Stratifin bound chitosan particles were dispersed in a 12.5% solution of PLGA in dichloromethane (chitosan:PLGA, 1:12.5 (w/w)). The mixture was vortexed for 30 s. It was slowly pipetted into 100 mL aqueous solution of PVA 1% (w/v) and stirred at 400 rpm. After 2 h the microspheres were separated by gravity, washed 3 times with distilled water, and dried under nitrogen gas for 1 h. The average size of stratifin-containing microspheres was 130 μm, and the overall encapsulation efficiency was 70% using the method previously described (Rahmani-Neishaboor et al., 2009)

3.2.5 Preparation of PVA composites

PVA (50:50 w/w, 98%:86% hydrolyzed) was dissolved in deionized water by heating to 80°C to obtain a 10% (w/w) solution under aseptic conditions. Glycerol (2% w/v) was added as a plasticizer after PVA dissolution. Composites were fabricated by casting the dispersion inside 2 × 1 cm slide chambers. 1.2 mL of the 10% PVA solution was pipetted into slide chambers and incubated at 37 °C for 1.5 h. Following incubation, 100 mg of microspheres containing either empty or stratifin-loaded microspheres were dispersed in the PVA solution. Borate solutions (4 mM) were prepared by dissolving sodium tetrahydroborate in deionized water and then gently added to the PVA solution in chambers without shaking. They were then incubated at –20°C for 20 h to freeze them. Samples were thawed at room temperature, and the excess borate buffer was decanted. Crosslinked PVA films were dried at 37°C overnight.

3.2.6 Stratifin *in vitro* release studies

The *in vitro* release of stratifin was obtained from PLGA microspheres, PVA hydrogels, chitosan particles embedded in PVA hydrogels, and PLGA microspheres embedded in PVA hydrogels. Under these experimental conditions, stratifin was released within the sink condition determined. SFN-FITC was used to prepare formulations and was analyzed by spectrofluorometry. 150 mg of PLGA microspheres were weighed and put into a microcentrifuge tube containing 1 mL of PBS, pH 7.4, and kept in an incubator at 37°C. Samples were taken at 1 h and 1, 2, 3, 5, 10, 15, 20, 30, 40, 50, and 60 days. At each sampling time, the release medium was collected after centrifugation and replaced

by the same amount of fresh buffer. The samples were analyzed with an Infinite F500 fluorescence plate reader at excitation wavelength of 485 nm and emission wavelength of 535 nm. PVA films containing either 10 μg SFN-FITC or 10 mg of unencapsulated chitosan particles or 100 mg of PLGA microspheres were assessed for *in vitro* release studies. These films were put on top of the Millicell cell culture inserts (PTFE, 0.4 μm) (Millipore, USA) and were then placed into 6-well cell culture plates containing 1.5 mL PBS, pH 7.4, containing 0.1% BSA. The release media contained 0.1% BSA as a carrier to reduce protein adsorption to the surface of the plates. In fact, 0.1% BSA did not interfere with fluorescence measurement of FITC under these conditions. The plates were kept in an incubator at 37°C, and samples were taken at 1 h and 1, 2, 3, 5, 10, 15, 20, 30, 40, 50, and 60 days. At each sampling time, the release medium was removed from the bottom chamber and replaced by the same amount of fresh buffer. The samples were analyzed using an Infinite F500 fluorescence plate reader, and percent cumulative release was determined for each time point. The experiments were repeated three times using n = 4 samples.

3.2.7 Rat surgical wound model

Ethics approval for this study was obtained from the University of British Columbia Clinical Research Ethics Board. All of the animal work was reviewed and approved by the University of British Columbia Animal Care Committee. Ten male Sprague-Dawley (SD) rats, age 5 weeks and weighing 200-250 g, were kept under standard conditions at the University of British Columbia Animal Care Center. Anesthesia was induced and maintained using isoflurane inhalation. Four full-thickness 1 cm long incisions were made on the back of each rat. Wounds were divided into three groups: untreated incisions, incisions inserted with stratifin-free implants, and incisions inserted with stratifin-eluting implants. All wounds were closed using Vetbond® (3M, USA) adhesive glue. Wounds were observed daily for signs of bleeding and infection. Tissue response (pharmacodynamics) was determined through serial sacrifice to investigate early (week 1) and chronic (week 3) healing process, inflammation, and fibrotic deposition. Tissues were harvested using a 12 mm circular biopsy punch (Acuderm Inc., USA). Samples were cut at the middle. One half of each wound was fixed in 10% neutral buffered formaldehyde, dehydrated, embedded in paraffin, sectioned at

5 μm thickness, and stained with hematoxylin and eosin (H&E). The other half was stored at -80ºC for RNA extraction.

3.2.8 Quantitative analysis of scar area

A histopathological evaluation of excised tissue samples from the site of implantation was performed. Standard histological protocols were used. H&E staining was used to measure the scar area at 21 days post surgery. Untreated incisions and those containing either stratifin-free or stratifin-eluting implants were compared. All measurements were taken within the confines of the wounded area at 100× magnification from the hematoxylin-eosin-stained tissue sections. The microsphere implant mass was not considered in calculations.

3.2.9 Epidermal thickness index

The epidermal thickness index (ETI) was used to determine the degree of epidermal hypertrophy after surgery. It was based on measurements taken from hematoxylin-eosin-stained tissue sections at 400× magnification. The entire cross-section of scar was measured for epidermal thickness, which corresponded to a total of approximately five fields. The epidermal thickness from five fields of uninjured skin was also measured from both sides of the scar. The ETI was then determined by calculating the ratio of the averaged epidermal height in scar tissue to the averaged epidermal height in normal uninjured skin (Brown et al., 2008; Tandara and Mustoe, 2008). ETI > 1 denotes hypertrophic epidermis formation. The ETI of untreated incisions and those containing either stratifin-free or stratifin-eluting implants were compared.

3.2.10 *In vivo* biologic activity; MMP-1 expression

The level of expression of MMP-1 in tissue was analyzed in order to determine the biologic activity of encapsulated stratifin. MMP-1 expression in tissue samples was examined by extracting RNA from tissue using the RNeasy fibrous tissue mini kit (Qiagen, Canada) according to manufacturer's instructions. RNA concentrations were measured with the NanoDrop spectrophotometer (NanoDrop Technologies, Denmark). Equal concentrations of RNA samples were then reverse transcribed to cDNA by the Thermo Script RT-PCR system (Invitrogen, Canada) following the manufacturer's protocol. The resulting cDNAs were used to perform polymerase chain reactions (PCRs)

for the primers of MMP-1 ([fwd] CAGCTTTATGGGAGCCAGTC and [rev] TGTTCCTCACCCTCCAGAAC, product size: 200 bp). Glyceraldehyde-3-phosphate dehydrogenase (GAPDH) was used as an endogenous control gene in order to normalize PCRs for the RNA loaded to reverse transcription reactions. The sequences of GAPDH primers were ([fwd] GAGCTGAACGGGAAACTCAC and [rev] TGCTGTAGCCAAATTCGTTG, product size: 300 bp).

3.2.11 Collagen density

Collagen deposition was used to quantify the anti-fibrogenic efficacy of controlled release of stratifin from implants. Excised tissue from untreated incisions and incisions inserted with either stratifin-free or stratifin-eluting implants were compared. Paraffin-embedded sections (4 μm) were mounted on glass slides and stained for collagen with Masson's trichrome. For each wound, five randomly chosen fields of dermis were photographed under 100× magnification. Collagen deposition areas were estimated by the Image Pro Plus 4.5 software (Rahmani-Neishaboor et al., 2010). Relative density of collagen in each group was calculated by normalizing to the unwounded skin collagen density.

3.2.12 Total tissue cellularity and infiltrated $CD3^+$ immune cells

Total tissue cellularity and infiltrated $CD3^+$ T cells were counted to characterize and quantify acute (day 7) and chronic (day 21) fibrosis and inflammation, respectively. Excised tissue from untreated incisions and incisions inserted with either stratifin-free or stratifin-eluting implants were analyzed and compared. Briefly, paraffin-embedded sections (5 μm) were deparaffinized and rehydrated through 100%, 95%, and 70% ethanol followed by incubation in double distilled water for 2 min. To retrieve cellular antigens, a microwave oven heating pretreatment was performed in sodium citrate buffer before blocking with 5% albumin in phosphate-buffered saline solution. For antibody staining, sections were incubated with rabbit anti-T cell CD3 peptide (1:50; Abcam, Cambridge, MA) at room temperature for 1 h. The second antibody, Alexa Fluor® 488 goat anti-rabbit IgG (Invitrogen, Burlington, ON), was used in a concentration of 1:1000. The slides were counterstained with 4′,6-diamidino-2-phenylindole (DAPI) for 5 s, and then sections were dehydrated and mounted. For each wound, five randomly chosen

fields of dermis were photographed under 400×magnification (high power field (HPF)) using a digital camera attached to a fluorescence microscope. Photographs were subsequently coded and randomized, and the number of nuclei and $CD3^+$ immune cells were counted using Image Pro Plus 4.5 software. The counts from the corresponded fields were averaged and normalized by cell counts from normal skin, and the ratio was shown.

3.2.13 Statistical analysis

Statistical significance of these results was evaluated using Instat version 3 for Macintosh. Multiple comparisons were assessed using one way analysis of variance (ANOVA) followed by post hoc analysis using Tukey's multiple comparison test. Results were considered significant when probability values were <0.05.

3.3 Results and Discussions

Localized controlled release delivery of anti-fibrogenic factors to regulate the healing process offer a great potential to reduce the propensity of scarring in surgical wounds. In this work the anti-fibrogenic effect of controlled release of stratifin was investigated from a PLGA microsphere/PVA hydrogel composite implant. To avoid activity lost during the encapsulation procedure and to reduce the burst release effect, stratifin was complexed with chitosan and then encapsulated in PLGA (Rahmani-Neishaboor et al., 2009). PLGA is a commonly used biopolymer for drug delivery applications for a wide range of small molecules as well as proteins and peptides (Cleland, 1997; Kim and Park, 2004; Okada, 1997; Weber et al., 2002). PLGA is widely accepted as a biomedical polymer that is used for sutures and other implants (Shive and Anderson, 1997). Nonetheless, one commonly reported problem is the presence of fibrous tissue formation surrounding biodegradable PLGA implants (Kontio et al., 1998).

In this study, the matrix in which the PLGA microspheres are embedded is composed of a PVA hydrogel that is biologically inert and possesses attractive swelling and mechanical properties (Galeska et al., 2005).

3.3.1 *In vitro* release studies

The *in vitro* release profiles of stratifin from PVA hydrogels, chitosan particles embedded in PVA hydrogels, and non-embedded and PVA hydrogel embedded PLGA microspheres are shown in Fig. 3.1A. PVA hydrogels demonstrated a high burst release of 22 ± 3% in 24 h. Complexing stratifin with chitosan particles reduced the burst release of stratifin to 11 ± 2% in 24 h. Encapsulating stratifin complexed chitosan particles into PLGA microspheres followed by embedding in PVA hydrogels reduced the burst release even more, 6 ± 0.3% in 24 h. Burst release is speculated to be due to the immediate discharge of drugs associated with the peripheral surface of microspheres that was not encapsulated into microspheres in the manufacturing process (McGinity and O'Donnell, 1997). This very low burst release of stratifin did not appear to interfere with wound closure and the observed *in vivo* healing process.

To identify and compare controlled release characteristics of stratifin from hydrogel embedded and non-embedded PLGA microspheres, the post-burst data were analyzed using a zero-order kinetics equation, and regression analysis was performed on the fitted curves (Fig. 3.1b). The zero-order plots of stratifin release from either hydrogel embedded or non-embedded PLGA microspheres were approximately linear, as indicated by their high R^2 values of 0.99 for both profiles. Post-burst release stratifin diffused from non-embedded PLGA microspheres at a constant rate of 286 pg/day, whereas hydrogel embedded PLGA microspheres exhibited a higher rate of 663 pg/day. In fact, the higher post-burst release rate of stratifin from hydrogel embedded microspheres demonstrated a more complete release of stratifin (63% in 60 days). Comparatively, non-embedded PLGA microspheres were able to release only 40% of stratifin in 60 days. Although the exact mechanism of release remains unknown, release of stratifin is considered to be at least in part due to diffusion from composite matrix along with simultaneous degradation of the PLGA polymer. This release pattern may be explained by the incorporation of surface-active boric acid in the PVA hydrogel matrix. Boric acid is speculated to facilitate surface degradation of the microspheres as a result of preferential adsorption at the PLGA/PVA interface and consequent local reduction in pH (Galeska et al., 2005). A combination of surface degradation along with the typical core degradation of the

microspheres is hypothesized to produce a higher release rate of stratifin with approximately zero-order kinetics, post-burst release (Patil et al., 2007).

3.3.2 Pharmacodynamics: reduced scar area and epidermal thickness

Topical application of stratifin in a rabbit ear model is known to prevent hypertrophic scar formation (Rahmani-Neishaboor et al., 2010). To investigate the efficacy of localized, controlled release of stratifin to prevent post-surgical scarring, stratifin-eluting implants were inserted in full thickness incisions created on the backs of rats. In order to investigate the effect of stratifin-releasing implants on the local tissue environment, the following controls were also studied: stratifin-free implants and untreated incisions.

Incisions treated with stratifin-free implants demonstrated a significantly larger scar area on day 21 post-surgery compared with the untreated incisions ($n = 5$, $p < 0.001$) (Fig. 3.2 A). However, local controlled release of stratifin significantly reduced the scar area ($n = 5$, $p < 0.001$) (Fig. 3.2 B). The scar area related to the incisions inserted with stratifin-eluting implants had a size similar to untreated incisions. This scar reducing effect of stratifin is explained by reduction in collagen deposition and also tissue cellularity, as shown in Figs. 3.4 and 3.5.

Epidermal thickness was measured for different wounds as described in Section 3.2. The mean epidermal thickness of untreated incisions and incisions inserted with stratifin-free implants was 1.5 and 2 times greater than normal unwounded skin, respectively ($n = 5$, $p < 0.001$) (Fig. 3.2 C, D).

Epidermal thickness significantly decreased in incisions inserted with stratifin-containing implants, and it was even less than ETI of untreated incisions ($n = 5$, $p < 0.001$). ETI for the wounds inserted with stratifin-containing implants was 1, which was equivalent to normal tissue ($n = 5$, $p > 0.001$).

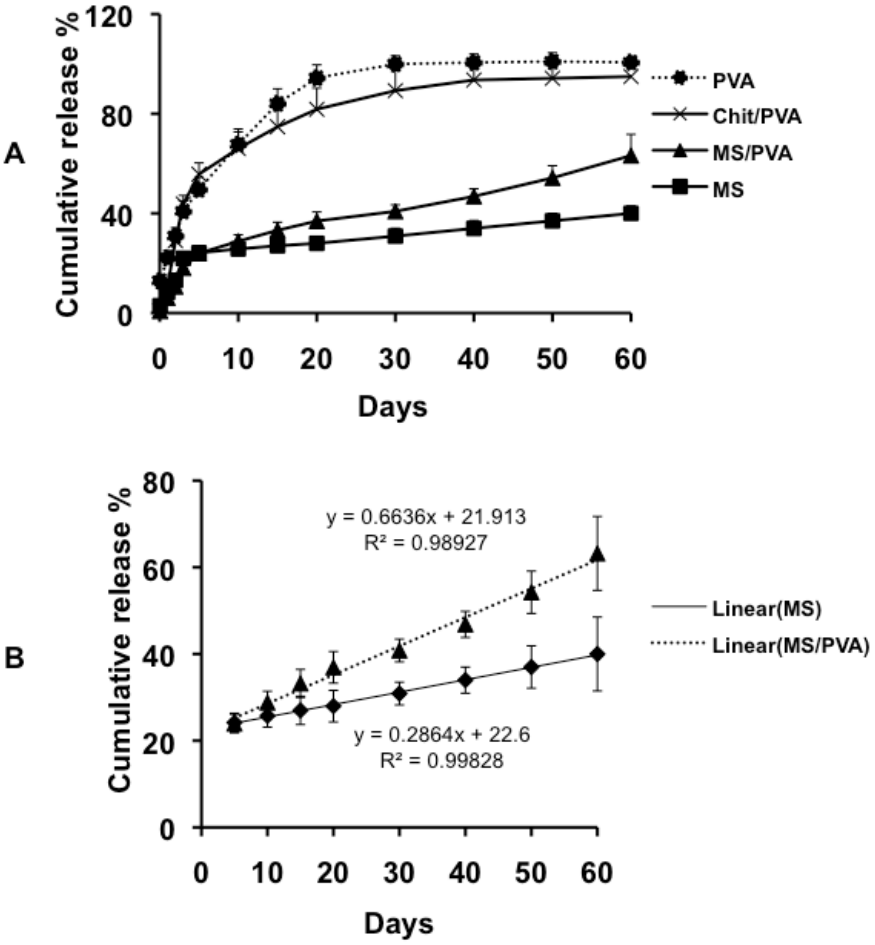

Fig. 3.1. *In vitro* release profiles of SFN-FITC. (A) *In vitro* release profiles of SFN-FITC from PLGA microspheres, PVA hydrogels, chitosan particles embedded in PVA hydrogels, and PLGA microspheres embedded in PVA hydrogels. Cumulative release % was plotted vs. days (mean ± SD, $n = 4$). (B) Post-burst release kinetics of SFN-FITC from non-embedded and PVA hydrogel-embedded PLGA microspheres. Data suggest linear release with approximate zero-order kinetics ($R^2 = 0.99$) for both non-embedded and hydrogel embedded PLGA microspheres.

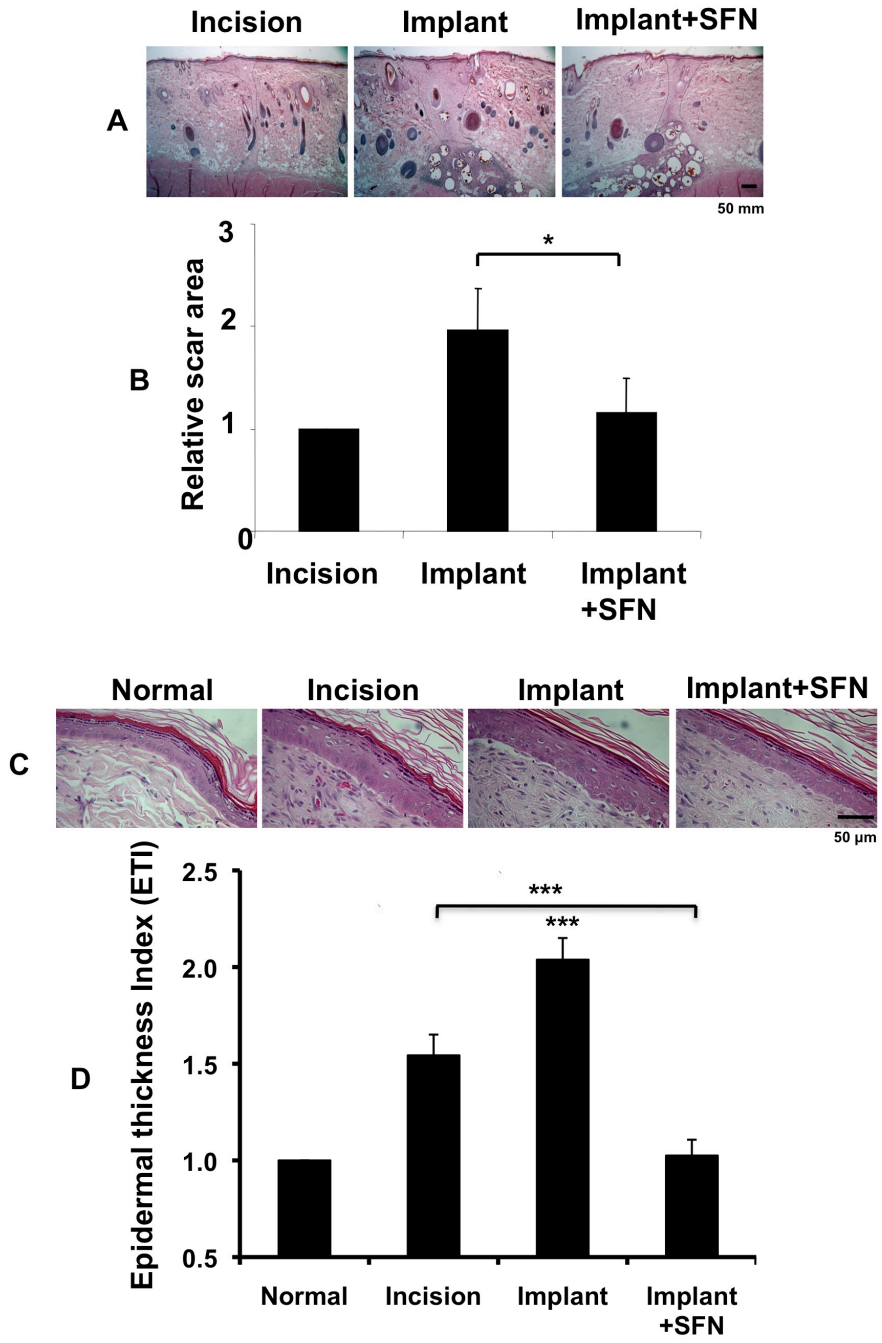

Fig. 3.2. Pharmacodynamic changes in representative tissue sections of rats. (A) Quantitative analysis of scar area in H&E stained tissue samples at day 21. (B) Relative scar area was calculated for untreated incisions (Incision), stratifin-free implants (Implant), and stratifin-eluting implants (Implant + SFN) and compared. Data represent the mean ± SD for $n = 5$. (C) Microscopic histology of epidermis of normal skin (Normal), untreated incisions (Incision), stratifin-free implants (Implant), and stratifin-eluting implants (Implant + SFN) on day 21 at 400× magnifications, H&E staining. (D) Epidermal hypertrophy was displayed by ETI. The ETI was measured for normal skin (Normal), untreated incisions (Incision), implants (Implant), and stratifin-associated implants (Implant + SFN). ETI > 1 depicts a hypertrophic epidermis. Data represent the mean ± SD for $n = 5$.

3.3.3 Biologic activity; increased MMP-1 mRNA expression in tissue

Figure 3.3 A shows the level of MMP-1 mRNA expression in normal skin, untreated incisions, and incisions inserted with either stratifin-free or stratifin-containing implants after 7 and 21 days post-surgery. GAPDH was shown as internal control. To quantify the data, the ratio of MMP-1 to GAPDH in normal skin was arbitrarily set to 1.0 based on band signal intensity (Fig 3.3 B). As was expected, the level of MMP-1 expression in untreated incisions was significantly higher than in normal skin on post-surgery day 7 ($n = 5$, $p < 0.001$) (Fig. 3.3 A , B). This increase can be explained by trauma after the surgical procedure. Inserting stratifin-free implants and even stratifin-containing implants did not significantly affect the level of MMP-1 expression in tissue on day 7 post-surgery ($n = 5$, $p < 0.001$) (Fig. 3.3 A, B). This evidence might be due to the observed reduction in burst release of stratifin from PVA composite implants (Fig. 3.1). In fact, this data reaffirms the safety of stratifin-eluting implants with regards to tissue integrity in acute phase of healing.

Tissue samples of normal skin, untreated incisions, and incisions inserted with stratifin-free implants did not express a detectable level of MMP-1 at day 21 post-surgery (Fig. 3.3 A, B). Interestingly, the local release of stratifin significantly increased the level of MMP-1 expression in tissue ($n = 5$, $p < 0.001$) (Fig. 3.3 A, B, D21). This result confirms the *in vivo* biological activity of stratifin released from the implants up to 21 days.

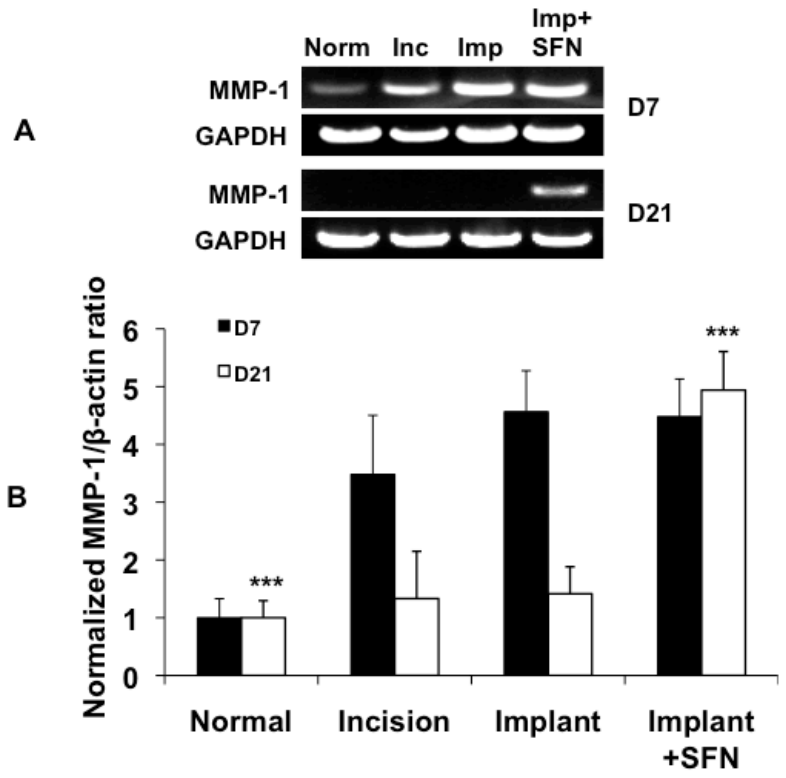

Fig. 3.3. Biological activity of controlled release stratifin. (A) The levels of expression of MMP-1 mRNA in normal skin (Norm), untreated incision (Inc), incisions inserted with stratifin-free implants (Imp), and incisions inserted with stratifin-eluting implants (Imp+SFN) were analyzed by RT-PCR. RNA loadings were compared using GAPDH internal control. (B) Semi-quantitative level of MMP-1 mRNA expression for each group was analyzed by densitometry of the corresponding bands. The results were represented as normalized ratio of MMP-1/GAPDH. Data represent the mean ± SD for $n = 5$.

3.3.4 Pharmacodynamics; reduced collagen deposition

Collagen is one of the major components of extracellular matrix, whose balance in synthesis and degradation is an essential factor for normal wound healing (Chen and Davidson, 2005; Singer and Clark, 1999). Areas of collagen deposition within the wound bed were quantified by evaluating Masson's trichrome stained slides using Image Pro Plus 4.5 software. Collagen density was analyzed in normal skin, untreated incisions, and incisions inserted with either stratifin-free or stratifin-containing implants after 7 and 21 days post-surgery (Fig. 3.4 A, B). Twenty-five microscopic high power fields from each group were analyzed. The results showed that the density of collagen is comparable in all treatment groups on day 7 ($n = 5$, $p > 0.001$) (Fig4 A, B, D7). Furthermore, these results coincide with the MMP-1 expression in tissue samples on day 7. Therefore, it can be concluded that the collagen deposition would not be compromised during the first 7 days of stratifin release from implants.

On the other hand, in the latter stages of wound healing (day 21 post-surgery) incisions treated with stratifin-containing implants demonstrated a significantly reduced collagen density compared to the incisions inserted with stratifin-free implants ($n = 5$, $p > 0.001$) (Fig. 3.4 A, B, D21). In fact, collagen density of incisions treated with stratifin-containing implants was similar to the untreated incisions at day 21 post-surgery ($n =5$, $p < 0.001$). Interestingly, the insertion of stratifin-free implants significantly increased collagen deposition on day 21. Collectively, these data suggest that local and controlled release of stratifin from implants markedly reduced collagen deposition by increasing the expression of MMP-1 and therefore collagen degradation in the surrounding tissue.

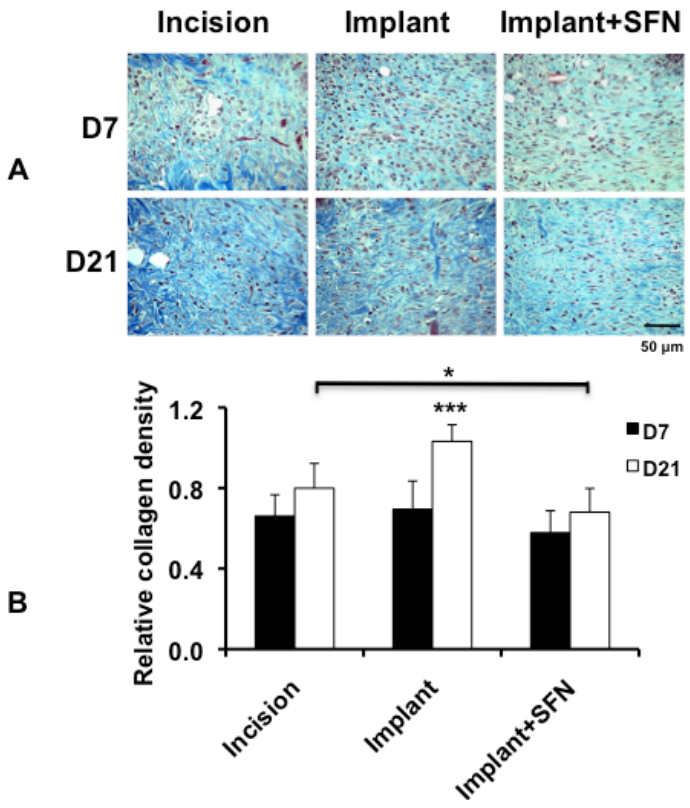

Fig. 3.4. Measurement of relative collagen density in tissue**.** (A) Collagen deposition in representative sections of normal skin (Normal), untreated incision (Incision), incisions inserted with stratifin-free implants (Implant), and incisions inserted with stratifin-eluting implants (Implant+SFN) stained with Masson trichrome. (B) Collagen density was analyzed by densitometry of the blue color in Masson trichrome stained sections. The average collagen density of each group was divided by the average collagen density of normal skin and represented as relative collagen density. Data represent the mean ± SD for $n = 5$.

3.3.5 Pharmacodynamics; reduced tissue cellularity and infiltrated $CD3^+$ immune cells

Often in the mid stages of wound healing and following the insertion of implantable materials, T-cell infiltration and cellularity can serve as a marker of inflammation (Forouzandeh et al., 2010; Tredget et al., 1997). In Fig. 3.5 A, total dermal cells are stained in blue and $CD3^+$ cells in green. Untreated incisions showed an 8- and 5-fold increase in total cellularity and $CD3^+$ immune cells on day 7 post-surgery, respectively (Fig. 3.5 A, B, C, Incision D7). Inserting stratifin-free implants into the incisions induced a significant increase in total cells and $CD3^+$ immune cells compared with the untreated incisions ($n = 5$, $p < 0.001$) (Fig. 3.5 A, B, C, Implant D7). Controlled

release of stratifin from drug-eluting implants significantly reduced total cells, as well as $CD3^+$ immune cells ($n = 5$, $p < 0.001$) (Fig. 3.5 A, B, C, Implant+SFN D7). In fact, the total number of cells in stratifin-containing implants and untreated incisions were comparable and not significantly different ($n = 5$, $p > 0.001$) (Fig. 3.5 A, B, D7). These data show that localized delivery of stratifin had a potent anti-fibrogenic effect that could suppress foreign body reactions induced by implantation, namely total tissue cellularity and $CD3^+$ cells.

Tissue sections from day 21 displayed a dense fibrotic tissue formed as a result of tissue repair (Fig. 3.2 A). This fibrous tissue was narrow in untreated incisions (Fig. 3.2 A, Incision), whereas it was extended in incisions treated with stratifin-free implants (Fig. 3.2 A, Implant). Localized, controlled release of stratifin significantly reduced the fibrous area (Fig. 3.2 A, Implant+SFN). Histological observation demonstrated that this fibrous area has low cell density in untreated incisions, whereas a significantly higher cell density is observed in incisions treated with stratifin-free implants. Further, immunohistochemistry results showed that $CD3^+$ T cells in the fibrous area of untreated incisions were reduced on day 21 compared with stratifin-free implants. Indeed, total cells and $CD3^+$ T cells were significantly reduced in incisions treated with stratifin-eluting implants ($n = 5$, $p < 0.001$) (Fig. 3.5 A, B, C D21 Implant+SFN). In fact, the number of $CD3^+$ T cells in incisions treated with stratifin-containing implants was as negligible as untreated incisions ($n = 5$, $p > 0.001$) (Fig. 3.5 A, B, C, Implant+SFN D21). Stratifin-containing implants resulted in a marked reduction of total tissue cellularity and $CD3^+$ cell count, 52% and 81%, respectively, compared with those of stratifin-free implants. This observation would appear to be a result of the local release of stratifin, which increased the expression of MMP-1 in surrounding tissue and reduced collagen deposition. These changes in cell secretary behaviors and surrounding matrix may alter cell proliferation behavior and fibrous tissue formation. This is consistent with present findings, as shown in Fig. 3.2 C and D.

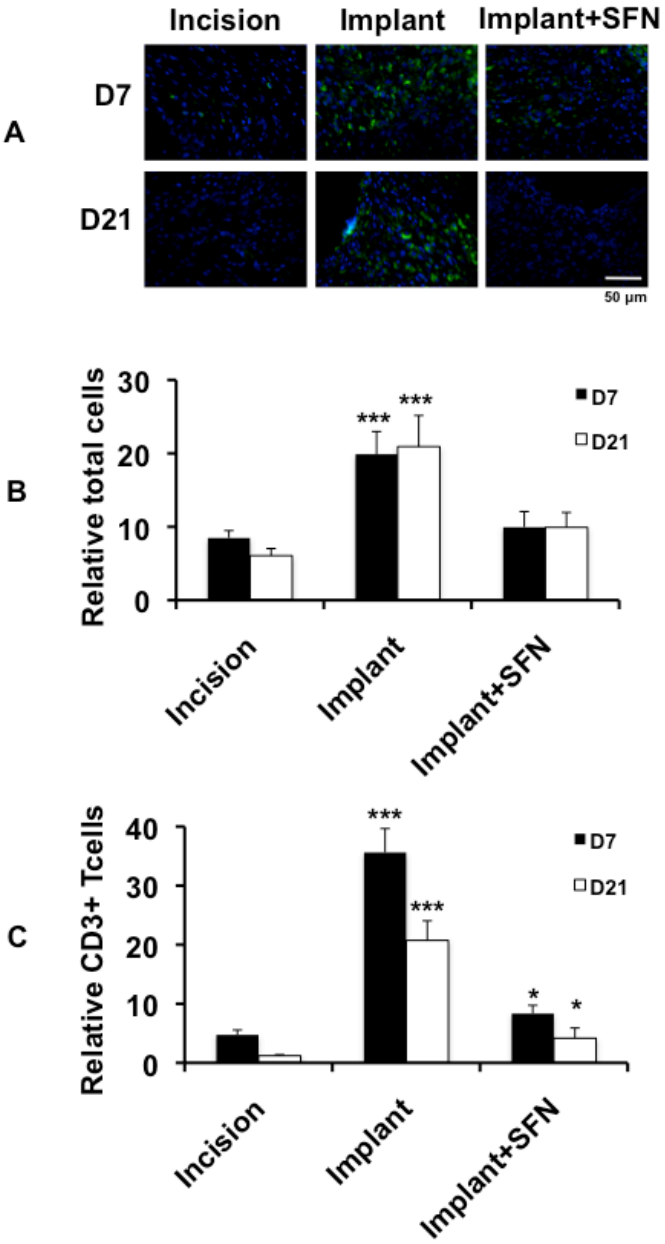

Fig. 3.5. Measurement of total tissue cellularity and infiltrated $CD3^+$ immune cells. (A) Total tissue cellularity (blue) and $CD3^+$ T cells (green) are shown in representative tissue sections of normal skin (Normal), untreated incision (Incision), incisions inserted with stratifin-free implants (Implant), and incisions inserted with stratifin-eluting implants (Implant+SFN) at days 7 and 21 post-surgery.
(B) Quantifies and compares total tissue cellularity.(C) Quantifies and compares infiltrated $CD3^+$ immune cells at day 7 (solid bars) and day 21 (open bars). The average number of the cell population in each group were divided by the average number of the cell population in normal skin and represented as relative total tissue cellularity and relative $CD3^+$ immune cells. Data represent the mean ± SD for $n = 5$.

3.6 Conclusion

PLGA microsphere/PVA hydrogel composites containing stratifin effectively reduced scar formation while minimizing T cell associated inflammation in a surgical incision model. These observations are attributed to an initial burst release of stratifin (18%) in the first 3 days followed by a controlled release of stratifin over 3 weeks. Complexing stratifin with chitosan prior to microencapsulation successfully preserved the protein bioactivity. These PLGA microsphere/PVA hydrogel composites may be particularly suitable for delivery of growth factors or other anti-fibrogenic factors that are susceptible to systemic degradation. However, the observed local tissue response to the implants remains an important consideration in product design. An implantable slow releasing system for localized delivery of anti-fibrogenic factors has a great potential in preventing post-surgical scarring.

Chapter 4. Improvement of Hypertrophic Scarring by using Topical Anti-fibrogenic/Anti-inflammatory Factors in a Rabbit Ear Model[3]

4.1 Introduction

Hypertrophic scarring is a dermal fibroproliferative disorder that often occurs following deep trauma, severe burn injury, and surgical incision. Clinically, HS is raised, red, and pruritic, and frequently results in contractures and cosmetic deformity. Abnormal patterns of tissue cellularity, extracellular matrix (ECM) expression, and accumulation are some of the characteristic features of this devastating clinical condition (Fumagalli et al., 2007; Tredget et al., 1997; Zitelli, 1996). Prolongation of the inflammatory phase has been cited as an etiologic factor in the development of HS and this may result from infection, a foreign body within the wound, excessive wound tension, or persistent mobilization of wound edges (Saulis et al., 2002; Singer and Clark, 1999).

The first consideration in scar treatment is prevention. Controlling this complication after ECM formation is very difficult. Despite the vast amount of research on the pathogenesis of hypertrophic scarring, the exact mechanism of its formation has not yet been fully elucidated. There is no single treatment modality that produces consistently favorable results. Therapeutic options include surgical excision, steroid injections, silicone sheeting, radiation therapy, and compression (Leventhal et al., 2006).

Topical agents are frequently applied to wounds for homeostasis and to promote healing. Topical steroids are also commonly applied to wounds. Steroids and nonsteroidal anti-inflammatory drugs inhibit wound healing and delay the development of tensile strength if given before or during the first 3 days after wounding. This is due to inhibition of migration of the important monocytes and formation of granulation tissue. After

[3] A version of this chapter has been published. Rahmani-Neishaboor, E., F.M. Yau, R. Jalili, R.T. Kilani, and A. Ghahary. 2010. Improvement of hypertrophic scarring by using topical anti-fibrogenic/anti-inflammatory factors in a rabbit ear model. *Wound Repair Regen*. 18:401-408.

3 days, high doses of anti-inflammatory agents are needed to affect fibroplasia and collagen remodeling (Zitelli, 1996).

Aspirin, acetylsalicylic acid (ASA), is among the most effective oral anti-inflammatory medications. It retards inflammation, making it a potential agent for preventing HS formation (Kaushal et al., 2007). It reduces human T cells by inhibiting the production of prostaglandin E2. T cells are among the most infiltrated immune cells present in both active and remission phases of hypertrophic scarring, and they affect fibroblasts and keratinocytes by releasing cytokines (Castagnoli et al., 1997). Resolution of a keloid was noted in a patient treated with topical tacrolimus, an immunosuppressive agent that inhibits T cell activation, for atopic dermatitis (Berman et al., 2004). The effect of topical application of ASA on HS has not been studied previously at the cellular, molecular, and also clinical levels.

Delays in reepithelialization by keratinocytes are known to increase the frequency of hypertrophic scarring (Ghahary et al., 2004; Lam et al., 2005; Medina et al., 2007). A recently identified factor known as stratifin or 14-3-3σ protein has been recognized as an important factor in this keratinocyte-fibroblast communication. Stratifin is a member of a large family of highly conserved dimeric 14-3-3 proteins, several of which are expressed ubiquitously (Ghahary et al., 2004). Stratifin expression, however, appears to be specific to stratified epithelial cells. In dermal fibroblasts, stratifin has been shown to function as a potent mediator of matrix metalloproteinase (MMP) expression, including collagenase (MMP-1) (Ghaffari et al., 2006; Lam et al., 2005; Medina et al., 2007). MMPs are a group of diverse proteolytic enzymes that, in addition to removing barriers such as collagen, function to regulate ECM composition and facilitate cell migration (Deitch et al., 1983; Ghahary et al., 2004; Murphy et al., 2002; Nagase and Woessner, 1999; Stamenkovic, 2003). Stratifin, therefore, appears to be an appropriate target for modulating the formation of HS.

Carboxymethylcellulose (CMC) gel dressing is one of the most common hydrogel dressings for wound healing. In the presence of wound exudate, this hydrogel absorbs liquid and forms a gel. This dressing is permeable to water, and the loss of water through the gel enhances the ability of the product to cope with exudate production (Thomas et al., 1997). It promotes gentle but effective debridement and desloughing.

To address the goal of this study, a fibrotic rabbit ear model described by Morris et al (Morris et al., 1997) has been used. This model is a highly reliable fibrotic model for quantifying the effects of various treatments on HS. Full-thickness wounds in the rabbit ear do not heal by contraction. Therefore, delays in reepithelialization result in raised scars, which resemble human HSs morphologically and histologically (Morris et al., 1997).

The present study was undertaken to discover the effect on the reduction of HS of topical application of CMC gel dressing containing either ASA or stratifin after the granulation tissue is formed.

4.2 Materials and Methods

Ethics approval for this study was obtained from the University of British Columbia Clinical Research Ethics Board. All of the animal work was reviewed and approved by the University of British Columbia Animal Care Committee.

4.2.1 Preparation of human recombinant stratifin

Human recombinant stratifin protein was prepared as described previously with slight modifications (Ghahary et al., 2004). Briefly, the cDNA of stratifin from human keratinocytes was cloned into a pGEX-6P-1 expression vector (Amersham/Pharmacia Biotech, Piscataway, NJ) and transformed into protein-expressing bacteria BL-21(DE3) (Novagene, Madison, WI). A single positive clone was grown in 100 mL of LB medium containing 50 mg/mL of ampicillin for 4–6 h at 37°C until an OD 600 nm of 0.4–0.6 was attained. Bacteria were then diluted to 1:10 with LB medium plus 0.1 mM IPTG for 12 h. To purify the protein, bacteria were centrifuged and lysed by sonication using short cut bursts (30 s intervals). GST-fused stratifin was purified by adding to glutathione sepharose-4B beads and subsequently digested using PreScission protease according to the manufacturer's procedure (GE Healthcare Bio-Sciences AB, Uppsala, Sweden). Recombinant stratifin protein produced as described has been shown previously to be >95% pure (Ghahary et al., 2004).

4.2.2 Preparation of CMC gel

Sodium CMC gel (2.5%) (Sigma-Aldrich, St. Louis, MO) was prepared by dispersing a weighed amount of CMC powder in cold water at high shear (Ammar et al., 2006). Once the powder was well dispersed 20% propylene glycol was added, and the solution was heated with moderate shear to 60°C. The prepared gel was allowed to cool and then mixed with ASA at a concentration of 0.5% or stratifin at a concentration of 0.002% using Teflon-coated magnetic stirrers.

4.2.3 Hypertrophic scarring model

The fibrotic rabbit ear model of cutaneous scarring was used as described previously with minor modifications (Brown et al., 2008; Morris et al., 1997; Tandara and Mustoe, 2008). Five New Zealand White rabbits weighing 4.5–5 kg were kept under standard conditions at the University of British Columbia Animal Care Center. Animals were anesthetized with an intramuscular injection of ketamine (22.5 mg/kg) and xylazine (2.5 mg/kg) followed by isoflurane gas through tracheal intubation. Four full-thickness wounds were created down to the cartilage on the ventral side of each ear using an 8 mm punch biopsy. The perichondrial membrane was then dissected off the cartilage. Two wounds, separated by at least 1 cm, were made on each side of the midline, carefully avoiding the central ear artery and marginal ear veins. Occasional bleeding was treated by manual compression. Each wound was covered with polyurethane Tegaderms dressing (3M, St. Paul, MN) separately to prevent interference between treatments. Wounds were kept covered until post-operative day 5. When granulation tissue formation had begun from the wound corners, treatments were started.

4.2.4 Treatment with either stratifin or ASA-containing CMC gel

Wounds were divided into four groups. Each group consisted of the wounds on both lateral and medial sides of the ear. Previous dose–response studies performed *in vitro* (Ghaffari et al., 2006; Ghahary et al., 2004) found the effective dose of stratifin to be 2 mg/ml. In this study, the dose was increased to 20 mg/g of gel to increase the accessibility of stratifin to the ECM-embedded fibroblasts. The dose of ASA was chosen as 0.5% based on the non irritant anti-inflammatory dose of salicylates that can be topically applied on the wounds (Reller). Treatment groups received either 150 mg of

CMC gel containing 0.002% (w/w) stratifin, 150 mg of CMC gel containing 0.5% (w/w) ASA, or 150 mg of CMC gel alone. Treatments were applied twice daily. Upon removal of Tegaderms, the wounds were cleaned, re-treated, and covered with new Tegaderms. The last group received no treatment, with healing by secondary intention. Wounds were observed daily and photographs were taken on post-operative days 20 and 28. Animals were sacrificed on post-operative day 28, and scars were harvested.

4.2.5 Tissue preparation and histologic analysis

Scars were harvested with a 0.5 cm margin of surrounding unwounded tissue and bisected through the maximum point of scar hypertrophy on visualization and palpation. One half of each wound was fixed in 10% neutral buffered formaldehyde, dehydrated, embedded in paraffin, cut in 5 mm sections, and stained with hematoxylin and eosin (H&E). The other half was stored at –80°C for RNA extraction.

4.2.6 MMP-1 expression by reverse transcription-polymerase chain reaction

MMP-1 expression in tissue samples was examined by extracting RNA from tissue using the RNeasy fibrous tissue mini kit (Qiagen, Valencia, CA) according to the manufacturer's recommendations. RNA concentrations were measured using the NanoDrop spectrophotometer (NanoDrop Technologies, Wilmington, DE). Equal concentrations of RNA samples were then reverse transcribed to cDNA by the Thermo Script RT-PCR system (GIBCO-Invitrogen Corporation, Burlington, ON) following the manufacturer's protocol. The resulting cDNAs were used to perform PCRs for the primers of MMP-1 ([fwd] CA GCTTTATGGGAGCCAGTC and [rev] TGTTCCTCA CCCTCCAGAAC, product size: 200 bp). Glyceraldehyde-3-phosphate dehydrogenase (GAPDH) was used as an endogenous control gene in order to normalize PCRs for the RNA loaded to reverse transcription reactions. The sequences of GAPDH primers were ([fwd] GAGCTGAACGGGAAA CTCAC and [rev] TGCTGTAGCCAAATTCGTTG, product size: 300 bp).

4.2.7 Scar elevation index

The scar elevation index (SEI) was used for histomorphometric analysis. The SEI measures the ratio of total scar area to the area of normal underlying dermis, as described previously by Morris et al. (Morris et al., 1997).The SEI was measured for treated and

untreated wounds. The height of the underlying dermis is determined based on the height of the adjacent unwounded dermis. All measurements were taken within the confines of the wounded area at 100× magnification from the H&E-stained tissue sections. The epithelial height is not considered in SEI calculations. An SEI = 1 indicates no newly formed hypertrophied dermis, whereas an index >1 denotes HS formation.

4.2.8 Epidermal thickness index

The epidermal thickness index (ETI) was used to determine the degree of epidermal hypertrophy and was based on measurements taken from H&E-stained tissue sections at 400× magnification. The entire cross-section of the scar was measured for epidermal thickness, which corresponded to a total of approximately five fields. The epidermal thickness from five fields of uninjured skin was also measured from both sides of the scar. The ETI was then determined by calculating the ratio between the averaged epidermal height in scar tissue and the averaged epidermal height in normal uninjured skin (Tandara and Mustoe, 2008). An ETI > 1 denotes hypertrophic epidermis formation.

4.2.9 Tissue cellularity and immunohistochemistry

Paraffin-embedded sections (5 mm) were deparaffinized and rehydrated through 100%, 95%, and 70% ethanol followed by incubation in double distilled water (DDW) for 2 min. To retrieve cellular antigens, a microwave oven heating pretreatment was performed in sodium citrate buffer before blocking with 5% albumin in phosphate-buffered saline solution. For antibody staining, sections were incubated with rabbit anti-T cell CD3 peptide (1:50; Abcam, Cambridge, MA) at room temperature for 1 h. The second antibody was rhodamine-conjugated goat anti-rabbit IgG (Bio-Rad Life Science, Mississauga, ON). The second antibody was used in a concentration of 1:4000. The slides were counterstained with 4′,6-diamidino-2-phenylindole (DAPI) for 5 s, and then sections were dehydrated and mounted. For each wound, five randomly chosen 1.8 mm × 1.8 mm fields of dermis were photographed under 400× magnification using a digital camera attached to a fluorescence microscope. Photographs were subsequently coded and randomized, and the number of nuclei were counted by a blinded observer. The counts from the corresponding fields were averaged and used for comparison.

4.2.10 Collagen density

Paraffin-embedded sections (4 mm) were mounted on glass slides and stained for collagen with Masson's trichrome, in which collagen stained blue. For each wound, five randomly chosen fields of dermis were photographed under 100× magnification. Collagen deposition areas were estimated using the Image Pro Plus 4.5 software (de Carvalho Pde et al., 2010). The relative density of collagen in each group was calculated by normalizing to the unwounded skin collagen density.

4.2.11 Statistical analysis

All data are expressed as mean ± SD. Data were analyzed using the analysis of variance Tukey–Kramer multicomparisons test to compare the means between study groups and their controls. The level of significance was set to p values <0.05.

4.3 Results

4.3.1 Qualitative wound assessment

Wounds that received no treatment became raised and firm as early as day 17. However, the wounds treated with CMC gel were closed 3 days later (postwounding day 20) (Fig. 4.1 A, day 20, Gel). As shown in Fig. 4.1 A, day 20, wounds treated with CMC gel containing either stratifin or ASA were still open. The ASA and stratifin-treated wounds closed several days later on postwounding days 23 and 25, respectively. They appeared slightly contracted with a minimal amount of raised tissue resembling early scar formation (Fig. 4,1 A, day 28, ASA and SFN). Scars were harvested on postwounding day 28. At this time, wounds that were either untreated or treated with CMC gel showed a visibly raised and palpable scar with evidence of HS (Fig. 4.1 B, Untrt and Gel). Wounds treated with CMC gel containing ASA also had some evidence of HS, but the scar was less raised (Fig. 4.1 B, ASA). Wounds treated with CMC gel-containing stratifin had the appearance of mature scars and appeared the flattest among all other treatment groups (Fig. 4.1 B, SFN).

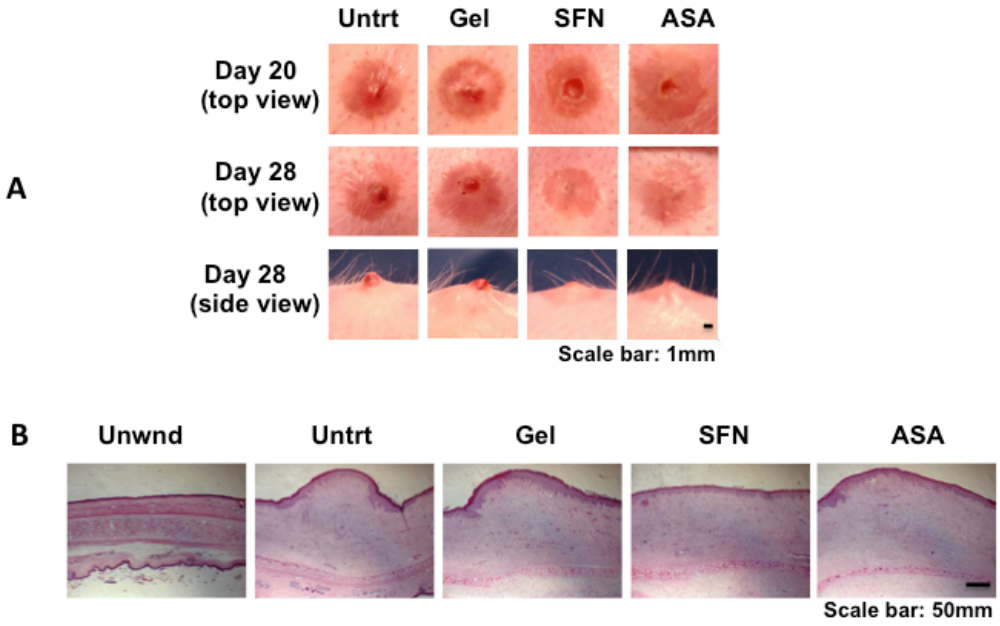

Fig. 4.1. Clinical appearance and histology of wound and scars. (A) represents the clinical appearance of wounds received either nothing (Untrt), CMC gel (Gel), ASA, or stratifin (SFN) on day 20 (top panel) and 28 (middle panel). The third row represents the side view of wounds on day 28. As can be seen, the wounds receiving stratifin and ASA are flattened relative to controls.(B) shows microscopic histology of unwounded skin (Unwnd), wounds received either nothing (Untrt), CMC gel (Gel), aspirin (ASA), or stratifin (SFN) on day 28 at 40× magnification, H&E stain.

4.3.2 Scar elevation index

Histomorphometric quantification of HSs was performed on post-operative day 28. All wounds had adequate scar maturation and showed histologic evidence of scarring. To quantify the degree of scar formation, SEI was measured for nine different wounds as described in Section 4.2. The mean SEI in untreated wounds was 1.84 ± 0.15, which was higher compared with that of treated wounds with either stratifin (SEI = 1.15 ± 0.14, $n = 9$, $p < 0.001$) or ASA-impregnated CMC gel (SEI = 1.23 ± 0.07, $n = 9$, $p < 0.001$) (Fig. 4.2 A). This represents a significant reduction in HS of 82% and 73%, respectively. The mean SEI of wounds treated with CMC gel (Fig. 4.2 A) was 1.79 ± 0.19, which was lower than that of untreated scars (Fig. 4.2 A, Untrt), but not statistically different ($p > 0.05$).

4.3.3 Epidermal thickness index

The ETI was measured for nine different wounds as described in Section 4.2. The mean epidermal thickness of untreated wounds was 3.6 times greater than that of normal unwounded skin ($n = 9$, $p < 0.001$) (Fig. 4.2 B). Epidermal thickness decreased in wounds treated with either stratifin or ASA-containing CMC gel to a mean ETI of 1.31 ± 0.2 and 2.18 ± 0.04, respectively, compared with that of untreated controls (3.57 ± 0.32) (Fig. 4.2 B). This corresponds to a respective 88% ($p < 0.001$) and 54% ($p < 0.001$) ETI reduction. The ETI of wounds treated with CMC gel was 3.01 ± 0.21, which corresponds to a 22% reduction in ETI ($p < 0.001$).

4.3.4 Total cellularity of dermis and $CD3^+$ T cell subset

Total cellularity of dermis was assessed using DAPI blue emission nuclear staining (Fig. 4.3 A). For quantitative analysis, 45 microscopic high-power fields of DAPI-stained slides from each group of wounds were counted. Cell count was highest in untreated wounds with an average of 114.1 ± 12.6 cells/hpf. Total dermal cellularity was significantly reduced in wounds treated with stratifin and ASA-containing gels (Fig. 4.3 B, solid bars). The result shows a mean of 46.1 ± 10.6 and 67.8 ± 15.1 cells/hpf for stratifin and ASA-treated wounds, respectively. This corresponds to a respective 57% ($p < 0.001$) and 41% ($p < 0.001$) reduction in dermal cellularity. Cell count in wounds treated with CMC gel had a mean of 88.9 ± 17.1 cells/hpf, which corresponds to a 22% reduction in dermal cellularity ($p < 0.01$) compared with those of untreated controls.

The number of $CD3^+$ cells in the dermis was assessed using the rabbit anti-T cell CD3 peptide (1:50; Abcam) (Fig.4.3 A). $CD3^+$ T cells in the dermis of unwounded skin were not detectable. Untreated scars had the highest $CD3^+$ T cell count with a mean of 46.5 ± 8.9 cells/hpf. The number of $CD3^+$ T cells in the dermis was reduced in scars treated with stratifin and ASA-impregnated gels to a mean of 9.8 ± 1.9 and 4.0 ± 1.7 cells/hpf, respectively (Fig. 4.3 B, open bars). This corresponds to a respective 79% ($p < 0.001$) and 91% ($p < 0.001$) reduction in the dermal $CD3^+$ T cell count. Wounds treated with CMC gel had a mean of 37.8 ± 10.3 cells/hpf, which corresponds to a 19% decrease in the number of $CD3^+$ T cells in the dermis ($p < 0.001$) (Fig. 4.3 B, open bars).

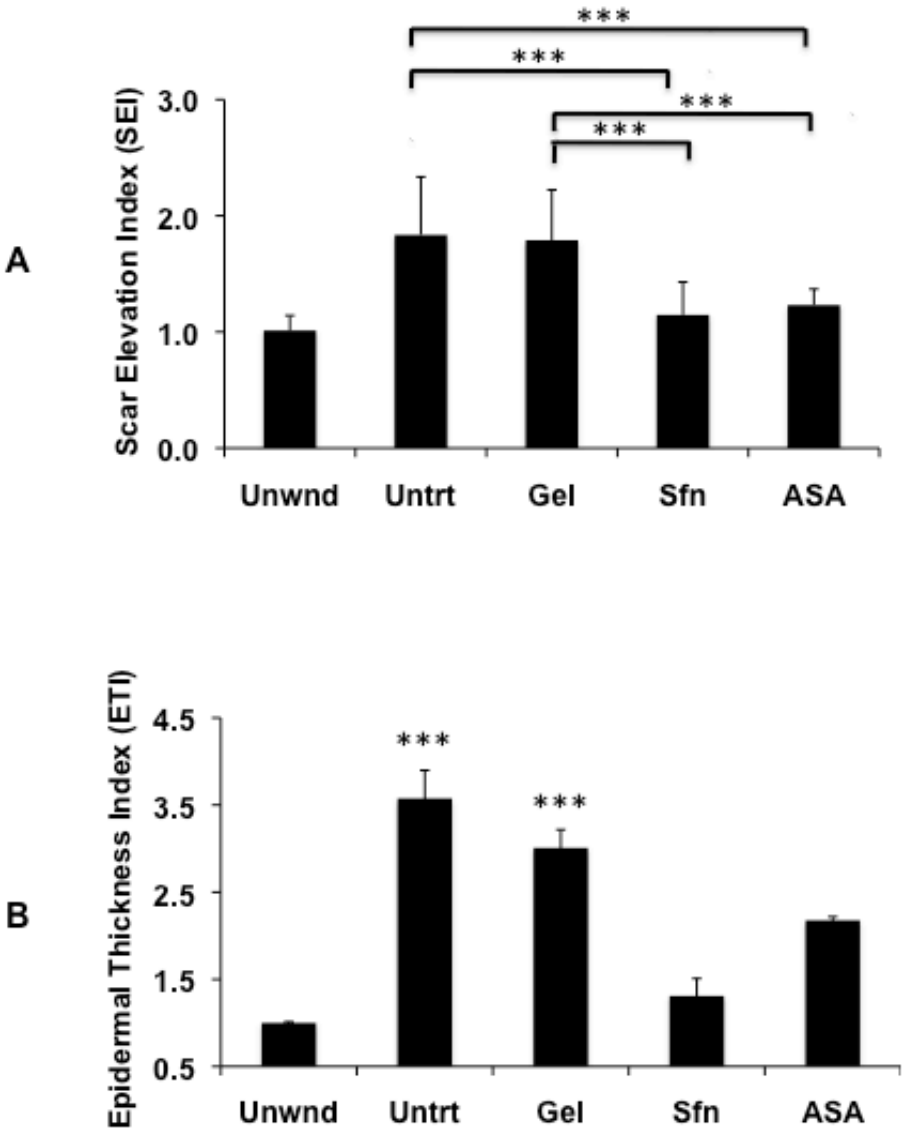

Fig. 4.2. Scar elevation index and epidermal thickness index. (A) Dermal hypertrophy was displayed by the SEI. SEI was measured for the wounds treated with either stratifin (SFN) or aspirin (ASA) and compared to the controls. SEI was measured for unwounded skin (Unwnd), untreated wound (Untrt), wounded skin treated with CMC gel only (Gel), or gel containing either stratifin (SFN) or aspirin (ASA). SEI >1 depicts a hypertrophic scar. Data represent the mean ± SD for $n = 9$. (B) Epidermal hypertrophy was displayed by ETI. The ETI was measured for unwounded skin (Unwnd), untreated wound (Untrt), wounded skin treated with CMC gel only (Gel), or gel containing either stratifin (SFN) or aspirin (ASA). ETI > 1 depicts a hypertrophic epidermis. Data represent the mean ± SD for $n = 9$.

4.3.4 MMP-1 mRNA expression

As shown in Fig. 4.5 A, MMP-1 mRNA expression was the highest in wounds treated with stratifin-impregnated gels. GAPDH was used as the internal control. To quantify the data, the ratio of MMP-1/GAPDH in unwounded skin was arbitrarily set to 1.0 based on band signal intensities. The ratio of MMP-1/GAPDH in wounds treated with stratifin-impregnated CMC gel was approximately 3-fold higher by comparison (mean of 3.2 ± 0.5, $n = 9$, $p < 0.001$) (Fig. 4.4 B). Averaged MMP-1/GAPDH ratios for wounds treated with ASA-impregnated CMC gel, CMC gel only, and untreated wounds were 1.8 ± 0.7, 1.6 ± 0.2, and 1.2 ± 0.2, respectively. These were statistically insignificant when compared with that of unwounded skin ($p > 0.05$).

4.3.5 Collagen density

Collagen deposition areas were measured using Image Pro Plus 4.5 software on Masson's trichrome-stained slides. Forty-five microscopic high-power fields from each group of wounds were analyzed. As a result, the relative density of collagen in untreated wounds was 0.74 ± 0.19 ($p < 0.01$). The collagen density was significantly reduced in wounds treated with stratifin-impregnated CMC gel compared with the untreated wounds (Fig. 5.5). The mean value for stratifin-treated wounds was 0.38 ± 0.13, which corresponds to a 48% reduction in collagen density compared with that of untreated controls. The mean values of relative collagen density for wounds treated with ASA-impregnated CMC gel and CMC gel only were 0.58 ± 0.17 and 0.57 ± 0.16, respectively. These values were not statistically different from the relative density of collagen in untreated wounds ($p > 0.05$).

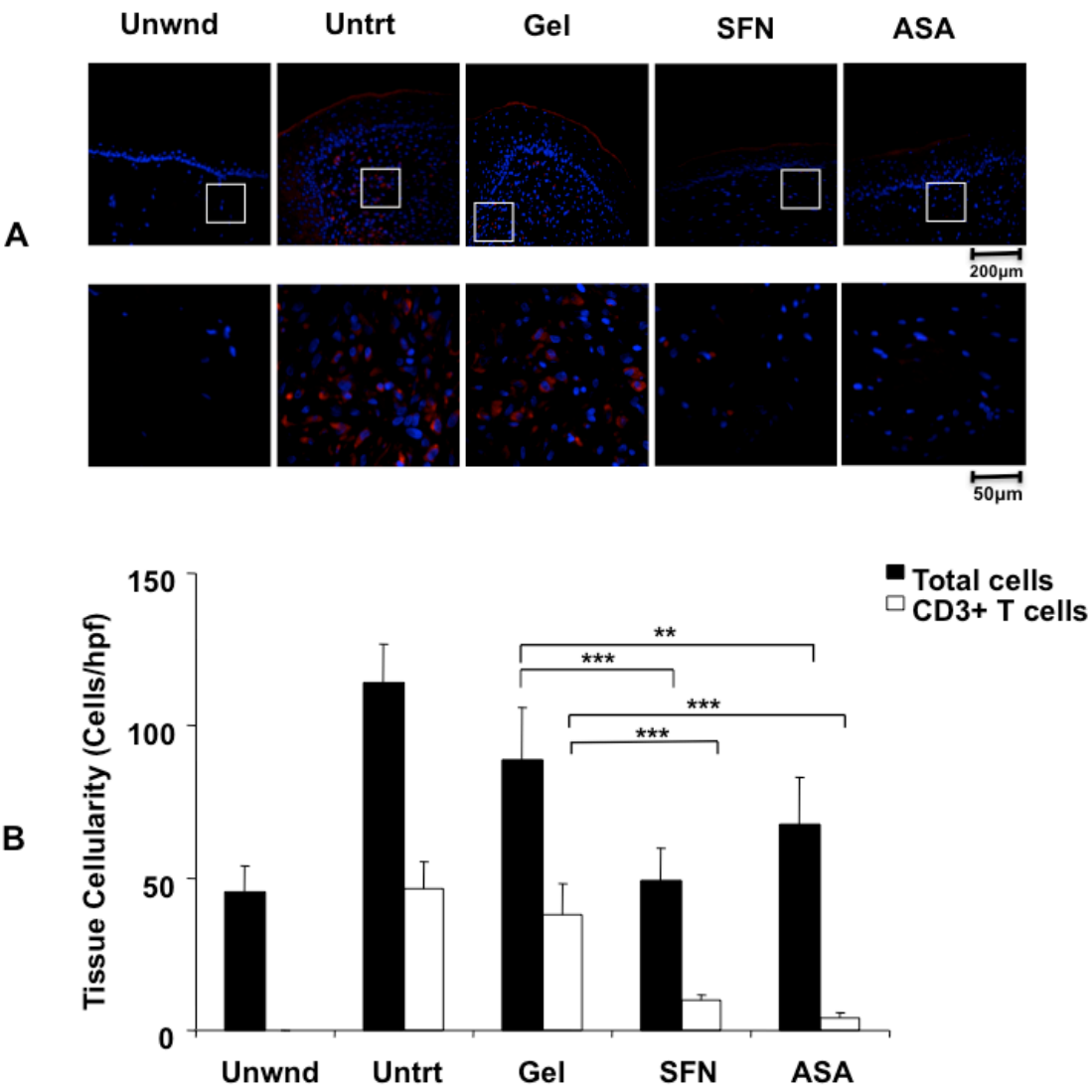

Fig. 4.3. Quantifying the total tissue cellularity and $CD3^+$ T cells within wounds at post-wounding day 28. (A) Total tissue cellularity and $CD3^+$ T cells were quantified in tissue sections using DAPI staining (blue) and specific immunohistochemical staining (red), respectively. **(**B) Total tissue cellularity (solid bars) and $CD3^+$ T cells (open bars) in sections of unwounded skin (Unwnd), untreated wound (Untrt), wounds treated with CMC gel only (Gel), or gel containing either stratifin (SFN) or aspirin (ASA) are quantified and compared. Data represent the mean ± SD for $n = 45$.

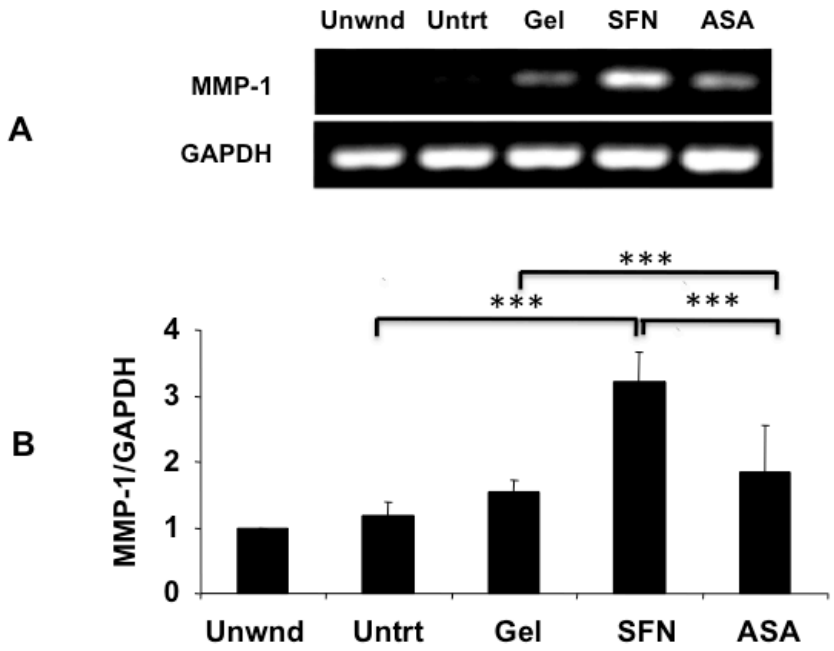

Fig. 4.4. Efficacy of topical application of stratifin on the expression of matrix metalloproteinase (MMP-1) in tissue at post-wounding day 28. **(**A**)** The levels of expression of MMP-1 mRNA in unwounded tissue (Unwnd), untreated wound (Untrt), wounds treated with CMC gel alone (Gel), and gel containing either stratifin (SFN) or aspirin (ASA) were analyzed by RT-PCR. RNA loadings were compared using GAPDH internal control. **(**B**)** Semi quantitative level of MMP-1 mRNA expression for each treatment group was analyzed by densitometry of the corresponding bands and represented as the ratio of MMP-1 expression to GAPDH. Data represent the mean ± SD for $n = 9$.

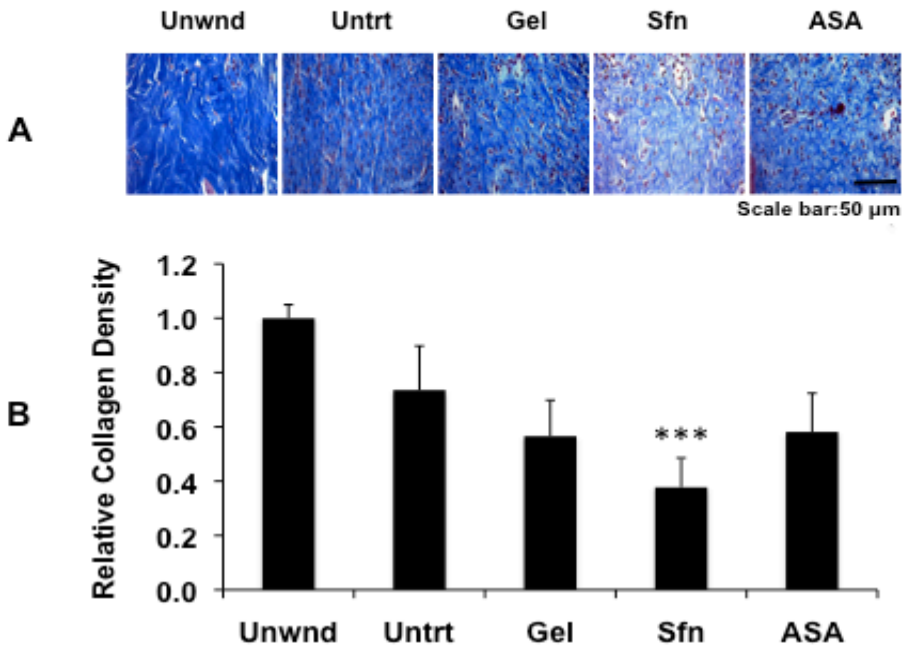

Fig. 4.5. Measurement of relative collagen density in tissue. **(**A**)** Collagen deposition areas in Masson's trichrome stained histology sections. **(**B**)** Relative collagen density in sections of unwounded skin (Unwnd), untreated wound (Untrt), wounds treated with CMC gel only (Gel), or gel containing either stratifin (SFN) or aspirin (ASA) are quantified and compared. Data represent the mean ± SD for $n = 45$.

4.4. Discussion

A mounting body of evidence indicates that epidermal–mesenchymal interactions during wound healing are important in controlling the expression of collagen and other ECM components (Ghahary et al., 2004; Lam et al., 2005; Medina et al., 2007). Normally, there exists a balance between ECM synthesis and degradation. When this balance is altered, wounds may heal with some difficulties causing either nonhealing wounds or excessive matrix accumulation leading to keloid and hypertrophic scar formation. During the proliferative phase of wound healing, excessive scar formation can result from an increased matrix synthesis, a reduced breakdown, or both (Fumagalli et al., 2007; Tredget et al., 1997).

One of the main strategies to reduce scar formation is to induce or accelerate scar degradation. Stratifin has been shown to function as a potent stimulator of fibroblast MMP-1, -3, -8, and -24 levels through the activation of c-Fos and mitogen-activated protein kinase pathway (Lam et al., 2005). As such, stratifin may be a good candidate to function as an anti-fibrogenic factor.

Although inflammation is important for healing, it is also a potent stimulator of scarring (Niessen et al., 1999; Slemp and Kirschner, 2006). In fact, scarless fetal wounds are characterized by a relative lack of inflammation (Dang et al., 2003). Aspirin is one of the most effective oral anti-inflammatory medications, making it a potential agent for preventing HS formation (Kaushal et al., 2007).

Stratifin increases the expression of MMP-1 in wound tissue. It is known that stratifin slows down the healing process by reducing matrix accumulation. Early application of stratifin might compromise granulation tissue formation, which will result in delayed healing. On the other hand, reducing the volume of the mature scar is very difficult if treatment is applied near the cessation of the maturation phase of wound healing. As such, an essential component of normal wound healing is its timely cession. Termination of wound healing, therefore, requires a fine balance between ECM deposition and its hydrolysis. In this study, the scar reduction effect of either stratifin or aspirin was combined with the healing-promoting effect of CMC hydrogel in order to modulate healing.

Use of the rabbit ear model established by Mastue's group for HS made it possible to see a significant improvement in healing quality(Kloeters et al., 2007; Morris et al., 1997). A critical time point for starting the treatment appears to be around post-wounding day 5 for both aspirin and stratifin; this is when granulation tissue started to form in all wounds. Wounds treated with CMC gel only underwent wound closure and complete epithelialization 3 days later than untreated wounds.

Measuring the epidermal thickness revealed that epidermal thickness significantly decreased in scars treated with CMC gel. Less epidermal proliferation and epithelilization rates in wounds treated with hydrogels were reported previously by Tandara et al. (Tandara and Mustoe, 2008). This evidence was explained to be the result of the inhibitory effect of hydrogel as a water evaporation barrier on epidermal proliferation. It

was observed that the epidermis responds to water loss and perturbation of homeostasis with epidermal proliferation to restore the stratum corneum and hence the functional barrier. The more effective the water barrier, the thinner the epidermis (low ETI) and the less the HS (Tandara and Mustoe, 2008). It is assumed that hydration of the stratum corneum using silicone gel sheeting would reduce water evaporation from the skin surface and would mimic the conditions of mature epidermis with a full-thickness stratum corneum, thus restoring homeostasis to the injured epidermis and removing a stimulus for epidermal proliferation (Tandara and Mustoe, 2008). It has also been suggested that these effects are mediated in part through interleukin (IL-1) and tumor necrosis factor a (TNF-a) (Tandara et al., 2007). Results of the present study showed that treatment of the wounds with the CMC gel alone significantly reduced both epidermal and dermal cellularity.

A previous study by Tandara et al. (Tandara et al., 2007) showed that hydration of keratinocytes modifies the levels of releasable cytokines, which alter the secretary behavior of dermal fibroblasts. In an *in vitro* keratinocyte fibroblast co-culture model, hydration of keratinocytes significantly affected the MMP activity (Tandara et al., 2008). CMC gel may create a moist environment in which keratinocytes produce MMP-1 stimulating factor for fibroblasts. This may be the reason for an increase observed in the level of MMP-1 expression in CMC-treated wounds.

As expected, using stratifin or aspirin delayed the wound closure by about 6–8 days, respectively, compared with time of closure of untreated wounds. Stratifin- and ASA-treated wounds were not raised. In these wounds, CMC gel worked as a water barrier, resulting in less epidermal hypertrophy and lower epidermal thickness. When the wounds were treated with aspirin, a significant reduction of 73% was achieved in scar formation compared with that of untreated wounds. It is well established that HS is associated with high cellularity. As such, low cellularity seen in ASA-treated wounds causes less ECM accumulation, which is the hallmark of HS. Topical application of aspirin inhibited the infiltration of $CD3^+$ T cells to the injured tissue. As immune cells produce fibrogenic factors such as transforming growth factor (TGF)-b and insulin-like growth factor (IGF)-1, fewer infiltrated immune cells produce fewer fibrogenic factors, which results in less HS. Considering the fact that TGF-b and IGF-1 are MMP- 1-

suppressing factors, less production of these factors increases the level of MMP-1 (Wang et al., 2007). However, the relationship between high tissue cellularity and MMP-1 is not known.

The high number of $CD3^+$ observed in untreated wounds can be due to either the prolongation of the inflammatory phase or the higher number of lymphocytes in rabbit blood (40%–50% in rabbit vs. 25%–30% in human) or both (Castagnoli et al., 1997; Poljicak-Milas et al., 2009). Topical application of aspirin significantly reduced the infiltration of $CD3^+$ T cells to the injured tissue (91%). As a result, aspirin controlled the excessive accumulation of granulation tissue. This inhibitory effect on the early inflammatory phase of wound healing had a significant outcome on the later events in the wound-healing process, namely a reduction in dermal cellularity and hypertrophy. Aspirin also reduced the total tissue cellularity by 46%, which was significantly higher than the reduction due to the occlusive effect of the CMC gel. It was observed that stratifin enhanced degradation of collagen by increasing the expression of MMP-1 in wound tissue. Applying CMC gel containing stratifin after 5 days resulted in a marked reduction of both components of HS tissue, collagen and the cells, 48% and 57%, respectively, compared with those of untreated controls. These effects led to a 82% reduction in HS compared with that of untreated wounds. When the fact that MMPs degrade the chemoattractants for immune cells including monocytes is considered, it is expected that there will be fewer infiltrated immune cells when the level of MMP-1 is high (McQuibban et al., 2002). Although it needs to be confirmed, stratifin-induced TGF-b is likely to be involved in the suppression of the number of cells in general and $CD3^+$ cells in particular. This assumption is based on a previous report (Lam et al., 2005) indicating that stratifin increases c-Fos and c-Jun, two components of AP-1 complex involved in TGF-b stimulation.

In summary, we believe that topical application of anti-fibrogenic factors such as stratifin and anti-inflammatory factors like aspirin applied at the appropriate time during the wound healing process will improve or prevent HS formation. Controlling the inflammation and degradation of collagen are important regulatory control points with potential for novel therapeutic intervention. Combination of both strategies appears to be an ultimate way to manage HS. The objective of my future studies is to create a modified

thermoreversible CMC gel formulation containing both stratifin and aspirin with a stronger water barrier capacity and film-forming capability that can control the release of these medications while enhancing their skin penetration efficiency.

Chapter 5. Controlled Release of Stratifin and Acetyl Salicylic Acid from a Topically Applied Thermoreversible Submicron Emulgel Reduces Hypertrophic Scarring[4]

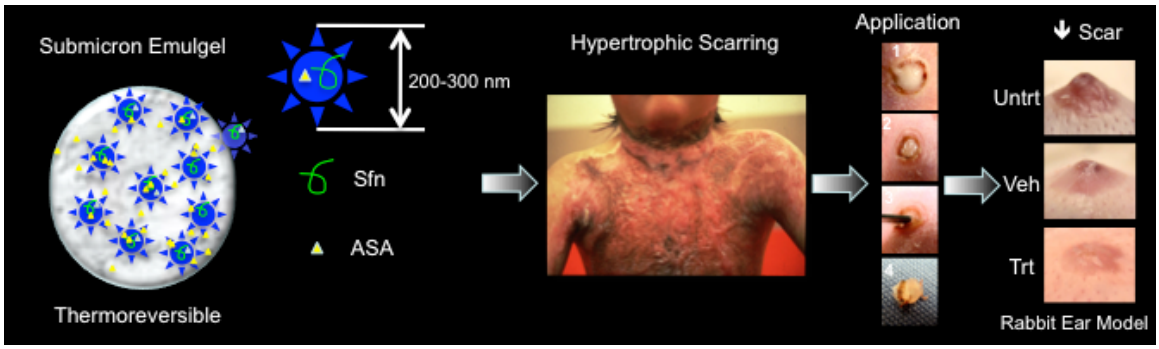

Fig. 5.1. Graphical abstract.

5.1 Introduction

Dermal fibrosis, such as hypertrophic scarring, remains a major clinical problem. For example, burn and traumatic injuries and even common surgical procedures can give rise to excessive scarring that results in permanent functional loss and disfigurement (Aarabi et al., 2007; Dockery, 1995; Tredget et al., 1997). Therapeutic intervention using controlled release of anti-fibrogenic and anti-inflammatory agents would be an advantageous strategy to reduce excess fibrosis following wound closure (Aarabi et al., 2007; Boutli-Kasapidou et al., 2005; M, 2005; Mutalik, 2005b; Occleston et al., 2008; Tredget et al., 1997).

Stratifin (14-3-3σ protein) is an important wound healing factor that is involved in keratinocyte-fibroblast communication (Ghahary et al., 2004). Stratifin is specifically expressed in stratified epithelial cells and increases the expression of matrix metalloproteinases (MMPs) in dermal fibroblasts (Ghaffari et al., 2006; Ghahary et al.,

[4] A version of this chapter is submitted for publication. Rahmani-Neishaboor, E. Jalili, R. Hartwell, R. Carr, N. and A. Ghahary. Controlled Release of Stratifin and Acetyl Salicylic Acid from a Topically Applied Thermoreversible Submicron Emulgel Reduces Hypertrophic Scarring.

2004; Lam et al., 2005; Medina et al., 2007). MMPs are a group of diverse proteolytic enzymes that function to facilitate cell migration by breaking down collagen and other extracellular matrix components (Murphy et al., 2002; Nagase and Woessner, 1999; Stamenkovic, 2003). Thus, stratifin has great potential to be used as an anti-fibrogenic factor for HS prevention.

Although inflammation is important for healing, it is a potent stimulator of scarring (Niessen et al., 1999). Fetal skin wounds heal without scarring. Scar specimens and tissue biopsies from fetal wounds suggest that a robust inflammatory response may underlie the excessive fibrosis seen in HS formation (Singer and Clark, 1999; Yang et al., 2003). Treatment with anti-inflammatory agents, such as acetylsalicylic acid (ASA) has a great potential to treat hypertrophic scarring. In a previous study (Rahmani-Neishaboor et al., 2010) the scar-reducing efficacy of topically applied stratifin and ASA using CMC gel was tested on a rabbit ear fibrotic model. The results showed that twice a day application of either stratifin or ASA-containing CMC gel reduces HS formation when it is applied post injury prior to re-epithelialization (Rahmani-Neishaboor et al., 2010).

Submicron emulsions (SMEs) are innovative colloidal systems that have unique physical-chemical characteristics, making them very attractive in many pharmaceutical applications (Sakulku et al., 2009). Cationic SMEs have been widely used as an ophthalmic controlled release delivery system for oligonucleotides (ODNs) and small molecules (Ammar et al., 2010; Hagigit et al., 2010; Sznitowska et al., 2001), pulmonary DNA immunization (Bivas-Benita et al., 2004) (Makidon et al., 2010a), ODN delivery for cancer therapy (Shi et al., 2005; Tagne et al., 2008), and as a topical delivery system for antibiotics and anti-inflammatory agents for the management of burn wounds (Hemmila et al., 2010). In fact, SMEs are attractive topical drug delivery systems, primarily owing to their small size, which thereby enhances the bioavailability and penetration of agents through the skin (Alves et al., 2007; Kim et al., 2008; Shakeel et al., 2008; Shakeel et al., 2009). Hydrophilic gels containing submicron vesicles have been able to promote drug penetration in the stratum corneum and/or in the layer of viable skin compared with a non-particulated formulation and also to control the release of incorporated drugs, unlike simple CMC gels (Alves et al., 2007). This is of particular importance when developing a delivery system for therapeutics that will interfere with

the latter stages of wound healing. Additionally, these hydrocolloid formulations provide a cooling and soothing effect, which is valuable in burns and severe wounds (Magnette et al., 2004).

In this study it was suggested that submicron emulgels (hydrophilic gels containing cationic submicron emulsions) might be effective for controlling the release of negatively charged stratifin and ASA. Thermoreversible characteristics of submicron emulgels allow them to form a thin film after absorbing the wound exudates, covering the wounds as a dressing while releasing the scar reducing factors. The efficiency of SFN/ASA-contained emulgels was evaluated in a fibrotic rabbit ear model described by Morris et al. (Morris et al., 1997).

5.2 Materials and Methods

5.2.1 Materials

MCT oil (medium chain triglyceride or caprylic/capric triglyceride) was purchased from Goldschmidt Chemical Corporation, Germany; sodium carboxymethyl cellulose (average MW ~ 700000), Oleylamine (Assay ≥ 70%, GC), Vitamin E (97%), glycerol (≥99%), 1,2-propanediol (99.5%), and acetylsalicylic acid were purchased from Sigma-Aldrich. Polyoxyethylene- polyoxypropylene-block copolymer (Lutrol F127) was received as gift from BASF, USA. Dulbecco's modified Eagle's medium (DMEM), keratinocyte serum free medium (KSFM), and antibiotic–antimycotic preparation (100 U/mL penicillin, 100 mg/mL streptomycin, 0.25 mg/mL amphotericin B) were purchased from GIBCO, USA.

5.2.2 Preparation of human recombinant stratifin (14-3-3σ)

Human recombinant stratifin (SFN) protein was prepared as previously described (Ghahary et al., 2004) with slight modification. Briefly, the cDNA of stratifin from human keratinocytes was cloned into a pGEX-6P-1 expression vector and transformed into protein expressing bacteria, BL-21(DE3). After lysing the bacteria, GST-fused stratifin was purified by adding to glutathione sepharose-4B beads and subsequently digested using PreScission protease. Recombinant stratifin protein produced as described was previously shown to be more than 95% pure (Ghahary et al., 2004).

5.2.3 Conjugation of stratifin with FITC

For detection and quantification purposes, stratifin was conjugated with fluorescein isothiocyanate. Fluorescence probe conjugation of stratifin was done by EZ-Label™ FITC protein labeling kit, as described previously (Rahmani-Neishaboor et al., 2009). Analytical quantification of FITC-conjugated stratifin (SFN-FITC) was done using an Infinite™ F500 microplate reader (TECAN Trading AG, USA) set at excitation and emission wavelengths of 485 and 535 nm, respectively.

5.2.4 Preparation of SFN/ASA-containing CMC gels and submicron emulgels

The CMC gel (2.5%, w/w) was prepared as described previously (Rahmani-Neishaboor et al., 2010). The blank SME was prepared according to the method described below. Glycerol and Lutrol F127 were dissolved in aqueous phase and adjusted to pH 7.4. The cationic lipid, oleylamine (OA), and vitamin E were dissolved in the MCT oil phase. Both phases were heated separately to 70°C, after which the two phases were mixed, stirred with the magnetic stirrer, and further heated to a temperature of 80°C. The resulting emulsion was then mixed by a high shear mixer, IKA® (IKA Works Inc, USA), at 2000 rpm over 5 min and rapidly cooled to <20°C. After cooling, the emulsions were homogenized using a TissueRuptur® (QIAGEN, Canada) at full speed for five cycles of 30 s on an ice bath. To prepare emulgels, CMC gel (2.5%, w/w) was added to the prepared SME under continuous stirring at 1500 rpm using the IKA® high shear mixer until a homogenous mixture was obtained. SFN 0.002% and ASA 0.5% (w/w) were blended at room temperature with the CMC gels and emulgels. Gels were sterilized according to US Pharmacopeia with 2.5 Mrad (USP 24).

5.2.5 Optimization of cationic submicron emulgels and thermal stability tests

A typical formulation consisted of (w/w%) MCT (4.5), Lutrol F127 (0.9), glycerol (1.8), oleylamine (0.45), and vitamin E (0.01), and double distilled water (DDW) up to 90. Preliminary trials were undertaken to establish the effect of the OA:MCT ratio ranging from 1:10 to 1:20 (w/w) on the physical characteristics and stability of emulgels. In all formulations, the percentage of excipients was kept constant. In order to test thermal stability 10 g of CMC gel and emulgel were put in glass bottles and subjected to stability studies at 4°C, 25°C, and 40°C for a period of 3 months. Samples were

withdrawn at 15-day intervals and inspected visually for their color, homogeneity, consistency, spreadability, and phase separation. The pH values of 1% aqueous solutions of either CMC gels or emulgel preparations were measured by an Acumet AB15 pH meter (Fisher Scientific Company, Toronto, ON).

5.2.6 Viscosity measurements

The viscosity of the submicron emulgels and CMC gels was determined using a Viscomate VM-10A (CBC Co.Ltd, Japan) at 25°C.

5.2.7 Swelling and dehydration assessment

The CMC gels and submicron emulgels were soaked in excess PBS, pH 7.4, at 37°C. The swollen hydrogels were weighed at regular time intervals after removal of the excess buffer and the buffer was replaced after each weighing. The swelling ratio was calculated by dividing the increase in the weight of swollen gel ($W_t - W_0$) to the original weight of the gel as shown below:

$$Q = [(W_t - W_0)/W_0]$$

where W_0 is the original weight of the gel and W_t is the weight of the gel at time t.

To measure the dehydration rate, CMC gels and submicron emulgels were incubated at 37°C in a vacuum chamber containing silica powder. The CMC gels and emulgels were weighed at regular time intervals. The dehydration ratio (D) was calculated by dividing the reduction in the weight of the gel ($W_t - W_0$) to the original weight of the gel as shown below:

$$D= [(W_t - W_0)/W_0]$$

where W_0 is the original weight of the gel and W_t is the weight of the gel at time t.

5.2.8 SME characterization following ASA and stratifin association

Droplet size, polydispersity, and zeta potential (ζ) of SMEs following association with ASA and stratifin were measured with Zetasizer Nano Series ZS (Malvern Instruments, Ltd, USA). SMEs with different concentrations of oleylamine (OA) (0.00%,

0.45%, 0.90 %, w/w) were examined. Stratifin and ASA associated SMEs were incubated overnight at 4°C. Samples were diluted 1000 times using DDW and measured at 25°C. Measurements were conducted using 3 preparations (n = 3). Mean values and standard deviations were calculated.

5.2.9 Determination of stratifin and ASA loadings

SFN-FITC and ASA-loaded CMC gels and emulgels (100 mg) were suspended in 10 mL of PBS 7.4 and incubated overnight at 37°C. Bovine serum albumin (BSA) in concentration of 0.1 % (w/w) was added to the SFN-FITC contained buffers in order to reduce surface protein adsorption. The solutions were vortexed and centrifuged, and the supernatant was analyzed to determine SFN-FITC content using an Infinite® F500 microplate reader (TECAN Trading AG, USA) at excitation and emission wavelengths of 485 nm and 535 nm, respectively. Samples were assayed spectrophotometrically for ASA content at 302 nm using BioTek™ absorbance microplate reader (BioTek Instruments Inc, USA).

5.2.10 *In vitro* release studies of ASA and SFN-FITC

100 mg of CMC gel and submicron emulgel containing either ASA (0.5 %, w/w) or SFN-FITC (0.002 %, w/w) were placed on Millicell inserts (PTFE, 0.4 μm) (Millipore, USA) and then placed into 24-well cell culture plates containing 1 mL PBS, pH 7.4, as described previously (Rahmani-Neishaboor et al., 2009). The release media for SFN-FITC associated formulations contained 0.1% BSA to reduce surface protein adsorption. The plates were kept in an incubator at 37 ± 0.5°C with constant agitation at 100 rpm. Samples were taken at 15 and 30 min followed by at 1, 1.5, 2, 3, 4, 6, 7, 8, 10, 12, 14, 16, 18, 20, 22, and 24 h. One millilitre of PBS was periodically withdrawn from the bottom chamber and replaced to maintain the drug concentration within sink conditions. ASA release was analyzed using a BIOTEK™ absorbance microplate reader set at 302 nm. SFN-FITC release was detected by an Infinite® F500 microplate reader set at excitation and emission wavelengths of 485 and 535 nm, respectively. *In vitro* release studies were conducted using 4 preparations (n = 4). Care was taken to ensure that sink conditions were not violated for both ASA and SFN-FITC. The effect of OA concentration ranging

from 0% to 0.9% (w/w) was evaluated on controlling the release of ASA and stratifin from submicron emulgels.

5.2.11 Biocompatibility of SFN/ASA-containing emulgels

In order to evaluate the biocompatibility of the SFN/ASA-containing submicron emulgels, cytotoxicity of the formulations were tested on human dermal fibroblasts and keratinocytes. Cultured fibroblasts and keratinocytes were prepared with the method as described previously (Li et al., 2009) and plated in 24-well plates with cell density of 1×10^5 and 2×10^5 per well, respectively. DMEM with 10% fetal bovine serum (FBS) was used for culturing fibroblasts, and KSFM supplemented with 25 μg/mL of bovine pituitary extract and 0.2 ng/mL of EGF was used for culturing keratinocytes.

Stock solutions of SFN and ASA (0.002% and 0.5%, w/w) containing emulgels were prepared using either DMEM for fibroblasts or KSFM for keratinocytes in the ratio of 6 mg/mL. Various dilutions were prepared at volume ratios of 1:1, 1:1.5, 1:3, 1:6, and 1:12 and added to the cells. As positive control cells were exposed to fresh media, and as negative control cells were exposed to 30% (v/v) ethanol for 30 min. Cell viability were measured using LIVE/DEAD® Viability/Cytotoxicity Kit (Invitrogen, Burlington, ON) (Stratton et al., 2009). The LIVE/DEAD assay uses calcein AM (ex. 500 nm/em. 520 nm) and ethidium (ex. 530 nm/em. 620 nm) homodimer to detect living or dead (dying) cells, respectively. Five randomly selected positions in each well were chosen, and images were taken using a fluorescence microscope (Carl Zeiss Ltd, Toronto, ON). Cells were counted using the particle analysis function of Image J software. The viability was determined by measuring the number of live cells divided by the total number of cells for each treatment.

5.2.12 Hypertrophic scar model

The fibrotic rabbit ear model of cutaneous scarring was used as previously described with minor modifications (Rahmani-Neishaboor et al., 2010). All of the animal work was reviewed and approved by the University of British Columbia Animal Care Committee. Three New Zealand White rabbits weighing 4.5-5 kg were kept under standard conditions at the University of British Columbia Animal Care Center. Animals were anesthetized with an IM injection of ketamine (22.5 mg/kg) and xylazine

(2.5 mg/kg) followed by isoflurane gas through tracheal intubation. Four full-thickness wounds were created down to cartilage on the ventral side of each ear using an 8-mm punch biopsy. Two wounds, separated by at least 1 cm, were made on each side of midline. Wounds were divided into three groups. Each group consisted of wounds on both lateral and medial sides of the ear. Wounds were cleaned every day and covered with Tegaderm® dressing (3M, Minnesota, MN). They were observed daily for signs of infection. Treatments were started on post-operative day 7, when granulation tissue formation had begun from the wound corners. Wounds were treated with submicron emulgels containing both stratifin (0.002%, w/w) and ASA (0.5%, w/w) once a day. Untreated and emulgel vehicle treated wounds were considered as controls.

5.2.13 Measurement of wound area

Wound size was determined every 3 days. Wound areas were measured using Image J image processing and analyzing software. The percent of wound closure was calculated using the following equation:

$$\% \text{ Wound closure} = (A_0 - A_t)/A_0 \times 100$$

where A_0 is the original wound area and A_t is the area of wound at the time of measurement (t).

Photographs were taken on post-operative days 17 and 28. Animals were sacrificed on post-operative day 28, and scars were harvested.

5.2.14 Tissue preparation and histologic analysis

Scars were harvested with a 0.5-cm margin of surrounding unwounded tissue and bisected through the maximum point of scar hypertrophy on visualization and palpation. One half of each wound was fixed in 10% (v/v) neutral buffered formaldehyde, dehydrated, embedded in paraffin, cut in 5 μm sections, and stained with hematoxylin and eosin (H&E). The other half was stored at –80 ºC for RNA extraction.

5.2.15 Scar elevation index and epidermal thickness index

The scar elevation index (SEI) measures the ratio of total scar area to the area of normal underlying dermis, as described previously by Morris et al (Morris et al., 1997).

All measurements were taken within the confines of the wounded area at 100× magnification from the H&E stained tissue sections. The epithelial height is not considered in SEI calculations. An SEI >1 denotes HS formation.

The epidermal thickness index (ETI) was used to determine the degree of epidermal hypertrophy and was based on measurements taken from H&E stained tissue sections at 400× magnification. The entire cross-section of scar was measured for epidermal thickness, which corresponded to a total of five fields. The epidermal thickness from five fields of uninjured skin was also measured from both sides of the scar. The ETI was then determined by calculating the ratio between the averaged epidermal height in scar tissue and the averaged epidermal height in uninjured skin (Brown et al., 2008; Tandara and Mustoe, 2008). ETI > 1 denotes hypertrophic epidermis formation.

5.2.16 Total tissue cellularity and infiltrated $CD3^+$ immune cells

Paraffin-embedded sections (5 μm) were deparaffinized using standard protocol. Antigen retrieval was performed to expose surface antigens, which have become masked by the tissue fixation process as described before (Rahmani-Neishaboor et al., 2010). For antibody staining, sections were incubated with rabbit anti-T cell CD3 peptide (1:50; Abcam, Cambridge, MA) at room temperature for 1 h. The second antibody was Alexa Fluor® 488 goat anti-rabbit IgG (Invitrogen, Burlington, ON). The second antibody was used in a concentration of 1:1000. The slides were counterstained with 4′,6-diamidino-2-phenylindole (DAPI). For each wound, five randomly chosen fields of dermis were photographed under 400× magnification (high power field (hpf)) using a Zeiss fluorescent microscope and Axiovision software. Photographs were subsequently coded and randomized, and the number of nuclei and $CD3^+$ immune cells were counted using Image Pro Plus 4.5 software. The counts from the corresponding fields were averaged and shown as cells/hpf.

5.2.17 MMP-1 expression in tissue

MMP-1 expression in tissue samples was examined by extracting RNA from tissue using the RNeasy fibrous tissue mini kit (Qiagen, USA) according to the manufacturer's instructions. Extracted RNA were then reverse transcribed to cDNA by the Thermo Script RT-PCR system (Invitrogen, Canada). The resulting cDNAs were used

to perform polymerase chain reactions (PCRs) for the primers of MMP-1 ([fwd] CAGCTTTATGGGAGCCAGTC and [rev] TGTTCCTCACCCTCCAGAAC, product size: 200 bp). Glyceraldehyde-3-phosphate dehydrogenase (GAPDH) was used as a endogenous control gene in order to normalize PCRs for the loaded RNA. The sequences of GAPDH primers were ([fwd] GAGCTGAACGGGAAACTCAC and [rev] TGCTGTAGCCAAATTCGTTG, product size: 300 bp).

5.2.18 Collagen density

Paraffin-embedded sections (4 μm) were mounted on glass slides and stained for collagen with Masson's trichrome, in which collagen stained blue. For each wound, five randomly chosen fields of dermis were photographed under 400× magnification. Collagen deposition areas were estimated by the Image Pro Plus 4.5 software (Rahmani-Neishaboor et al., 2010) and normalized by dividing by the unwounded skin collagen density.

5.2.19 Statistical analysis

All data are expressed as mean ± SD. Data were analyzed using the ANOVA Tukey-Kramer multicomparisons test to compare the means between study groups and their controls. The level of significance was set to *P* values less than 0.05.

5.3 Results and Discussion

5.3.1 Formulation and thermal stability of cationic submicron emulgels

The sensitivity of the wound environment limits material options to be used in formulation. An ideal formulation should be able to absorb wound exudate and form an occlusive film that eliminates dehydration of the wound and prevents bacterial contamination.

To meet these criteria, a non-ionic tri-block copolymer, Lutrol F127 was used as emulsifier to form an O/W emulsion. Lutrol F127 has low irritability and also been shown to accelerate healing in third degree burns (Escobar-Chavez et al., 2006). Non-saturated medium chain triglycerides were used as the main component of the oil phase. Oleylamine was used as a co-emulsifier to stabilize the nano droplets and also sustain the release of negatively charged stratifin and ASA. The thermoreversible property of Lutrol

F127 resulted in the formation of an occlusive film on wound bed. Emulgels with an OA:MCT ratio of 1:10 (w/w) were found to be stable upon storage for 3 months at 4°C, 25°C, and 40°C.

5.3.2 Physicochemical characterization of submicron emulgels

The emulgel formulations developed are white, odorless preparations with smooth, homogenous appearances. They are easily spreadable and have good aesthetic appeal. Viscosity studies were carried out using Viscomate VM-10A to check formulation flow properties. The values were found to be 340 and 290 Cps for CMC gels and submicron emulgels at room temperature, respectively. The reduction in viscosity for emulgels corresponded to an easier application on the wound bed when compared with CMC gels.

5.3.3 Swelling and dehydration properties of CMC gels and submicron emulgels

Swelling studies were performed for the CMC gels and submicron emulgels. The maximum swelling ratio of the emulgels was 177% and for CMC gels was 62% (Fig. 5.2 A). The higher swelling property of the emulgels could be due to tri-block co-polymer and amphipathic lipid contents. On the other hand, the *in vitro* dehydration results showed that the dehydration rate of submicron emulgels was not significantly different from that of CMC gels (Fig. 5.2 B), which emphasizes the ability of emulgels to absorb wound exudates while preventing maceration. Additionally, emugels were able to form thin film on the wound; this film is easily removed when wetted (Fig. 5.2 C).

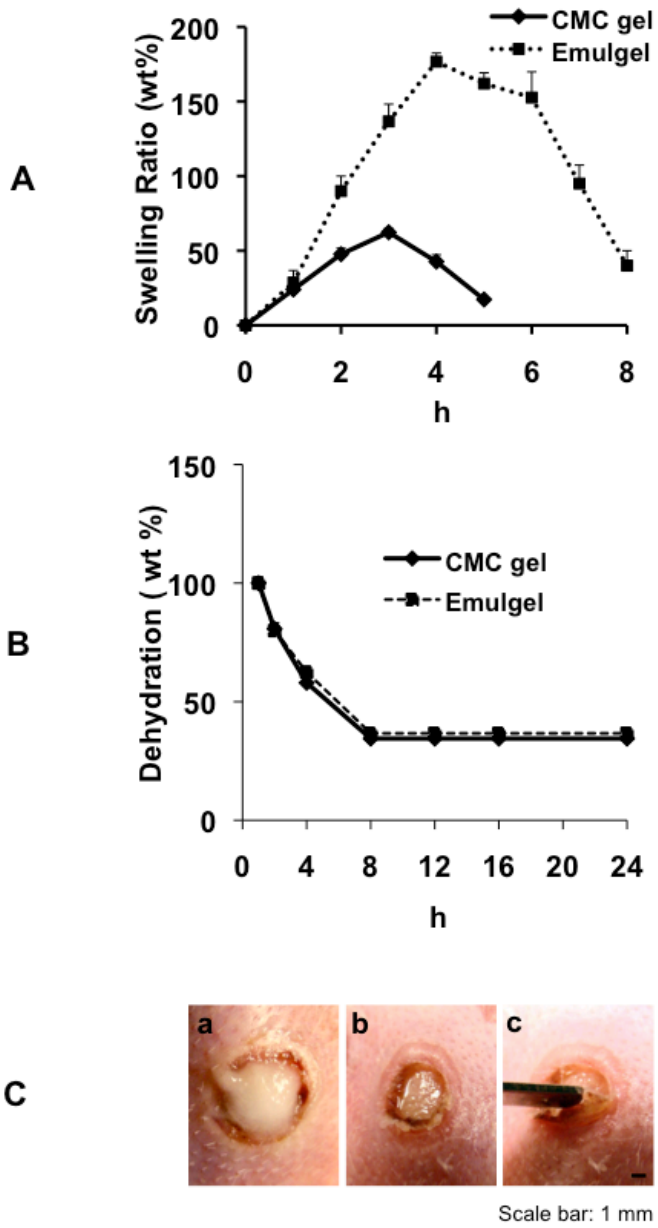

Fig. 5.2. (A) Swelling and (B) dehydration behavior of submicron emulgels and CMC gels. (C) Emulgels (a) at time of application, (b) after 24 h, (c) emulgels can be easily removed following wetting with normal saline.

5.3.4 Submicron emulsion droplet size and zeta potential following SFN/ASA association

In order to examine the effect of different charge balances for micelle emulsified stratifin and ASA, droplet size and zeta potential were evaluated (Table 5.1). Emulsions in the absence of OA had a mean droplet size of 620.5 nm with negative charge of –6.5 ± 4.1 mV. When the concentration of OA was increased to 0.45% (w/w), the mean diameter of oil droplets decreased to 300 ± 23 nm and zeta potential increased to 40.1 ± 5.3 mV. Further increase of OA concentration to 0.9% (w/w) did not significantly alter the size and zeta potential of oil droplets.

Table 5.1. Physicochemical properties, droplet size (DI), and zeta potential (ζ), of submicron emulsions prepared with various concentration of oleylamine (OA) following ASA and stratifin (SFN) association

SME type	Blank SME		ASA associated SME		SFN associated SME		SFN/ASA associated SME	
	DI (nm)	ζ (mV)	DI (nm)	ζ (mV)	DI (nm)	ζ (mV)	DI (nm	ζ (mV)
Without OA	620±47	–6.5±4.1	430±33	–0.1±4.1	219±18	–6.6±4.4	205±23	–8.1±2.4
OA 0.45	300±23	40.1±5.3	271±25	37.3±4.7	194±21	4.1±3.4	113±11	5.8±5.5
OA 0.90	250±19	40.3±4.7	136±12	41.4±5.5	147±11	–5.1±2.4	152±16	31.5±4.8

Incorporating SFN (0.002%, w/w) or ASA (0.5%, w/w) individually into SMEs (OA, 0.45% w/w) dropped the zeta potential of oil droplets from 40.1 ± 5.3 mV to 4.1 ± 3.4 mV or 37.3 ± 4.7 mV, respectively. Combining both SFN and ASA into a single emulgel formulation (OA, 0.45% w/w) dropped the zeta potential to 5.8 ± 5.5mV. This depletion in zeta potential of oil droplets could be attributed to the interaction of positively charged OA with negatively charged drugs, mostly stratifin (Hagigit et al., 2008). This surface charge interaction could be one of the reasons that SFN and ASA are sustainably released from cationic submicron emulgels. In fact, this interaction did not have any negative effect on the droplet size and stability of the submicron emulsions.

5.3.5 SFN-FITC and ASA loading and *in vitro* release

The average loading efficiency of CMC gels for ASA and SFN-FITC were 103 ± 4% and 100 ± 1.5%, respectively. Loading efficiency for submicron emulgels was 102 ± 1% for ASA and 103 ± 3% for SFN-FITC on average.

The *in vitro* release profiles of SFN-FITC and ASA from CMC gels and submicron emulgels are shown in Fig. 5.3. Stratifin-FITC demonstrated a 3-fold difference in sustained release from emulgels compared with CMC ($p < 0.001$) (Fig. 5.3 A, B). Similarly, ASA exhibited a 3.5 fold slower release from emulgel compared with CMC ($p < 0.001$). The reduction in burst release exhibited by emulgels could be a result of the amphipathic polymers and lipids. The observation that ASA released faster than stratifin is likely because smaller molecules will diffuse at a faster rate.

To define the effect of oleylamine (OA) on controlling the release of SFN and ASA, release kinetics of SFN-FITC and ASA from submicron emulgels containing various OA concentrations, 0% to 0.9% (w/w), were studied (Fig. 5.3 C and D). Increasing the OA concentration from 0% to 0.9% (w/w) did not significantly control the release of ASA (Fig. 5.3 C). This observation can be attributed to the low surface charge interaction between ASA and oil droplets, as obtained from zetametry data. It was observed that ASA association with the concentration of (0.5%, w/w) did not significantly alter the zeta potential of oil droplets ($p > 0.05$) (Table 5.1). However, increasing the OA concentration from 0% to 0.45% (w/w) controlled the release of SFN-FITC significantly. Since increasing the OA percentage to 0.9% (w/w) had no significant effect, data suggest that 0.45% OA is the preferred concentration. It has been reported that adding OA to submicron emulsions causes a decrease in release rate of the negatively charged drugs due to a greater partitioning into the micellar region within the gel structure (Hagigit et al., 2008).

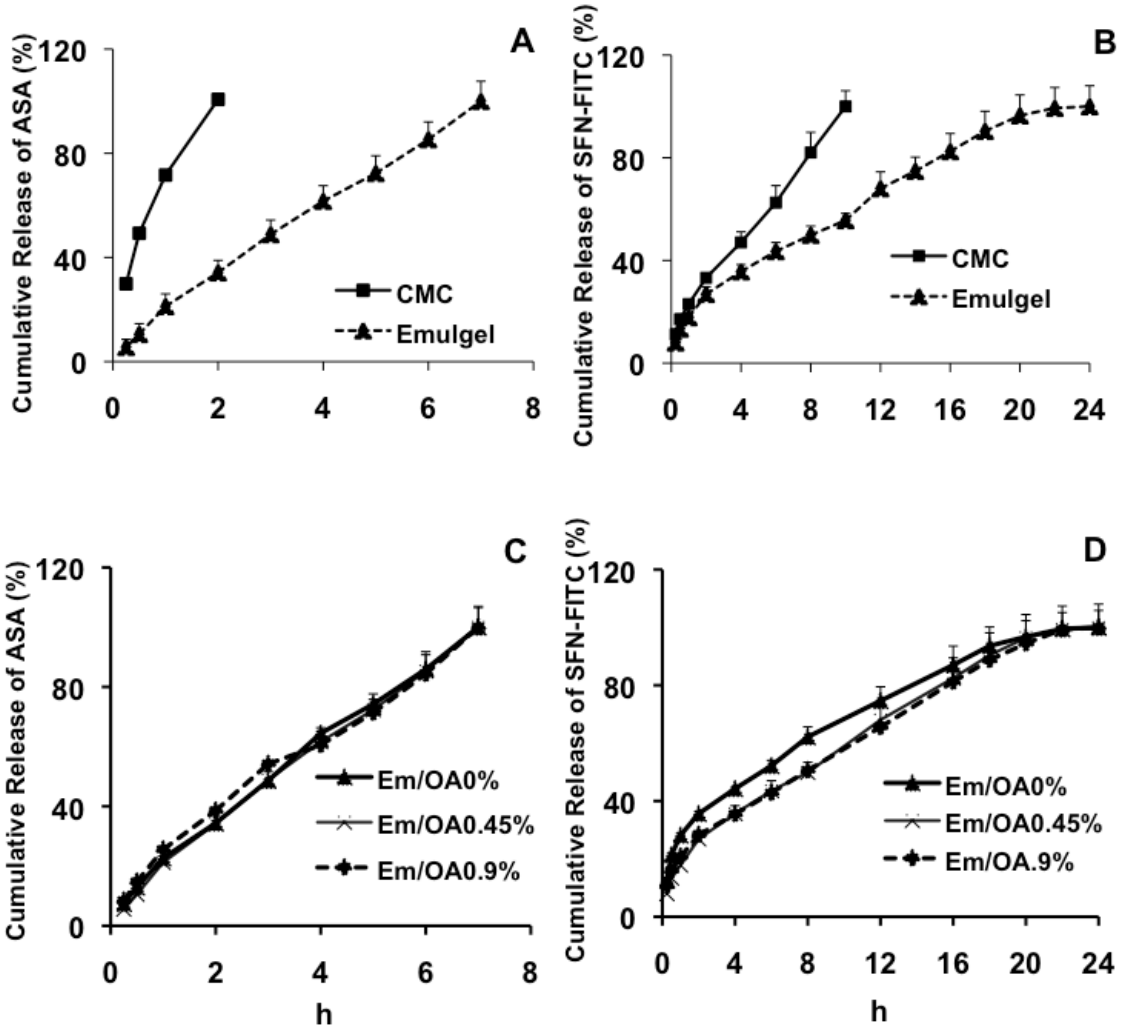

Fig. 5.3. *In vitro* release profiles of (A) SFN-FITC and (B) ASA from submicron emulgels and CMC gels. *In vitro* release profiles of (C) SFN-FITC and (D) ASA from submicron emulgels as a function of various concentrations of oleylamine.

5.3.6 Biocompatibility of SFN/ASA- containing emulgels

The biocompatibility of SFN/ASA-containing submicron emulgels was tested on human skin fibroblasts and keratinocytes using a LIVE/DEAD assay. The number of viable cells was assessed after treatment with emulgel extracts with actual concentrations of 0.5, 1, 2, 4, and 6 µg/mL in culture media (Fig. 5.4 A, F, and K). Results showed that there was no significant reduction in viable cells following incubation of emulgel extracts in different concentrations with either fibroblasts or keratinocytes (Fig. 5.4 B) ($p > 0.05$, $n = 4$) when compared with untreated controls.

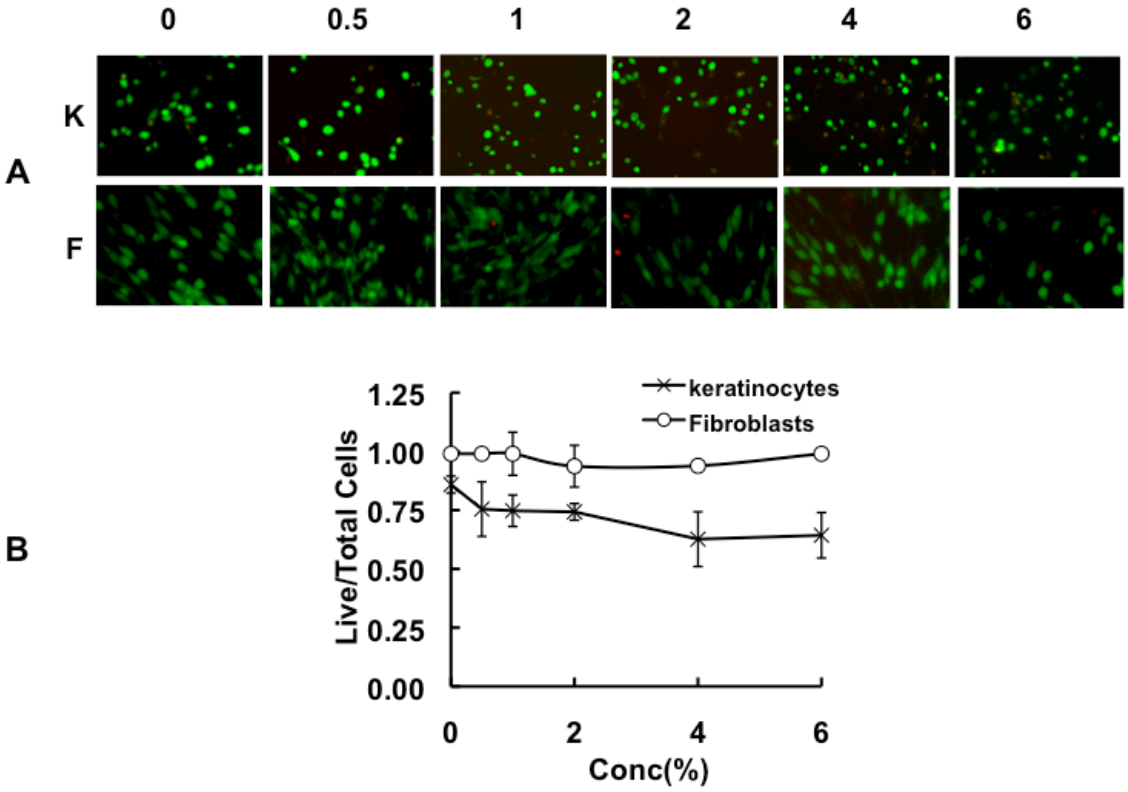

Fig. 5.4. (A) Biocompatibility of various concentrations of SFN/ASA-containing submicron emulgels (0.5, 1, 2, 4, and 6 mg/mL) by LIVE/DEAD assay on human skin keratinocytes (K) and fibroblasts (F). Green and red areas represent live and dead cells, respectively. (B) The cell viability was determined by measuring the number of viable cells divided by the total number of cells for each treatment group.

5.3.7 Qualitative wound assessment

Macroscopic analysis of the wounds indicated that wound closure was significantly faster in untreated and emulgel treated wounds compared with SFN/ASA treated ones (Fig.5.5). SFN/ASA treated wounds were still open while untreated and emulgel treated wounds were 100% and 97% closed by post-operative day 17, respectively (Fig. 5.5 A, D17). Qualitative wound assessments showed that SFN/ASA treated wounds were closed with the constant rate of 3.3 mm^2/day (Fig. 5.5 B). Untreated and emulgel treated wounds exhibit a higher closure rate during the first 2 weeks, yet emulgel treated wounds exhibited a slower rate on week 3. This observation could be due to the moisture balance demonstrated by the gel and or the stimulation of MMP-1 (Tandara et al., 2008). Complete wound closure for all groups was achieved within 21 days, which suggests that prolonged wound closure does not result in a chronic non-healing wound.

On day 28 scar sections were collected for evaluation of visibly raised and palpable scar with HS evidence (Fig. 5.5 A, D28, Untrt). Emulgel treated wounds exhibited less hypertrophic scarring compared with the untreated controls (Fig. 5.5 A, D28, Emulgel). Wounds treated with SFN/ASA-containing emulgel had the appearance of mature scars and appeared the flattest amongst all other treatment groups (Fig. 5.5 A, D28)

5.3.8 Reduced scar elevation index and epidermal thickness index

SEI and ETI were measured to quantify the degree of dermal and epidermal hypertrophy for different wounds, as described in Section 5.2. The mean SEI in SFN/ASA treated wounds was 1.18 ± 0.16 ($n = 12$), which was significantly lower than that of untreated (SEI = 1.9 ± 0.18, $n = 9$, $p < 0.001$) and emulgel treated wounds (SEI = 1.49 ± 0.19, $n = 9$, $p < 0.01$) (Fig. 5.5 C, D). This represents a significant reduction in dermal hypertrophy of 80% and 63% compared with the untreated and emulgel treated wounds. Treatment with a vehicle emulgel showed a significant reduction of 46% in the mean SEI compared with that of untreated wounds ($n = 9$, $p < 0.001$) (Fig. 5.5 C, D), which may in part be due to the hydrating qualities of the gel, which may alter cytokine and growth factor secretion from keratinocytes (Tandara et al., 2008).

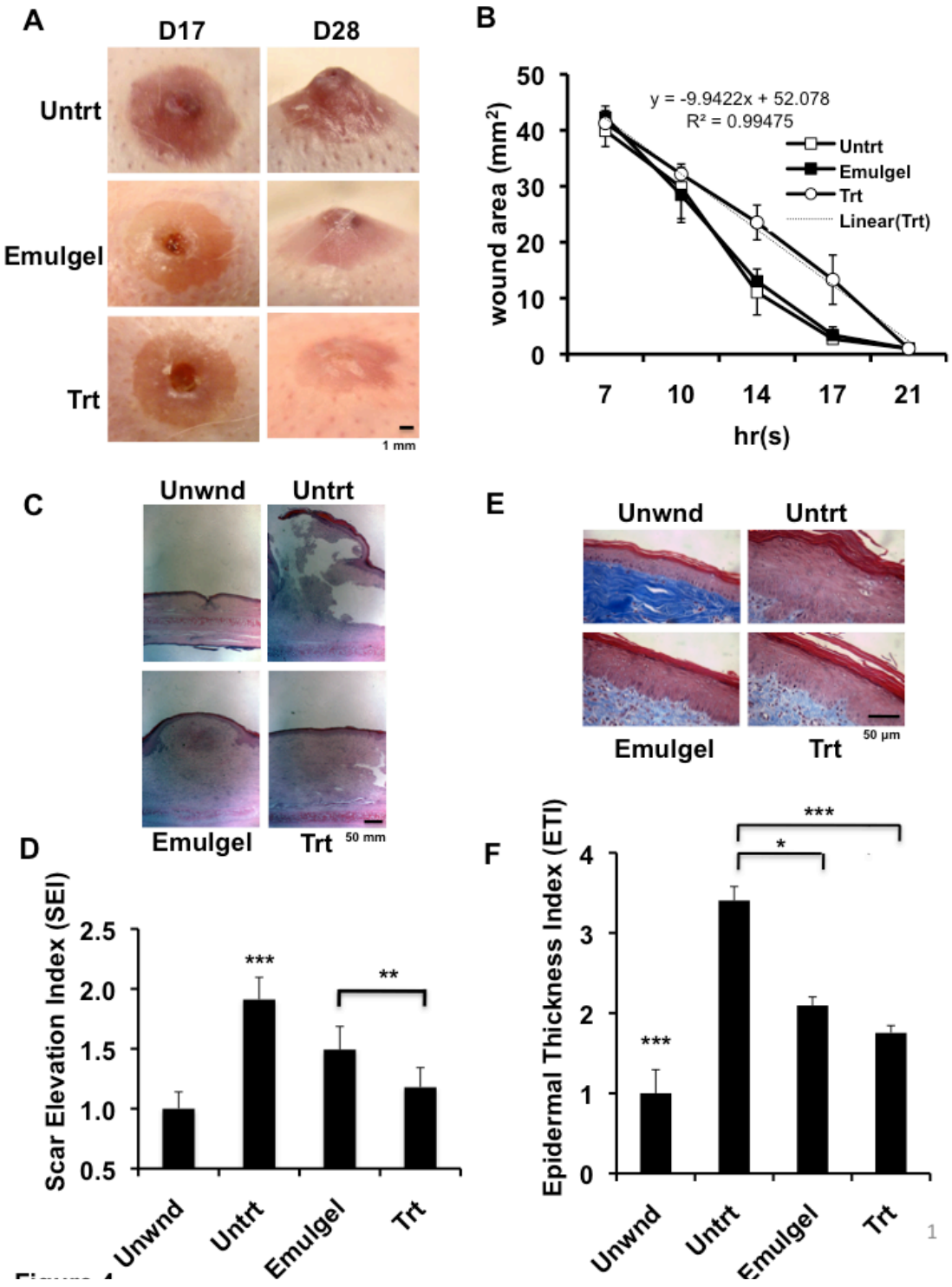

Fig. 5.5. (A) Clinical appearance of the wounds at post-operative days 17 and 28, (B) profile of wound closure, (C) microscopic histology of normal skin and scars, H&E staining, (D) scar elevation index, (E) microscopic histology of epidermis, Masson trichrom staining, and (F) epidermal thickness index calculated for unwounded skin (Unwnd), untreated wounds (Untrt), and wounds treated with emulgel alone (Emulgel) or SFN/ASA-containing emulgels (Trt).

The mean ETI of untreated wounds was 3.4 times greater than that of normal unwounded skin ($n = 9$, $p < 0.001$) (Fig. 5.5 E, F). Epidermal thickness decreased in wounds treated with SFN/ASA-containing emulgel to a mean ETI of 1.8 ± 0.09 compared with that of untreated controls (3.4 ± 0.17) (Fig. 5.5 F, Trt). This corresponds to a respective 66 % ($p < 0.001$) ETI reduction. The ETI of wounds treated with emulgel only was 2.1 ± 0.11, which corresponds to a 54% reduction in ETI ($p < 0.001$). It has been reported that epidermis responds to water loss with epidermal proliferation to restore the stratum corneum functional barrier. These data suggest that emulgel is superior to CMC at reducing ETI. In our previous studies, we demonstrated that CMC alone can reduce the ETI (Rahmani-Neishaboor et al., 2010). Furthermore, this confirms that the synergic effect of emulgels with active ingredients stratifin and ASA reduces epidermal hypertrophy.

5.3.9 Reduced total tissue cellularity and infiltrated $CD3^+$ immune cells

Total tissue cellularity and infiltrated $CD3^+$ T cells were counted to characterize and quantify fibrosis and inflammation. T cells as a marker of inflammation are among the most infiltrated immune cells present in both the active and remission phases of hypertrophic scarring (Castagnoli et al., 1997). Total cellularity of dermis was assessed using DAPI nuclear staining (Fig. 5.6 A). Untreated wounds showed the highest cell count with an average of 157 ± 35 cells/hpf. Total dermal cellularity was significantly reduced in wounds treated with SFN/ASA-containing emulgels (Fig. 5.6 B, solid bars), with 88 ± 17 cells/hpf. This corresponds to a 60% ($p < 0.01$) reduction in dermal cellularity. Cell counts in wounds treated with emulgel alone had a mean of 113 ± 29 cells/hpf, which corresponds to a 38% reduction in dermal cellularity ($p < 0.01$) compared with those of untreated controls. Once a day application of SFN/ASA-containing emulgels showed comparable reduction in cellularity to a twice a day application of SFN-containing CMC gels. This effect was significantly higher than the effect of twice a day application of ASA-containing CMC gels (Rahmani-Neishaboor et al., (2010).

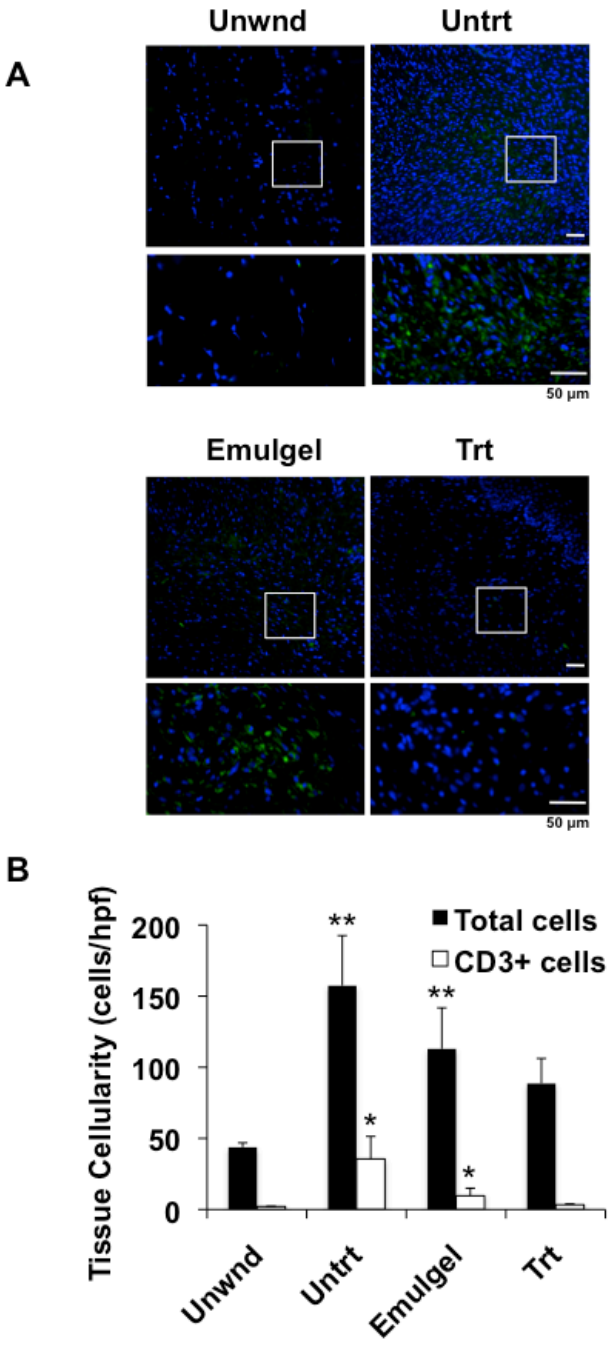

Fig. 5.6. (A) Total tissue cellularity (blue, Dapi staining) and infiltrated $CD3^+$ T immune cells (green, immunostaining) within wounds at post-operative day 28. (B) Total tissue cellularity (solid bars) and $CD3^+$ T cells (open bars) in sections of unwounded skin (Unwnd), untreated wounds (Untrt), wounds treated with emulgel alone (Emulgel), or SFN/ASA-containing emulgels (Trt) are quantified and compared.

It is well established that hypertrophic scarring is associated with high cellularity. Additionally, it is expected that low cellularity following wound healing is suggestive of either reduced inflammatory response or less ECM deposition. Therefore, to evaluate the inflammatory response following wound healing, the numbers of infiltrating $CD3^+$ T cells were compared among treatment groups. $CD3^+$ T cells in the dermis of unwounded skin were barely detectable (Fig. 5.6 A, green fluorescence). Untreated scars had the highest $CD3^+$ T cell count with a mean of 36 ± 6 cells/hpf. The number of $CD3^+$ T cells in the dermis was reduced in wounds treated with SFN/ASA-containing emulgels to a mean of 3 ± 1 cells/hpf (Fig. 5.5 B, open bars). This corresponds to a 97% ($p < 0.001$) reduction in the dermal $CD3^+$ T cell count. Wounds treated with emulgel had a mean of 10 ± 2 cells/hpf, which corresponds to a 76% decrease in the number of $CD3^+$ T cells in the dermis ($p < 0.05$) (Fig. 5.6 B, open bars). The high number of $CD3^+$ T cells observed in untreated wounds may be due to the prolongation of the inflammatory phase, as discussed in a previous study (Rahmani-Neishaboor et al., 2010).

Topical application of SFN/ASA-containing emulgel significantly reduced the infiltration of $CD3^+$ T cells to the injured tissue (97%). In fact, the combination of stratifin and ASA exhibited a greater reduction in $CD3^+$ cells compared with using either drug alone (Rahmani-Neishaboor et al., 2010).

5.3.10 MMP-1 mRNA expression

As shown in Fig. 5.7 A, MMP-1 mRNA expression was the highest in wounds treated with SFN/ASA-containing emulgels. To quantify the data, the ratio of MMP-1/GAPDH in unwounded skin was arbitrarily set to 1.0, based on band signal intensities. The ratio of MMP-1/GAPDH in wounds treated with SFN/ASA-containing emulgel was approximately 4-fold higher by comparison (mean of 4.1 ± 0.3, $n = 12$, $p < 0.001$) (Fig. 5.7 B). Averaged MMP-1/GAPDH ratio for wounds treated with emulgel only was 3.0 ± 0.3, which was not statistically significant when compared with that of untreated wounds ($p > 0.05$).These results suggest a greater expression of MMP-1 in emulgel treated wounds relative to those treated with CMC (Makidon et al., 2010b). In fact, Tandra et al. demonstrated in an *in vitro* keratinocyte-fibroblast co-culture model, hydration of

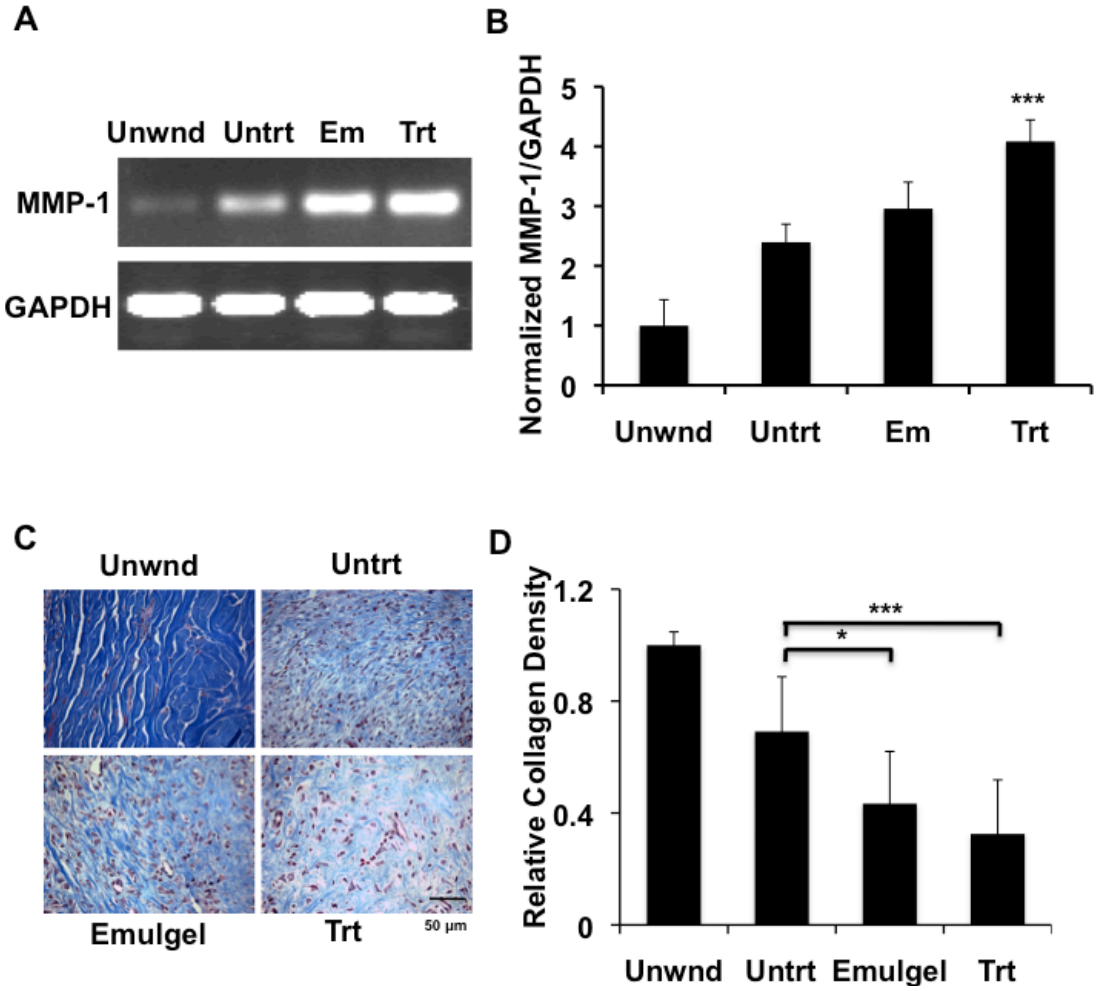

Fig. 5.7. (A) MMP-1 mRNA expression in unwounded tissue (Unwnd), untreated wound (Untrt), wounds treated with emulgel alone (Em), and SFN/ASA-containing emulgel (Trt) were analyzed by RT-PCR. RNA loadings were compared using GAPDH internal control. (B) Semi-quantitative level of MMP-1 mRNA expression for each group was analyzed by densitometry of the corresponding bands and represented as the ratio of MMP-1 expression to GAPDH. (C) Microscopic histology of Masson's trichrome stained sections for collagen, (D) Relative collagen density in sections of unwounded skin (Unwnd), untreated wound (Untrt), wounds treated with emulgel alone (Emulgel), or SFN/ASA-containing emulgel (Trt) are quantified and compared.

keratinocytes significantly affected on MMP activity (Tandara et al., 2008). As such, emulgels are able to create a moisture-balanced environment owing to their film forming ability within which keratinocytes produce MMP-1 stimulating factor for fibroblasts. This would be, at least in part, the reason for increased MMP-1 expression in emulgel treated wounds.

5.3.11 Collagen density

In order to determine if the increase MMP-1 expression correlated with a decrease in collagen deposition, wound sections were stained with Masson's trichrome. The relative density of collagen in untreated wounds was 0.69 ± 0.19, which was significantly lower than that of unwounded skin ($p < 0.001$). Collagen density was significantly reduced in wounds treated with SFN/ASA-containing emulgel compared with that of untreated wounds (Fig.5.7 C, D). The mean value for SFN/ASA treated wounds was 0.32 ± 0.11, which corresponds to 54 % reduction in collagen density compared with that of untreated controls. Wounds treated with a combination of SFN/ASA appeared to have a superior effect on reducing collagen deposition compared with either drug alone, observed in our previous study (Rahmani-Neishaboor et al., 2010).

5.4 Conclusions

A thermoreversible submicron emulgel formulation was created to regulate the late-stage wound healing through a controlled release of stratifin and acetylsalicylic acid. These emulgels were able to absorb excess wound exudates and form an occlusive film on wound surface. Submicron emulgels provided a significantly improved controlled release of stratifin and ASA compared with conventional CMC gels. Moreover, thermoreversible submicron emulgels effectively reduced the number of required applications when compared with CMC gels, which should translate to improved patient comfort and compliance. Interestingly, emulgels in the absence of any drug significantly mitigate scar size. Finally, wounds treated with SFN/ASA-containing emulgels on a daily basis showed a significant reduction in both collagen density and tissue cellularity. The findings of this study suggest that submicron emulgels provide a feasible means by which the delivery of both stratifin and acetylsalicylic acid is controlled to the wound bed of patients who are at risk of developing dermal fibrosis.

Chapter 6. Conclusions and Suggestions for Future Work

6.1 General Discussion

Wound healing is a dynamic process that strikes a fine balance between synthesis and degradation of extracellular matrix (ECM) (Singer and Clark, 1999; Yang et al., 2003). Non-healing and over-healing are two extreme cases in which the biomechanical processes of normal tissue are disturbed owing to either deficiencies or alterations in ECM composition and organization. Although the promotion of healing in patients is clearly desirable, its cessation is equally important. Prolonged "early-stage" healing events can lead to excessive matrix components and deleterious fibrotic conditions (Norton, 2008). Over-healing processes such as keloid and post-burn hypertrophic scarring are disfiguring and devastating, resulting in bulky, itchy, and inelastic scars that pose serious cosmetic and functional problems for millions of patients who suffer from burn wounds or are exposed to surgical incision and skin trauma (Tredget et al., 1997). Current treatment modalities for dermal fibrosis such as hypertrophic scarring and keloid remain unsatisfactory (Mutalik, 2005). Pressure garment therapy, intralesional injections of corticosteroids, and surgical revision are routinely used for treatment of post-burn hypertrophic scarring, but all of these treatments have significant shortcomings. Pressure garments must be worn for up to two years to be effective; steroid use is limited by the risk of systemic side effects and is not suitable for scars covering large areas; and surgical revision often results in recurrence of the condition. These treatments are particularly devastating for pediatric patients who, by virtue of their limited life experiences, have difficulty dealing with these problems and often develop acute or long-term psychological disorders (Leventhal et al., 2006; Mutalik, 2005; Niessen et al., 1999; Poston, 2000; Sallstrom et al., 1989; Sawada and Sone, 1990). Novel approaches are under development (Occleston et al., 2008).

Epidermal–mesenchymal interactions during wound healing are important in controlling the expression of collagen and other ECM components (Ghahary et al., 2004; Lam et al., 2005; Medina et al., 2007). Normally, there exists a balance between ECM synthesis and degradation. When this balance is altered, wounds may heal with some problems that cause either non-healing wounds or generate excessive matrix

accumulation leading to keloid and hypertrophic scar formation. It has been demonstrated that keratinocytes synthesize and release a strong collagenase-stimulating factor for dermal fibroblasts, which was identified to be stratifin or 14-3-3σ protein (Ghahary et al., 2004). These findings suggest that stratifin, whose anti-fibrogenic effect was established previously, is an ideal natural factor for reducing and/or preventing excessive scarring. It is thought that stratifin slows down the healing process by reducing matrix accumulation (Ghahary et al., 2004).

In this thesis research, the goal was to investigate the potential of stratifin in prevention of hypertrophic scarring in both open and surgically closed wounds. To address the first objective of this study, which was reducing hypertrophic scarring in surgically closed wounds, a microsphere/hydrogel based controlled release system for stratifin was developed. This implant was designed to be placed in surgical wounds before closure and sustainably release stratifin to stimulate the expression of matrix metalloproteinase and degrade excessive collagen produced during the healing process. As reported in chapter 2, this microsphere/hydrogel implant has two advantages: (1) controlling the release of stratifin over 30 days without compromising its bioactivity, (2) reducing the burst release of stratifin to a negligible amount for up to 3 days (Rahmani-Neishaboor et al., 2009). The key to success in this study was to complex stratifin with chitosan (hydrophophilic polymer) before encapsulating into PLGA (hydrophobic polymer), which preserves the protein bioactivity during the microencapsulation procedure. Poly(lactic-co-glycolic acid) (PLGA), a hydrophobic polymer whose biodegradability is adjustable by changing the ratio of lactic acid to glycolic acid monomers, is one of the most appropriate polymers used for the controlled delivery of protein molecules. The main potential problems with using PLGA for this purpose are protein aggregation during the microencapsulating process and a high burst phase of proteins (Diwan and Park, 2001; Sanchez et al., 2003).

The use of composite microspheres containing both hydrophobic and hydrophilic regions for sustaining the release of bioactive proteins has been previously described (Li et al., 2006; Zheng et al., 2004); it typically still produced a burst release of protein. For example, gelatin nanoparticles containing bFGF loaded in PLGA microspheres produced 30% release of bFGF in the first 24 h (Li et al., 2006). Using a composite of alginate–

chitosan in PLGA microspheres, Zheng et al. (2004) reported a reduction in the burst phase of BSA release from 53% to 39%. To further reduce early protein release, some groups have blended protein-loaded microspheres in hydrogel films (DeFail et al., 2006; Huang et al., 2006; Kempen et al., 2008; Lee et al., 2004). Defail et al. (2006) reported the controlled release of TGF-ß1 from PLGA microspheres incorporated into PEG-genipin hydrogels. Within 1 day, the microspheres demonstrated a high burst release of protein (69 ± 29%), while the PEG-genipin scaffold delayed the burst release up to 17 days (72 ± 11%).

Interestingly, the encapsulation of chitosan particles in PLGA microspheres significantly reduced the burst release of stratifin from 73% to 18% in 24 h. Blending PLGA microspheres into hydrogel films reduced the release of stratifin to 5% in 3 days and then controlled it for 30 days so that 60% of the total stratifin loaded was released. This microsphere/hydrogel system exhibited a biphasic release profile for stratifin that was tailored to the wound healing process, with a very low burst release phase in the beginning followed by a faster release phase over 30 days. The released stratifin significantly stimulated the expression of MMP-1 in cultured fibroblasts without compromising cell viability.

In order to test the therapeutic effect of a local controlled delivery of stratifin in reduction of hypertrophic scarring in closed surgical wound; as reported in chapter 3, a rat surgical-wound model was established and used for this purpose. A high swelling ratio was the major downfall of using hyaluronic acid as the implant substrate, which created inappropriate stress on the tissue and made it difficult to surgically close the wound. To solve this problem, the microsphere/hydrogel implant was modified using polyvinyl alcohol (PVA), a synthetic equivalent of hyaluronic acid with a low swelling propensity.

Stratifin-releasing PVA:PLGA implants also demonstrated a reduced burst release of stratifin. This minimum burst release of stratifin did not appear to interfere with wound closure and the observed *in vivo* healing process. Interestingly, the local controlled release of stratifin demonstrated a significant reduction in fibrosis and inflammation induced by stratifin-free microsphere/hydrogel implants. The local and controlled release of stratifin from implants markedly reduced collagen deposition by increasing the

expression of MMP-1 and therefore collagen degradation in the surrounding tissue. This result confirms the *in vivo* biological activity of stratifin released from the implants. Localized delivery of stratifin also suppressed foreign body reactions induced by implantation, namely total tissue cellularity and $CD3^+$ cells. This observation would appear to be a result of the increased MMP-1 expression in surrounding tissue and reduced matrix deposition, which might alter cell proliferation behavior and fibrous tissue formation.

In chapter 4, to address the second objective of this research project, which was testing the therapeutic effect of topically applied stratifin on the reduction of hypertrophic scarring in large open wounds, a rabbit ear fibrotic model was used. Noninvasive delivery of protein macromolecules across intact skin is challenging, as these molecules have typically high molecular weights and poorly permeate across the epithelium layer. One successful strategy to enhance dermal delivery of macromolecules to the healing wounds for prevention of hypertrophic scarring is to apply the medication before complete epithelialization. Liposome associated IFN-alpha-2b applied 5 days post-wounding reduced mRNA for the pro-alpha1 chain of type 1 collagen, confirming its transepidermal penetration and effectiveness (Ghahary et al., 2000).

For topical delivery of stratifin to the healing wounds it was decided to use carboxymethylcellulose (CMC) hydrophilic gels. CMC gel has been used extensively for wound debridement as Intrasite® gel. It is able to donate water to the necrotic and dry wounds. CMC gel also has been used in the formulation of Regranex® for the topical delivery of recombinant PDGF to promote healing in non-healing diabetic foot ulcers.

The therapeutic effect of a topically applied non-steroidal anti-inflammatory drug, acetylsalicylic acid (ASA), in the reduction of hypertrophic scarring in this fibrotic model was also investigated. A critical time point for starting the treatment appears to be around post-wounding day 5 for both ASA and stratifin when granulation tissue started to form in all wounds. Combining the scar reducing effect of either stratifin or ASA with the healing-promoting effect of CMC hydrogel produced a significant improvement in healing quality (Rahmani-Neishaboor et al., 2010). Qualitative wound assessment showed a reduced hypertrophic scarring in stratifin- and ASA-treated wounds when compared with the controls. This study showed that topical application of either stratifin-

or ASA-impregnated CMC gel reduced hypertrophic scar formation following dermal injuries in a rabbit ear fibrotic model. Controlling the inflammation and degradation of collagen were both important for regulating wound healing process resulting in reduced hypertrophic scarring. Combination of both strategies may appear to be an ultimate way to manage hypertrophic scarring.

Histological analysis of the wounds at day 28 post-wounding demonstrated a significant reduction in hypertrophic scar formation in the wounds treated with either stratifin (82%) or ASA (73%) compared with that of untreated controls. A reduction of 57% and 41% in total tissue cellularity and 79% and 91% reduction in infiltrated $CD3^+$ T cells were observed in response to treatment with stratifin and ASA, respectively, compared with those of untreated controls. Wounds treated with stratifin showed a 2.8-fold increase in matrix metalloproteinase-1 expression, which resulted in a 48% decrease in collagen density compared with those of untreated controls.

The objective of chapter 5 was to modify CMC gel into a thermoreversible emulgel containing both stratifin and aspirin with a stronger water barrier capacity and film-forming capability that can control the release of these medications in order to reduce the frequency of application to once a day and to enhance efficacy by promoting their penetration across intact skin. Biphasic vesicles, a novel lipid-based topical delivery system, have been shown to deliver macromolecules into the skin (Foldvari et al., 1999; Foldvari et al., 2010). Submicron O/W emulsions were formulated using pluronic F127 and dispersed in CMC gel to form an emulgel. Submicron emulgels provided a significantly improved controlled release of stratifin and ASA compared with conventional CMC gels. The emulgel formulations did not demonstrate any acute toxicity for primary human keratinocytes and dermal fibroblasts *in vitro*. Efficacy of anti-fibrogenic formulations was tested *in vivo* using a rabbit ear fibrotic model. Emulgels were able to form an occlusive film following topical application on the wounds. Wounds treated with stratifin- and ASA-containing emulgels showed an 80% reduction in hypertrophic scarring compared with the untreated controls. Inflammation was significantly controlled in treated wounds as shown by a reduced number of infiltrated $CD3^+$ T cells ($p > 0.001$). Stratifin and ASA treated wounds demonstrated a significantly

higher ($P > 0.001$) expression of matrix metalloproteinase-1 (MMP-1), which resulted in reduced collagen deposition.

Moreover, thermoreversible submicron emulgels effectively reduced the number of required applications when compared with CMC gels, which should translate to improved patient comfort and compliance. Interestingly, emulgels in the absence of any drug significantly mitigates scar size. Finally, wounds treated daily with SFN/ASA-containing emulgels showed a significant reduction in both collagen density and tissue cellularity. The findings of this study suggest that submicron emulgels provide a feasible means in which to control the delivery of both stratifin and acetylsalicylic acid to the wound bed of patients who are at risk of developing dermal fibrosis.

In this thesis, two delivery systems are formulated and reported on for the first time. First, in chapter 2, the development of a stratifin-releasing scaffold that can be implanted in surgical incisions before wound closure and sustainably release stratifin is described. In chapter 3, results of testing the therapeutic effect of these anti-fibrogenic implants in a rat model are presented. The importance of these results extends beyond the area of wound healing; they also provide additional information regarding the potential delivery of other bioactive proteins. Moreover, given the ubiquitous nature of scarring within the body, these results provided important potential treatment options for problematic scarring associated with implanted prostheses, such as vascular stents and breast implants. Taken as a whole, this body of research will provide a meaningful foundation for future research regarding the delivery of other bioactive proteins, as well as the management of scarring at various locations throughout the body.

In chapter 4, the efficacy of topically applied stratifin and ASA for reduction of hypertrophic scarring in open wounds is demonstrated, and results of tests in a rabbit ear fibrotic model are given. Chapter 5 describes the modification of CMC gel into a thermoreversible emulgel containing both stratifin and aspirin with a stronger water barrier capacity and film-forming capability that could control the release of these medications, which reduced the frequency of application to once a day. Interestingly, emulgels in the absence of any drug significantly mitigate scar size. This emulgel formulation can be used for the topical delivery of growth factors and antibiotics to the healing wounds.

In summary, in this research project I was able to (1) confirm anti-fibrogenic effect of stratifin in animal models, (2) design and develop a local controlled release and a topical formulation to deliver stratifin into surgically closed and open wounds, and (3) evaluate these systems in rat surgical and in rabbit ear fibrotic wound models.

6.2 Suggestions for Future Work

Although I believe that the findings of this thesis research are very promising, it is obvious that the research has only passed the proof of principal phase and these systems need further improvement. The following are suggested studies to be done as the next steps for improvement of these anti-fibrogenic products.

1. The anti-fibrogenic effect of local controlled release delivery of stratifin in a rat surgical wound model has been tested. A rat model is not an ideal fibrotic model. Using a better model such as the Duroc/Yorkshire pig, which better mimics human fibroproliferative scarring, and furthermore human clinical trials are suggested.
2. One of the adverse reactions of PLGA microspheres is dermal fibrosis and foreign body reactions. As such, fabricating stratifin-releasing dermal implants with nanofiber structures, which mimic the ultrafine structure of extracellular matrix in skin with much less probability of fibrosis, is proposed. This approach will help the delivery system be more translatable to the clinical situation.
3. The ultimate goal for development of the topical formulations of stratifin is its application to prevent post-burn hypertrophic scarring in humans, which will take about 2 years to be fully developed. The anti-fibrogenic effect of topically applied stratifin has been tested in a rabbit ear fibrotic model, which took only 28 days to be developed. Using a model like the Duroc/Yorkshire pig, which will allow study of the process of scarring for an extended period, and eventually human clinical trials are suggested.

References

Aarabi, S., M.T. Longaker, and G.C. Gurtner. 2007. Hypertrophic scar formation following burns and trauma: new approaches to treatment. *PLoS Med*. 4:e234.

Alves, M.P., A.L. Scarrone, M. Santos, A.R. Pohlmann, and S.S. Guterres. 2007. Human skin penetration and distribution of nimesulide from hydrophilic gels containing nanocarriers. *Int J Pharm*. 341:215-220.

Ammar, H.O., M. Ghorab, S.A. El-Nahhas, and R. Kamel. 2006. Design of a transdermal delivery system for aspirin as an antithrombotic drug. *Int J Pharm*. 327:81-88.

Ammar, H.O., H.A. Salama, M. Ghorab, and A.A. Mahmoud. 2010. Development of dorzolamide hydrochloride in situ gel nanoemulsion for ocular delivery. *Drug Dev Ind Pharm*. 36:1330-1339.

Aoyagi, S., H. Onishi, and Y. Machida. 2007. Novel chitosan wound dressing loaded with minocycline for the treatment of severe burn wounds. *Int J Pharm*. 330:138-145.

Atiyeh, B.S., M. Costagliola, and S.N. Hayek. 2005. Keloid or hypertrophic scar: the controversy: review of the literature. *Ann Plast Surg*. 54:676-680.

Atkinson, J.A., K.T. McKenna, A.G. Barnett, D.J. McGrath, and M. Rudd. 2005. A randomized, controlled trial to determine the efficacy of paper tape in preventing hypertrophic scar formation in surgical incisions that traverse Langer's skin tension lines. *Plast Reconstr Surg*. 116:1648-1656; discussion 1657-1648.

Babensee, J.E., L.V. McIntire, and A.G. Mikos. 2000. Growth factor delivery for tissue engineering. *Pharm Res*. 17:497-504.

Bauer, E.A., G.P. Stricklin, J.J. Jeffrey, and A.Z. Eisen. 1975. Collagenase production by human skin fibroblasts. *Biochem Biophys Res Commun*. 64:232-240.

Berman, B., A.M. Villa, and C.C. Ramirez. 2004. Novel opportunities in the treatment and prevention of scarring. *J Cutan Med Surg*. 8 Suppl 3:32-36.

Bivas-Benita, M., M. Oudshoorn, S. Romeijn, K. van Meijgaarden, H. Koerten, H. van der Meulen, G. Lambert, T. Ottenhoff, S. Benita, H. Junginger, and G. Borchard. 2004. Cationic submicron emulsions for pulmonary DNA immunization. *J Control Release*. 100:145-155.

Boateng, J.S., K.H. Matthews, H.N. Stevens, and G.M. Eccleston. 2008. Wound healing

dressings and drug delivery systems: a review. *J Pharm Sci*. 97:2892-2923.

Bode, W., C. Fernandez-Catalan, H. Tschesche, F. Grams, H. Nagase, and K. Maskos. 1999. Structural properties of matrix metalloproteinases. *Cell Mol Life Sci*. 55:639-652.

Boutli-Kasapidou, F., A. Tsakiri, E. Anagnostou, and O. Mourellou. 2005. Hypertrophic and keloidal scars: an approach to polytherapy. *Int J Dermatol*. 44:324-327.

Brown, R.J., M.J. Lee, M. Sisco, J.Y. Kim, N. Roy, and T.A. Mustoe. 2008. High-dose ultraviolet light exposure reduces scar hypertrophy in a rabbit ear model. *Plast Reconstr Surg*. 121:1165-1172.

Butler, G.S., R.A. Dean, E.M. Tam, and C.M. Overall. 2008. Pharmacoproteomics of a metalloproteinase hydroxamate inhibitor in breast cancer cells: dynamics of membrane type 1 matrix metalloproteinase-mediated membrane protein shedding. *Mol Cell Biol*. 28:4896-4914.

Castagnoli, C., C. Trombotto, S. Ondei, M. Stella, M. Calcagni, G. Magliacani, and S.T. Alasia. 1997. Characterization of T-cell subsets infiltrating post-burn hypertrophic scar tissues. *Burns*. 23:565-572.

Chen, J., W.L. Yang, G. Li, J. Qian, J.L. Xue, S.K. Fu, and D.R. Lu. 2004. Transfection of mEpo gene to intestinal epithelium in vivo mediated by oral delivery of chitosan-DNA nanoparticles. *World J Gastroenterol*. 10:112-116.

Chen, M.A., and T.M. Davidson. 2005. Scar management: prevention and treatment strategies. *Curr Opin Otolaryngol Head Neck Surg*. 13:242-247.

Cho, Y.S., J.W. Lee, J.S. Lee, J.H. Lee, T.R. Yoon, Y. Kuroyanagi, M.H. Park, D.G. Pyun, and H.J. Kim. 2002. Hyaluronic acid and silver sulfadiazine-impregnated polyurethane foams for wound dressing application. *J Mater Sci Mater Med*. 13:861-865.

Clark, R. 1996. Wound repair. Overview and general considerations. *In* The molecular and cellular biology of wound repair. e. Clark RAF, editor. Plenum, New York. 3-50.

Cleland, J.L. 1997. Protein delivery from biodegradable microspheres. *Pharm Biotechnol*. 10:1-43.

Clugston, P.A., M.D. Vistnes, L.C. Perry, G.P. Maxwell, and J. Fisher. 1995. Evaluation of silicone-gel sheeting on early wound healing of linear incisions. *Ann Plast Surg*. 34:12-15.

Daly, T.J., and W.L. Weston. 1986. Retinoid effects on fibroblast proliferation and

collagen synthesis in vitro and on fibrotic disease in vivo. *J Am Acad Dermatol*. 15:900-902.

Dang, C., K. Ting, C. Soo, M.T. Longaker, and H.P. Lorenz. 2003. Fetal wound healing current perspectives. *Clin Plast Surg*. 30:13-23.

de Carvalho Pde, T., I.S. da Silva, F.A. dos Reis, D.M. Perreira, and R.D. Aydos. 2010. Influence of ingaalp laser (660nm) on the healing of skin wounds in diabetic rats. *Acta Cir Bras*. 25:71-79.

DeFail, A.J., C.R. Chu, N. Izzo, and K.G. Marra. 2006. Controlled release of bioactive TGF-beta 1 from microspheres embedded within biodegradable hydrogels. *Biomaterials*. 27:1579-1585.

Deitch, E.A., T.M. Wheelahan, M.P. Rose, J. Clothier, and J. Cotter. 1983. Hypertrophic burn scars: analysis of variables. *J Trauma*. 23:895-898.

Diwan, M., and T.G. Park. 2001. Pegylation enhances protein stability during encapsulation in PLGA microspheres. *J Control Release*. 73:233-244.

Dockery, G.L. 1995. Hypertrophic and keloid scars. *J Am Podiatr Med Assoc*. 85:57-60.

Eisen, A.Z., J.J. Jeffrey, and J. Gross. 1968. Human skin collagenase. Isolation and mechanism of attack on the collagen molecule. *Biochim Biophys Acta*. 151:637-645.

Escobar-Chavez, J.J., M. Lopez-Cervantes, A. Naik, Y.N. Kalia, D. Quintanar-Guerrero, and A. Ganem-Quintanar. 2006. Applications of thermo-reversible pluronic F-127 gels in pharmaceutical formulations. *J Pharm Pharm Sci*. 9:339-358.

Foldvari, M., M.E. Baca-Estrada, Z. He, J. Hu, S. Attah-Poku, and M. King. 1999. Dermal and transdermal delivery of protein pharmaceuticals: lipid-based delivery systems for interferon alpha. *Biotechnol Appl Biochem*. 30 (Pt 2):129-137.

Foldvari, M., I. Badea, S. Wettig, D. Baboolal, P. Kumar, A.L. Creagh, and C.A. Haynes. 2010. Topical delivery of interferon alpha by biphasic vesicles: evidence for a novel nanopathway across the stratum corneum. *Mol Pharm*. 7:751-762.

Forouzandeh, F., R.B. Jalili, R.V. Hartwell, S.E. Allan, S. Boyce, D. Supp, and A. Ghahary. 2010. Local expression of indoleamine 2,3-dioxygenase suppresses T-cell-mediated rejection of an engineered bilayer skin substitute. *Wound Repair Regen*.

Franz, M.G., D.L. Steed, and M.C. Robson. 2007. Optimizing healing of the acute wound by minimizing complications. *Curr Probl Surg*. 44:691-763.

Franzke, C.W., P. Bruckner, and L. Bruckner-Tuderman. 2005. Collagenous transmembrane proteins: recent insights into biology and pathology. *J Biol Chem*. 280:4005-4008.

Fumagalli, M., T. Musso, W. Vermi, S. Scutera, R. Daniele, D. Alotto, I. Cambieri, A. Ostorero, F. Gentili, P. Caposio, M. Zucca, S. Sozzani, M. Stella, and C. Castagnoli. 2007. Imbalance between activin A and follistatin drives postburn hypertrophic scar formation in human skin. *Exp Dermatol*. 16:600-610.

Galeska, I., T.K. Kim, S.D. Patil, U. Bhardwaj, D. Chatttopadhyay, F. Papadimitrakopoulos, and D.J. Burgess. 2005. Controlled release of dexamethasone from PLGA microspheres embedded within polyacid-containing PVA hydrogels. *AAPS J*. 7:E231-240.

Garg, S., and P.W. Serruys. 2010. Coronary stents: current status. *J Am Coll Cardiol*. 56:S1-42.

Ghaffari, A., Y. Li, A. Karami, M. Ghaffari, E.E. Tredget, and A. Ghahary. 2006. Fibroblast extracellular matrix gene expression in response to keratinocyte-releasable stratifin. *J Cell Biochem*. 98:383-393.

Ghahary, A., F. Karimi-Busheri, Y. Marcoux, Y. Li, E.E. Tredget, R. Taghi Kilani, L. Li, J. Zheng, A. Karami, B.O. Keller, and M. Weinfeld. 2004. Keratinocyte-releasable stratifin functions as a potent collagenase-stimulating factor in fibroblasts. *J Invest Dermatol*. 122:1188-1197.

Ghahary, A., Y. Marcoux, F. Karimi-Busheri, Y. Li, E.E. Tredget, R.T. Kilani, E. Lam, and M. Weinfeld. 2005. Differentiated keratinocyte-releasable stratifin (14-3-3 sigma) stimulates MMP-1 expression in dermal fibroblasts. *J Invest Dermatol*. 124:170-177.

Ghahary, A., E.E. Tredget, Q. Shen, R.T. Kilani, P.G. Scott, and M. Takeuchi. 2000. Liposome associated interferon-alpha-2b functions as an anti-fibrogenic factor in dermal wounds in the guinea pig. *Mol Cell Biochem*. 208:129-137.

Gottrup, F., B. Jorgensen, T. Karlsmark, R.G. Sibbald, R. Rimdeika, K. Harding, P. Price, V. Venning, P. Vowden, M. Junger, S. Wortmann, R. Sulcaite, G. Vilkevicius, T.L. Ahokas, K. Ettler, and M. Arenbergerova. 2007. Less pain with Biatain-Ibu: initial findings from a randomised, controlled, double-blind clinical investigation on painful venous leg ulcers. *Int Wound J*. 4 Suppl 1:24-34.

Gregg, A.K., and M. Jones. 1999. Intermittent subcutaneous injections for postoperative pain relief. *Anaesthesia*. 54:200.

Grzybowski, J., E. Oldak, M. Antos-Bielska, M.K. Janiak, and Z. Pojda. 1999. New cytokine dressings. I. Kinetics of the in vitro rhG-CSF, rhGM-CSF, and rhEGF release from the dressings. *Int J Pharm*. 184:173-178.

Gu, F., B. Amsden, and R. Neufeld. 2004. Sustained delivery of vascular endothelial growth factor with alginate beads. *J Control Release*. 96:463-472.

Hagigit, T., M. Abdulrazik, F. Orucov, F. Valamanesh, M. Lambert, G. Lambert, F. Behar-Cohen, and S. Benita. 2010. Topical and intravitreous administration of cationic nanoemulsions to deliver antisense oligonucleotides directed towards VEGF KDR receptors to the eye. *J Control Release*. 145:297-305.

Hagigit, T., T. Nassar, F. Behar-Cohen, G. Lambert, and S. Benita. 2008. The influence of cationic lipid type on in-vitro release kinetic profiles of antisense oligonucleotide from cationic nanoemulsions. *Eur J Pharm Biopharm*. 70:248-259.

Hemmila, M.R., A. Mattar, M.A. Taddonio, S. Arbabi, T. Hamouda, P.A. Ward, S.C. Wang, and J.R. Baker, Jr. 2010. Topical nanoemulsion therapy reduces bacterial wound infection and inflammation after burn injury. *Surgery*. 148:499-509.

Hoffman, A.S. 2002. Hydrogels for biomedical applications. *Adv Drug Deliv Rev*. 54:3-12.

Howard, D., L.D. Buttery, K.M. Shakesheff, and S.J. Roberts. 2008. Tissue engineering: strategies, stem cells and scaffolds. *J Anat*. 213:66-72.

Huang, S., T. Deng, H. Wu, F. Chen, and Y. Jin. 2006. Wound dressings containing bFGF-impregnated microspheres. *J Microencapsul*. 23:277-290.

Jackson, J.K., T. Hung, K. Letchford, and H.M. Burt. 2007. The characterization of paclitaxel-loaded microspheres manufactured from blends of poly(lactic-co-glycolic acid) (PLGA) and low molecular weight diblock copolymers. *Int J Pharm*. 342:6-17.

Jackson, J.K., K.C. Skinner, L. Burgess, T. Sun, W.L. Hunter, and H.M. Burt. 2002. Paclitaxel-loaded crosslinked hyaluronic acid films for the prevention of postsurgical adhesions. *Pharm Res*. 19:411-417.

Jorgensen, B., P. Price, K.E. Andersen, F. Gottrup, N. Bech-Thomsen, E. Scanlon, R. Kirsner, H. Rheinen, J. Roed-Petersen, M. Romanelli, G. Jemec, D.J. Leaper, M.H. Neumann, J. Veraart, S. Coerper, R.H. Agerslev, S.H. Bendz, J.R. Larsen, and R.G. Sibbald. 2005. The silver-releasing foam dressing, Contreet Foam, promotes faster healing of critically colonised venous leg ulcers: a randomised, controlled trial. *Int Wound J*. 2:64-73.

Kang, N., B. Sivakumar, R. Sanders, C. Nduka, and D. Gault. 2006. Intra-lesional injections of collagenase are ineffective in the treatment of keloid and hypertrophic scars. *J Plast Reconstr Aesthet Surg*. 59:693-699.

Katti, D.S., K.W. Robinson, F.K. Ko, and C.T. Laurencin. 2004. Bioresorbable nanofiber-based systems for wound healing and drug delivery: optimization of fabrication parameters. *J Biomed Mater Res B Appl Biomater*. 70:286-296.

Katz, A.B., and L.B. Taichman. 1999. A partial catalog of proteins secreted by epidermal keratinocytes in culture. *J Invest Dermatol*. 112:818-821.

Kauh, Y.C., S. Rouda, G. Mondragon, R. Tokarek, M. diLeonardo, R.S. Tuan, and E.M. Tan. 1997. Major suppression of pro-alpha1(I) type I collagen gene expression in the dermis after keloid excision and immediate intrawound injection of triamcinolone acetonide. *J Am Acad Dermatol*. 37:586-589.

Kaushal, M., N. Gopalan Kutty, and C. Mallikarjuna Rao. 2007. Wound healing activity of NOE-aspirin: a pre-clinical study. *Nitric Oxide*. 16:150-156.

Kempen, D.H., L. Lu, T.E. Hefferan, L.B. Creemers, A. Maran, K.L. Classic, W.J. Dhert, and M.J. Yaszemski. 2008. Retention of in vitro and in vivo BMP-2 bioactivities in sustained delivery vehicles for bone tissue engineering. *Biomaterials*. 29:3245-3252.

Kietzmann, M., and M. Braun. 2006. [Effects of the zinc oxide and cod liver oil containing ointment Zincojecol in an animal model of wound healing]. *Dtsch Tierarztl Wochenschr*. 113:331-334.

Kim, A., J. DiCarlo, C. Cohen, C. McCall, D. Johnson, B. McAlpine, A.G. Quinn, E.R. McLaughlin, and J.L. Arbiser. 2001. Are keloids really "gli-loids"?: High-level expression of gli-1 oncogene in keloids. *J Am Acad Dermatol*. 45:707-711.

Kim, B.S., M. Won, K.M. Lee, and C.S. Kim. 2008. In vitro permeation studies of nanoemulsions containing ketoprofen as a model drug. *Drug Deliv*. 15:465-469.

Kim, H.K., and T.G. Park. 2004. Comparative study on sustained release of human growth hormone from semi-crystalline poly(L-lactic acid) and amorphous poly(D,L-lactic-co-glycolic acid) microspheres: morphological effect on protein release. *J Control Release*. 98:115-125.

Kirsner, R.S., and W.H. Eaglstein. 1993. The wound healing process. *Dermatol Clin*. 11:629-640.

Kloeters, O., A. Tandara, and T.A. Mustoe. 2007. Hypertrophic scar model in the rabbit ear: a reproducible model for studying scar tissue behavior with new observations on silicone gel sheeting for scar reduction. *Wound Repair Regen*. 15 Suppl 1:S40-45.

Kobayashi, H., M. Ishii, M. Chanoki, N. Yashiro, H. Fushida, K. Fukai, T. Kono, T. Hamada, H. Wakasaki, and A. Ooshima. 1994. Immunohistochemical

localization of lysyl oxidase in normal human skin. *Br J Dermatol*. 131:325-330.

Kobayashi, R., M. Deavers, R. Patenia, T. Rice-Stitt, J. Halbe, S. Gallardo, and R.S. Freedman. 2009. 14-3-3 zeta protein secreted by tumor associated monocytes/macrophages from ascites of epithelial ovarian cancer patients. *Cancer Immunol Immunother*. 58:247-258.

Koempel, J.A., S.E. Gibson, K. O'Grady, and D.M. Toriumi. 1998. The effect of platelet-derived growth factor on tracheal wound healing. *Int J Pediatr Otorhinolaryngol*. 46:1-8.

Kontio, R., A. Salo, R. Suuronen, C. Lindqvist, J.H. Meurman, and I. Virtanen. 1998. Fibrous wound repair associated with biodegradable poly-L/D-lactide copolymer implants: study of the expression of tenascin and cellular fibronectin. *J Mater Sci Mater Med*. 9:603-609.

Kwan, P., K. Hori, J. Ding, and E.E. Tredget. 2009. Scar and contracture: biological principles. *Hand Clin*. 25:511-528.

Ladak, A., and E.E. Tredget. 2009. Pathophysiology and management of the burn scar. *Clin Plast Surg*. 36:661-674.

Lam, E., R.T. Kilani, Y. Li, E.E. Tredget, and A. Ghahary. 2005. Stratifin-induced matrix metalloproteinase-1 in fibroblast is mediated by c-fos and p38 mitogen-activated protein kinase activation. *J Invest Dermatol*. 125:230-238.

Lee, K.W., J.J. Yoon, J.H. Lee, S.Y. Kim, H.J. Jung, S.J. Kim, J.W. Joh, H.H. Lee, D.S. Lee, and S.K. Lee. 2004. Sustained release of vascular endothelial growth factor from calcium-induced alginate hydrogels reinforced by heparin and chitosan. *Transplant Proc*. 36:2464-2465.

Levenson, S.M., E.F. Geever, L.V. Crowley, J.F. Oates, 3rd, C.W. Berard, and H. Rosen. 1965. The Healing of Rat Skin Wounds. *Ann Surg*. 161:293-308.

Leventhal, D., M. Furr, and D. Reiter. 2006. Treatment of keloids and hypertrophic scars: a meta-analysis and review of the literature. *Arch Facial Plast Surg*. 8:362-368.

Li, M., A. Moeen Rezakhanlou, C. Chavez-Munoz, A. Lai, and A. Ghahary. 2009. Keratinocyte-releasable factors increased the expression of MMP1 and MMP3 in co-cultured fibroblasts under both 2D and 3D culture conditions. *Mol Cell Biochem*. 332:1-8.

Li, S.H., S.X. Cai, B. Liu, K.W. Ma, Z.P. Wang, and X.K. Li. 2006. In vitro characteristics of poly(lactic-co-glycolic acid) microspheres incorporating gelatin particles loading basic fibroblast growth factor. *Acta Pharmacol Sin*. 27:754-759.

Li, Y.K., M.J. Chou, T.Y. Wu, T.R. Jinn, and Y.W. Chen-Yang. 2008. A novel method for preparing a protein-encapsulated bioaerogel: using a red fluorescent protein as a model. *Acta Biomater*. 4:725-732.

Luo, Y., K.R. Kirker, and G.D. Prestwich. 2000. Cross-linked hyaluronic acid hydrogel films: new biomaterials for drug delivery. *J Control Release*. 69:169-184.

MacLaughlin, F.C., R.J. Mumper, J. Wang, J.M. Tagliaferri, I. Gill, M. Hinchcliffe, and A.P. Rolland. 1998. Chitosan and depolymerized chitosan oligomers as condensing carriers for in vivo plasmid delivery. *J Control Release*. 56:259-272.

Maeda, M., K. Kadota, M. Kajihara, A. Sano, and K. Fujioka. 2001. Sustained release of human growth hormone (hGH) from collagen film and evaluation of effect on wound healing in db/db mice. *J Control Release*. 77:261-272.

Magnette, J., J.L. Kienzler, I. Alekxandrova, E. Savaluny, A. Khemis, S. Amal, M. Trabelsi, and J.P. Cesarini. 2004. The efficacy and safety of low-dose diclofenac sodium 0.1% gel for the symptomatic relief of pain and erythema associated with superficial natural sunburn. *Eur J Dermatol*. 14:238-246.

Majan, J.I. 2006. Evaluation of a self-adherent soft silicone dressing for the treatment of hypertrophic postoperative scars. *J Wound Care*. 15:193-196.

Makidon, P.E., J. Knowlton, J.V. Groom, 2nd, L.P. Blanco, J.J. LiPuma, A.U. Bielinska, and J.R. Baker, Jr. 2010a. Induction of immune response to the 17 kDa OMPA Burkholderia cenocepacia polypeptide and protection against pulmonary infection in mice after nasal vaccination with an OMP nanoemulsion-based vaccine. *Med Microbiol Immunol*. 199:81-92.

Makidon, P.E., S.S. Nigavekar, A.U. Bielinska, N. Mank, A.M. Shetty, J. Suman, J. Knowlton, A. Myc, T. Rook, and J.R. Baker, Jr. 2010b. Characterization of stability and nasal delivery systems for immunization with nanoemulsion-based vaccines. *J Aerosol Med Pulm Drug Deliv*. 23:77-89.

McGinity, J.W., and P.B. O'Donnell. 1997. Preparation of microspheres by the solvent evaporation technique. *Adv Drug Deliv Rev*. 28:25-42.

McQuibban, G.A., J.H. Gong, J.P. Wong, J.L. Wallace, I. Clark-Lewis, and C.M. Overall. 2002. Matrix metalloproteinase processing of monocyte chemoattractant proteins generates CC chemokine receptor antagonists with anti-inflammatory properties in vivo. *Blood*. 100:1160-1167.

Medina, A., A. Ghaffari, R.T. Kilani, and A. Ghahary. 2007. The role of stratifin in fibroblast-keratinocyte interaction. *Mol Cell Biochem*. 305:255-264.

Meier, K., and L.B. Nanney. 2006. Emerging new drugs for scar reduction. *Expert*

Opin Emerg Drugs. 11:39-47.

Mi, F.L., Y.C. Tan, H.F. Liang, and H.W. Sung. 2002a. In vivo biocompatibility and degradability of a novel injectable-chitosan-based implant. *Biomaterials*. 23:181-191.

Mi, F.L., Y.B. Wu, S.S. Shyu, J.Y. Schoung, Y.B. Huang, Y.H. Tsai, and J.Y. Hao. 2002b. Control of wound infections using a bilayer chitosan wound dressing with sustainable antibiotic delivery. *J Biomed Mater Res*. 59:438-449.

Miller, E., and S. Gay. 1992. Collagen structure and function *In* Wound Healing: Biochemical and Clinical Aspects. WB Saunders, Philadelphia. 130-155.

Morris, D.E., L. Wu, L.L. Zhao, L. Bolton, S.I. Roth, D.A. Ladin, and T.A. Mustoe. 1997. Acute and chronic animal models for excessive dermal scarring: quantitative studies. *Plast Reconstr Surg*. 100:674-681.

Murphy, G., V. Knauper, S. Atkinson, G. Butler, W. English, M. Hutton, J. Stracke, and I. Clark. 2002. Matrix metalloproteinases in arthritic disease. *Arthritis Res*. 4 Suppl 3:S39-49.

Mustoe, T.A. 2008. Evolution of silicone therapy and mechanism of action in scar management. *Aesthetic Plast Surg*. 32:82-92.

Mustoe, T.A., R.D. Cooter, M.H. Gold, F.D. Hobbs, A.A. Ramelet, P.G. Shakespeare, M. Stella, L. Teot, F.M. Wood, and U.E. Ziegler. 2002. International clinical recommendations on scar management. *Plast Reconstr Surg*. 110:560-571.

Mutalik, S. 2005. Treatment of keloids and hypertrophic scars. *Indian J Dermatol Venereol Leprol*. 17.

Myllyharju, J., and K.I. Kivirikko. 2001. Collagens and collagen-related diseases. *Ann Med*. 33:7-21.

Nagase, H., and J.F. Woessner, Jr. 1999. Matrix metalloproteinases. *J Biol Chem*. 274:21491-21494.

Niessen, F.B., P.H. Spauwen, J. Schalkwijk, and M. Kon. 1999. On the nature of hypertrophic scars and keloids: a review. *Plast Reconstr Surg*. 104:1435-1458.

Norton, J.A., Barie, P.S., Bollinger, R.R., Chang, A.E., Lowry, S., Mulvihill S.J., Pass, H.I., Thompson, R.W., Shirazi, M.K. . 2008. Surgery: Basic Science and Clinical Evidence.

Occleston, N.L., S. O'Kane, N. Goldspink, and M.W. Ferguson. 2008. New therapeutics for the prevention and reduction of scarring. *Drug Discov Today*. 13:973-981.

Okada, H. 1997. One- and three-month release injectable microspheres of the LH-RH superagonist leuprorelin acetate. *Adv Drug Deliv Rev*. 28:43-70.

Pardo, M., A. Garcia, B. Thomas, A. Pineiro, A. Akoulitchev, R.A. Dwek, and N. Zitzmann. 2006. The characterization of the invasion phenotype of uveal melanoma tumour cells shows the presence of MUC18 and HMG-1 metastasis markers and leads to the identification of DJ-1 as a potential serum biomarker. *Int J Cancer*. 119:1014-1022.

Park, S.N., H.J. Jang, Y.S. Choi, J.M. Cha, S.Y. Son, S.H. Han, J.H. Kim, W.J. Lee, and H. Suh. 2007. Preparation and characterization of biodegradable anti-adhesive membrane for peritoneal wound healing. *J Mater Sci Mater Med*. 18:475-482.

Patil, S.D., F. Papadmitrakopoulos, and D.J. Burgess. 2007. Concurrent delivery of dexamethasone and VEGF for localized inflammation control and angiogenesis. *J Control Release*. 117:68-79.

Pirard, B. 2007. Insight into the structural determinants for selective inhibition of matrix metalloproteinases. *Drug Discov Today*. 12:640-646.

Poljicak-Milas, N., I. Kardum-Skelin, M. Vudan, T. Marenjak, A. Ballarin-Perharic, and Z. Milas. 2009. Blood cell count analyses and erythrocyte morphometry in New Zealand white rabbits. *Vet Archiv*. 79:561–571.

Poston, J. 2000. The use of silicone gel sheeting in the management of hypertrophic and keloid scars. *J Wound Care*. 9:10-16.

Pulkkinen, L., F. Ringpfeil, and J. Uitto. 2002. Progress in heritable skin diseases: molecular bases and clinical implications. *J Am Acad Dermatol*. 47:91-104.

Puolakkainen, P.A., D.R. Twardzik, J.E. Ranchalis, S.C. Pankey, M.J. Reed, and W.R. Gombotz. 1995. The enhancement in wound healing by transforming growth factor-beta 1 (TGF-beta 1) depends on the topical delivery system. *J Surg Res*. 58:321-329.

Rahmani-Neishaboor, E., J. Jackson, H. Burt, and A. Ghahary. 2009. Composite hydrogel formulations of stratifin to control MMP-1 expression in dermal fibroblasts. *Pharm Res*. 26:2002-2014.

Rahmani-Neishaboor, E., F.M. Yau, R. Jalili, R.T. Kilani, and A. Ghahary. 2010. Improvement of hypertrophic scarring by using topical anti-fibrogenic/anti-inflammatory factors in a rabbit ear model. *Wound Repair Regen*. 18:401-408.

Reller, H. Topical composition containing acetyl salicylic acid. Vol. 4126681. US Patent.

Rhee, S.H., S.H. Koh, D.W. Lee, B.Y. Park, and Y.O. Kim. 2010. Aesthetic effect of

silicone gel on surgical scars in Asians. *J Craniofac Surg*. 21:706-710.

Sakulku, U., O. Nuchuchua, N. Uawongyart, S. Puttipipatkhachorn, A. Soottitantawat, and U. Ruktanonchai. 2009. Characterization and mosquito repellent activity of citronella oil nanoemulsion. *Int J Pharm*. 372:105-111.

Sallstrom, K.O., O. Larson, P. Heden, G. Eriksson, J.E. Glas, and U. Ringborg. 1989. Treatment of keloids with surgical excision and postoperative X-ray radiation. *Scand J Plast Reconstr Surg Hand Surg*. 23:211-215.

Sanchez, A., M. Tobio, L. Gonzalez, A. Fabra, and M.J. Alonso. 2003. Biodegradable micro- and nanoparticles as long-term delivery vehicles for interferon-alpha. *Eur J Pharm Sci*. 18:221-229.

Saray, Y., and A.T. Gulec. 2005. Treatment of keloids and hypertrophic scars with dermojet injections of bleomycin: a preliminary study. *Int J Dermatol*. 44:777-784.

Sarkhosh, K., E.E. Tredget, Y. Li, R.T. Kilani, H. Uludag, and A. Ghahary. 2003. Proliferation of peripheral blood mononuclear cells is suppressed by the indoleamine 2,3-dioxygenase expression of interferon-gamma-treated skin cells in a co-culture system. *Wound Repair Regen*. 11:337-345.

Saulis, A.S., J.H. Mogford, and T.A. Mustoe. 2002. Effect of Mederma on hypertrophic scarring in the rabbit ear model. *Plast Reconstr Surg*. 110:177-183; discussion 184-176.

Sawada, Y., and K. Sone. 1990. Treatment of scars and keloids with a cream containing silicone oil. *Br J Plast Surg*. 43:683-688.

Scott, P.G., A. Ghahary, and E.E. Tredget. 2000. Molecular and cellular aspects of fibrosis following thermal injury. *Hand Clin*. 16:271-287.

Shakeel, F., S. Baboota, A. Ahuja, J. Ali, and S. Shafiq. 2008. Skin permeation mechanism and bioavailability enhancement of celecoxib from transdermally applied nanoemulsion. *J Nanobiotechnology*. 6:8.

Shakeel, F., W. Ramadan, and M.A. Ahmed. 2009. Investigation of true nanoemulsions for transdermal potential of indomethacin: characterization, rheological characteristics, and ex vivo skin permeation studies. *J Drug Target*. 17:435-441.

Sherman, R., and H. Rosenfeld. 1988. Experience with the Nd:YAG laser in the treatment of keloid scars. *Ann Plast Surg*. 21:231-235.

Shi, R., L. Hong, D. Wu, X. Ning, Y. Chen, T. Lin, D. Fan, and K. Wu. 2005. Enhanced immune response to gastric cancer specific antigen Peptide by

coencapsulation with CpG oligodeoxynucleotides in nanoemulsion. *Cancer Biol Ther*. 4:218-224.

Shive, M.S., and J.M. Anderson. 1997. Biodegradation and biocompatibility of PLA and PLGA microspheres. *Adv Drug Deliv Rev*. 28:5-24.

Siepmann, J., and N.A. Peppas. 2000. Hydrophilic matrices for controlled drug delivery: an improved mathematical model to predict the resulting drug release kinetics (the "sequential layer" model). *Pharm Res*. 17:1290-1298.

Singer, A.J., and R.A. Clark. 1999. Cutaneous wound healing. *N Engl J Med*. 341:738-746.

Slemp, A.E., and R.E. Kirschner. 2006. Keloids and scars: a review of keloids and scars, their pathogenesis, risk factors, and management. *Curr Opin Pediatr*. 18:396-402.

Springate, C.M., J.K. Jackson, M.E. Gleave, and H.M. Burt. 2005. Efficacy of an intratumoral controlled release formulation of clusterin antisense oligonucleotide complexed with chitosan containing paclitaxel or docetaxel in prostate cancer xenograft models. *Cancer Chemother Pharmacol*. 56:239-247.

Stamenkovic, I. 2003. Extracellular matrix remodelling: the role of matrix metalloproteinases. *J Pathol*. 200:448-464.

Steenfos, H.H. 1994. Growth factors and wound healing. *Scand J Plast Reconstr Surg Hand Surg*. 28:95-105.

Stratton, T.R., J.L. Rickus, and J.P. Youngblood. 2009. In vitro biocompatibility studies of antibacterial quaternary polymers. *Biomacromolecules*. 10:2550-2555.

Sznitowska, M., S. Janicki, K. Zurowska-Pryczkowska, and J. Mackiewicz. 2001. In vivo evaluation of submicron emulsions with pilocarpine: the effect of pH and chemical form of the drug. *J Microencapsul*. 18:173-181.

Tagne, J.B., S. Kakumanu, and R.J. Nicolosi. 2008. Nanoemulsion Preparations of the Anticancer Drug Dacarbazine Significantly Increase Its Efficacy in a Xenograft Mouse Melanoma Model. *Mol Pharm*.

Takeuchi, M., E.E. Tredget, P.G. Scott, R.T. Kilani, and A. Ghahary. 1999. The antifibrogenic effects of liposome-encapsulated IFN-alpha2b cream on skin wounds. *J Interferon Cytokine Res*. 19:1413-1419.

Tandara, A., T. Mustoe, and J. Mogford. 2008. Impact of hydration on MMP activity. *Wound Repair Regen* 12:A6.

Tandara, A.A., O. Kloeters, J.E. Mogford, and T.A. Mustoe. 2007. Hydrated keratinocytes reduce collagen synthesis by fibroblasts via paracrine mechanisms. *Wound Repair Regen*. 15:497-504.

Tandara, A.A., and T.A. Mustoe. 2008. The role of the epidermis in the control of scarring: evidence for mechanism of action for silicone gel. *J Plast Reconstr Aesthet Surg*. 61:1219-1225.

Thomas, S., V. Banks, S. Bale, M. Fear-Price, S. Hagelstein, K.G. Harding, J. Orpin, and N. Thomas. 1997. A comparison of two dressings in the management of chronic wounds. *J Wound Care*. 6:383-386.

Tredget, E.E., B. Nedelec, P.G. Scott, and A. Ghahary. 1997. Hypertrophic scars, keloids, and contractures. The cellular and molecular basis for therapy. *Surg Clin North Am*. 77:701-730.

USP 24. Sterilization and Sterility Assurance. *US Pharmacopeia*.

Wang, J., H. Jiao, T.L. Stewart, H.A. Shankowsky, P.G. Scott, and E.E. Tredget. 2007. Increased TGF-beta-producing CD4+ T lymphocytes in postburn patients and their potential interaction with dermal fibroblasts in hypertrophic scarring. *Wound Repair Regen*. 15:530-539.

Weber, F.E., G. Eyrich, K.W. Gratz, F.E. Maly, and H.F. Sailer. 2002. Slow and continuous application of human recombinant bone morphogenetic protein via biodegradable poly(lactide-co-glycolide) foamspheres. *Int J Oral Maxillofac Surg*. 31:60-65.

Wong, T.W., H.C. Chiu, C.H. Chang, L.J. Lin, C.C. Liu, and J.S. Chen. 1996. Silicone cream occlusive dressing--a novel noninvasive regimen in the treatment of keloid. *Dermatology*. 192:329-333.

Wu, X., Z. Gao, N. Song, C. Chua, D. Deng, Y. Cao, and W. Liu. 2007. Creating thick linear scar by inserting a gelatin sponge into rat excisional wounds. *Wound Repair Regen*. 15:595-606.

Yang, G.P., I.J. Lim, T.T. Phan, H.P. Lorenz, and M.T. Longaker. 2003. From scarless fetal wounds to keloids: molecular studies in wound healing. *Wound Repair Regen*. 11:411-418.

Yeo, Y., T. Ito, E. Bellas, C.B. Highley, R. Marini, and D.S. Kohane. 2007. In situ cross-linkable hyaluronan hydrogels containing polymeric nanoparticles for preventing postsurgical adhesions. *Ann Surg*. 245:819-824.

zhang, x., J. Jackson, and H. Burt. 1996. Development of amphiphilic diblock copolymers as micellar carriers of taxol. *International journal of Pharmaceutics*. 132:195-206.

Zheng, C.H., J.Q. Gao, Y.P. Zhang, and W.Q. Liang. 2004. A protein delivery system: biodegradable alginate-chitosan-poly(lactic-co-glycolic acid) composite microspheres. *Biochem Biophys Res Commun*. 323:1321-1327.

Zhu, K.Q., G.J. Carrougher, N.S. Gibran, F.F. Isik, and L.H. Engrav. 2007. Review of the female Duroc/Yorkshire pig model of human fibroproliferative scarring. *Wound Repair Regen*. 15 Suppl 1:S32-39.

Zhu, X.H., Y. Tabata, C.H. Wang, and Y.W. Tong. 2008. Delivery of basic fibroblast growth factor from gelatin microsphere scaffold for the growth of human umbilical vein endothelial cells. *Tissue Eng Part A*. 14:1939-1947.

Zilberman, M., A. Kraitzer, O. Grinberg, and J.J. Elsner. 2010. Drug-eluting medical implants. *Handb Exp Pharmacol*:299-341.

Zitelli, J. 1996. Wound healing by first and second intention. MarcelDekker Inc., New York.